Mycol Progress
DOI 10.1007/s11557-008-0563-3

ORIGINAL ARTICLE

The *Trichoderma brevicompactum* clade: a separate lineage with new species, new peptaibiotics, and mycotoxins

Thomas Degenkolb · Ralf Dieckmann · Kristian Fog Nielsen · Tom Gräfenhan · Christoph Theis · Doustmorad Zafari · Priscila Chaverri · Adnan Ismaiel · Hans Brückner · Hans Von Döhren · Ulf Thrane · Orlando Petrini · Gary J. Samuels

Received: 8 January 2008 / Revised: 27 March 2008 / Accepted: 8 April 2008

Abstract The Brevicompactum clade is recognized as a separate lineage in *Trichoderma*/*Hypocrea*. This includes *T. brevicompactum* and the new species *T. arundinaceum, T. turrialbense, T. protrudens* and *Hypocrea rodmanii*. The closest relative of the Brevicompactum clade is the Lutea clade. With the exception of *H. rodmanii*, all members of this clade produce the simple trichothecene-type toxins harzianum A or trichodermin. All members of the clade produce peptaibiotics, including alamethicins. Strains previously reported as *T. harzianum* (ATCC 90237), *T. viride* (NRRL 3199) or *Hypocrea* sp. (F000527, CBS 113214) to produce trichothecenes are reidentified as *T. arundinaceum*. The Brevicompactum clade is not closely related to species that have biological application.

Taxonomic novelties *Hypocrea rodmanii* Samuels & Chaverri, *Trichoderma arundinaceum* Zafari, Gräfenhan & Samuels, *Trichoderma protrudens* Samuels & Chaverri, *Trichoderma turrialbense* Samuels, Degenkolb, K.F. Nielsen & Gräfenhan.

T. Degenkolb · C. Theis · H. Brückner
Interdisciplinary Research Centre for Biosystems, Land Use and Nutrition (IFZ), Department of Food Sciences, Institute of Nutritional Science, University of Giessen, Heinrich-Buff-Ring 26-32, 35392 Giessen, Germany

R. Dieckmann · H. Von Döhren
Technische Universität Berlin, Institut für Chemie, FG Biochemie und Molekulare Biologie, Franklinstraße 29, 10587 Berlin, Germany

K. F. Nielsen · U. Thrane
Center for Microbial Biotechnology (CMB), BioCentrum, Technical University of Denmark, Building 221, 2800 Lyngby, Denmark

T. Gräfenhan
Eastern Cereals and Oilseeds Research Centre, William Saunders Building, Agriculture and Agri-Food Canada, Ottawa, ON K1A OC6, Canada

D. Zafari
Faculty of Agriculture, Bu Ali Sina University, Hamadan, Iran

P. Chaverri
Department of Biology, Howard University, 415 College Street NW, Washington, DC 20059, USA

A. Ismaiel · G. J. Samuels (✉)
United States Department of Agriculture, ARS, Systematic Mycology & Microbiology Laboratory, B-011a, Rm. 304, 10300 Baltimore Ave., Beltsville, MD 20705, USA
e-mail: gary.samuels@ars.usda.gov

O. Petrini
Repubblica e Cantone Ticino, Istituto Cantonale di Microbiologia, Via Mirasole 22A, 6500 Bellinzona, Switzerland

Introduction

Visible phenotype, including microscopic and colony characters, has come to occupy a role subsidiary to molecular phylogenetics in *Trichoderma* and its corresponding teleomorph, *Hypocrea*. For example, *T. viride* is the most commonly reported species in the genus, but many, or most, of those reports are likely to have been based on misidentifications because it is now known that *T. viride* has a limited distribution in the northern hemisphere while the morphologically very similar *T. viridescens* is widely distributed at temperate latitudes (Jaklitsch et al. 2006). Similarly, *T. harzianum* also ranks among the most commonly reported species, on the basis of its morphology, but gradually this morphological concept is being refined. Thus, the cause of green mould disease of commercial mushrooms was originally identified as *T. harzianum* but is now known to be *T. aggressivum* (Samuels et al. 2002). While the physical differences between *T. viride* and *T. viridescens* and between *T. harzianum* and *T. aggressivum* are small but consistent, it was only through phylogenetic analysis that the respective pairs were seen to represent distinct species.

Trichoderma brevicompactum could be mistaken for *T. harzianum* on the basis of considerable shared micromorphology, but phylogenetic analysis shows them to be only distantly related (Kraus et al. 2004). Moreover, when it was originally described (Kraus et al. 2004), a combined ITS-*tef1* phylogram indicated two, highly supported, sister groups within *T. brevicompactum*. The two well-supported sister clades at least indicated distinct phylogenetic if not taxonomic species.

In their study of mycotoxin production in *Trichoderma*, Nielsen et al. (2005) found that the ex-type and other cultures of *T. brevicompactum* produced the simple trichothecene-type mycotoxin trichodermin, while isolates in the sister lineage to the ex-type produced harziaum A. Trichodermin is the first trichothecene for which the structure was fully elucidated; it was produced by a culture identified as *T. viride* LEO ND 8 (Godtfredsen and Vangedal 1964, 1965). That culture was reidentified by Nielsen et al. (2005) as *T. brevicompactum*. Harzianum A was isolated from a culture identified as *T. harzianum* (ATCC 90237, Corley et al. 1994) and later reidentified by Nielsen et al. (2005) as *T. brevicompactum*, although in the sister lineage mentioned above. Because the patterns of toxin production by isolates coincided with the phylogenetic lineages observed in the protologue of *T. brevicompactum*, Nielsen et al. (2005) suggested the existence of two phylogenetic species within the morphological species *T. brevicompactum*. However, the trichothecene results were ambiguous in that one of the cultures (CBS 112445) identified by Kraus et al. (2004) as being in the *T. brevicompactum*-type group produced harzianum A, not trichodermin. This culture was separated from the type group in a parsimony tree, but with only modest bootstrap support (69%) (Kraus et al. 2004).

Nielsen et al. (2005) demonstrated the production of alamethicins in extracts of *T. brevicompactum*. Alamethicins are a group of 20-residue polypeptides belonging to the so-called peptaibiotics. Almost 850 individual sequences of linear and 9 of cyclic peptaibiotics are reported to be produced by members of approximately 20 fungal genera. Peptaibiotics are defined as linear or cyclic polypeptide antibiotics which (1) have a molecular weight between 500 and 2,200 Dalton, thus containing 4–21 residues; (2) show a high content of α-aminoisobutyric acid (Aib); (3) are characterized by the presence of other non-proteinogenic amino acids such as isovaline (Iva) and/or lipoamino acids; (4) possess an acylated *N*-terminus, and (5), in the case of the linear compounds, have a *C*-terminal residue that in most of them consists of a free or acetylated amide-bonded 1,2-amino alcohol, but might also be an amine, amide, free amino acid, 2,5-dioxopiperazine, or sugar alcohol. The majority of linear Aib-containing peptides carries a *C*-terminal residue representing a 2-amino alcohol, and this subgroup is therefore referred to as peptaibols. Notably, half of the known peptaibiotics are produced by strains and species of the genus *Hypocrea/Trichoderma* (Degenkolb et al. 2003, 2006a, 2007, 2008a, b; Krause et al. 2006). Peptaibiotics were proposed to contribute to the disruption of the cell walls of fungal pathogens owing to their amphiphilicity and membrane activity (Lorito et al. 1996). Gräfenhan (2006, see also Degenkolb et al. 2006a) reported that cultures of *T. brevicompactum* had unusually high antagonistic activity against the causal agents of two grapevine diseases, Eutypa dieback (*Eutypa lata*) and Esca disease (*Phaeomoniella chlamydospora*, *Phaeoacremonium aleophilum*) when compared to other *Trichoderma* species so far used in biological control (*T. atroviride*, *T. harzianum*, *T. koningii*, and *T. viride*). In an effort to understand the in vitro antagonistic activity against the grape pathogens and, at the same time, to explore for any link between production of peptaibiotics and phylogeny within what they termed 'the *T. brevicompactum* complex,' Degenkolb et al. (2006a) documented the production of peptaibiotics in *T. brevicompactum*. They also showed that the alamethicin F30 patent strain NRRL 3199, originally identified as *T. viride* (Coats et al. 1974; Brückner and Jung 1980; Kirschbaum et al. 2003; Psurek et al. 2006), belonged to the sister clade of the ex-type strain of *T. brevicompactum*. Degenkolb et al. (2006a) found that in general the patterns of peptaibiotics produced in *Trichoderma*/*Hypocrea* are species-specific. The isolates in the type-group of *T. brevicompactum* did not produce trichobrevins while those belonging to its sister clade, including

NRRL 3199, did. Like other members of this clade, NRRL 3199 produced harzianum A. The peptaibiotics of CBS 112445, which was weakly linked to the type group of *T. brevicompactum* (Kraus et al. 2004), were more comparable to those of the type group than to those of the sister group.

Since the appearance of the publications cited above, we have found additional cultures of the morphological species *T. brevicompactum*. DNA sequence analysis showed that these cultures fall into the respective phylogenetic lineages that were seen in the protologue. In the course of our monographic studies of *Trichoderma* and *Hypocrea* we have found additional cultures of *Trichoderma*/*Hypocrea* that are closely related to *T. brevicompactum* s. lat. but that form independent lineages. In the present work, we re-examine the phylogenetic lineages within the morphological species *T. brevicompactum* and the phylogenetic relationships of *T. brevicompactum* and its closest relatives. We continue an examination of the secondary metabolites produced by members of this clade with descriptions of the peptaibiotics, hydrophobins, and small metabolites like trichothecenes, and the significance of these metabolites to taxonomy.

Materials and methods

Chemicals used

Solvents were HPLC grade and all other chemicals analytical grade unless otherwise stated. Water was 18.2 MΩ cm^{-1} purified.

Morphological analyses

The isolates studied are listed in Table 1. Most were obtained from the indicated culture collections. The strain CBS 121320 was isolated as an endophyte from sapwood of a cacao tree (*Theobroma cacao*) following the protocol described by Evans et al. (2003). Cultures of *Hypocrea rodmanii* were obtained by isolating single ascospores from freshly collected specimens on cornmeal-dextrose agar (CMD; cornmeal agar Difco + 2% dextrose).

Material to be used for microscopic measurements was first immersed in 3% KOH. Herbarium specimens of *Hypocrea* collections were rehydrated briefly in 3% KOH. Sections were made with an IEC-CTF microtome cryostat (International Equipment, Needham Heights, Mass.). Measurements and observations of sectioned perithecia were carried out in lactic acid preparations. Measurements of microscopic characters of the anamorph and teleomorph were made from 3% KOH, which was replaced with distilled water, following the protocol of Samuels et al. (2002). Microscopic characters of conidiophores and conidia were taken from CMD or SNA (synthetic low nutrient agar; Nirenberg 1976) within approximately 7 days, mostly using intermittent light (12 h cool white fluorescent lamps, 12 h darkness). Presence of chlamydospores was determined by examining the underside of colonies after 7–10 days on CMD with the 40× objective. Where possible, 30 units of each character were measured, using Scion Image for Windows™ (www.scioncorp.com). Observations were made with differential interference contrast (DIC), phase contrast (PC), and bright field (BF) microscopy. Helicon Focus™ version 4.21.5 Pro(MP) (Helicon Soft, http://HeliconFocus.com) was used to produce some composite images (e.g. Figs. 7o, 8b, 9i and 12c). Color standards are from Kornerup and Wanscher (1978) and are cited as "K&W."

Growth rates were determined on potato-dextrose agar (PDA, Becton, Dickenson, Sparks, Md.) and SNA following Samuels et al. (2002, 2006).

Statistical analysis

For each strain, descriptive statistics (minimum, mean, median, maximum, standard deviation and 95% confidence intervals of the mean) were computed for the morphological data. These are summarized in Table 8 (see later). Metabolite data were coded using categorical scales. Multidimensional scaling (MDS) was performed using standardized data matrices that included either the morphological data, expressed as means for each strain, or the metabolite data, or both. The characters used in the analysis are shown in Tables 7 and 8 (see later). Computation of descriptive statistics was performed using Systat 11 (Systat Software, San José, Calif.). Only strains for which no data were missing were included in the analysis. The MDS had exploratory character only and was aimed at detecting grouping of strains according to the variables measured. The ALSCAL procedure implemented in SPSS 16 (SPSS, Chicago, Ill.) was used for the MDS analysis.

Phylogenetic analysis

The extraction of genomic DNA was performed as reported previously (Dodd et al. 2002). Sixty-six cultures of diverse *Trichoderma* species were used in the phylogenetic analysis (Table 2).

The gene regions studied were RNA polymerase II subunit (*rpb2*), translation elongation factor 1α (*tef1*) and internal transcribed spacers ITS (ITS1, 5.8S, and ITS2) of the nrDNA gene repeat. The primers for *rbp2* amplification were fRPB2-and fRPB2-7cR (Liu et al. 1999). Primers for *Tef1* amplification were Ef728F (Carbone and Kohn 1999) and Tef1R (Samuels et al. 2002). The primers for ITS amplification were ITS5 and ITS4 (White et al. 1990).

Table 1 Members of the Brevicompactum Clade, their provenances, major peptaibiotics, hydrophobins and trichothecene toxins

Strain	Species	Geographic location	Substratum	Peptaibiotics (LC-ESI-MS)[a]	Peptaibiotics (MALDI-TOF-MS)	Hydrophobin biomarkers[c]	Trichothecene
CBS 113214 = F000527	*T. arundinaceum* (received as *Hypocrea* sp.)	Korea: Daejeon	Soil	n.d.	n.d.	n.d.	Harzianum A
CBS 119573 = IBT 40837	*T. arundinaceum*	Iran: Khormabad, Alshter	Soil	n.d.	n.d.	n.d.	Harzianum A
CBS 119574 = IBT 40836	*T. arundinaceum*	Iran: Khormabad	Soil	n.d.	n.d.	n.d.	Harzianum A
CBS 119575 = IBT 40842 (ex-type)	*T. arundinaceum*	Iran: Hamadan	Soil	ALM F50/F30, TBV, TCP, TFR-A	ALM, TBV, TFR	5605, 7126, 7172, 7225, 8649, 9651	Harzianum A
CBS 119576 = ATCC 90237 = IBT 9471	*T. arundinaceum* (received as *T. harzianum*)	Namibia: Windhoek	Micaceous clay from stream bed	TBV-B, TBV-A, ALM, TCP, TFR, traces of TCT-B	ALM, TFR, TBV	5605, 7197, 7231, 7256, 8644, 9649	Harzianum A
CBS 119577 = IBT 40863	*T. arundinaceum*	Iran: Shar-e Kord, Chahar Mahall va Bakhtiari	Soil	TBV-A, ALM F30, TBV-B, TCP, TFR-A	n.d.	n.d.	Harzianum A
CBS 119578 = IBT 40864	*T. arundinaceum*	Iran: Hamadan	Soil	n.d.	n.d.	n.d.	Harzianum A
CBS 121153 = G.J.S. 90-2	*T. arundinaceum*	USA: Miss.	Soil in soy bean field	ALM F30/F50, TBV-B, TBV-A, TCP, TFR-A	n.d.	n.d.	Harzianum A
NRRL 3199	*T. arundinaceum* (received as *T. viride*)	Not available. Patent strain (Coats et al. 1974)	Not available	ALM F30, TBV-B, TBV-A, TCP, TFR [b]	ALM, TBV	5602, 7143, 7165, 7201, 8648, 9653	Harzianum A
CBS 109720 = DAOM 231232 = IBT 40866 (ex-type)	*T. brevicompactum*	USA: Geneva, N.Y.	Soil under *Helianthus annuus*	ALM F30, TCT-A, TCT-B, TCP	TCT-A, TCT-B, ALM	6658, 6879, 6943, 7118, 7289, 7319, 8755, 9499, 9567	Trichodermin
CBS 112443 = IBT 40867	*T. brevicompactum*	Papua New Guinea: Kuriva Forest	Rhizosphere soil with *Glycosmis sapindoiodes*	n.d.	n.d.	n.d.	Trichodermin
CBS 112444 = IBT 40861	*T. brevicompactum*	St Vincent and the Grenadines: Union Island	Soil, maize field	ALM F30, TCP, TCT-A, TCT-B, TFR-A	TCT-A, TCT-B, ALM	6952, 7112, 7140, 7294, 8761, 9302, 9378, 9576, 10003	Trichodermin
CBS 112446 = IBT 40862	*T. brevicompactum*	India: Trivandrum	Soil in backyard	ALM F30/F50, TCP, TCT-A, TCT-B, TFR	TCT-A, TCT-B, ALM	6945, 6981, 7103, 9367, 9575	Trichodermin
CBS 112447	*T. brevicompactum*	México: Distrito Federal	Soil	ALM F30/F50, TCP, TCT-A, TCT-B, TFR	TCT-A, TCT-B, ALM	5598, 7107, 8813, 9382, 9585	Trichodermin
CBS 112945	*T. brevicompactum*	Not available	Not available	n.d.	n.d.	n.d.	n.d.
CBS 119569 = IBT 40839	*T. brevicompactum*	Iran: Aligoodarz	Soil	ALM F30, TCT-A, TCP	n.d.	n.d.	Trichodermin
CBS 119570 = IBT 40840	*T. brevicompactum*	Iran: Doroud	Soil	ALM F30, TCT-A, TCP	n.d.	n.d.	Trichodermin
CBS 119571 = IBT 40838	*T. brevicompactum*	Iran: Qazvin	Soil	n.d.	n.d.	n.d.	Trichodermin
CBS 119572 = IBT 40865	*T. brevicompactum*	Iran: Khoran Abad	Soil	n.d.	n.d.	n.d.	Trichodermin

CBS 121154 = G.J.S. 05–355	*T. brevicompactum*	Cameroon: Bokito	Soil under *Theobroma cacao*	ALM F30/F50, TCP, TCT-A, TBV-A, TBV-B (the latter two in trace amounts)	TCT-A, ALM	6950, 7115, 7288, 7449, 8750, 8777, 9275, 9300, 9355, 9564	Trichodermin
IBT 40841 = G.J.S. 05–176	*T. brevicompactum*	Iran: Alshter	Soil	n.d.	n.d.	n.d.	Trichodermin
MA 4103 = G.J.S. 04–380	*T. brevicompactum*	USA: N.Y.	Soil with *Cucurbita maxima*	n.d.	n.d.	n.d.	n.d.
CBS 121320 = DIS 119f (ex-type)	*T. protrudens*	India: Kerala	*Theobroma cacao,* trunk endophyte	TBV-B, TBV-A, ALMF30/F50, TCP, TFR	ALM, TBV-A, TBV-B, TFR	5570, 6895, 7191, 7252, 7278, 7665, 8741, 9235, 9619	Harzianum A
CBS 120895 = G.J.S. 91-88 (ex-type)	*Hypocrea rodmanii*	USA: Va.	Branchlets	HCP, HRC, TKO	HRC, TKO	7348, 7375, 7561	None detected
CBS 109719 = G.J.S. 91-91	*Hypocrea rodmanii*	USA: Va.	Decorticated wood	HCP, HRC, TKO	n.d.	n.d.	None detected
CBS 120897 = G.J.S. 91-89	*Hypocrea rodmanii*	USA: Va.	Bark	n.d.	n.d.	n.d.	None detected
CBS 112554 = BBA 72294	*T. turrialbense*	Costa Rica: Turrialba	Soil	ALM F30/F50, TCT-C, TCT-D,TCP, TFR-A, TBV-A, TBV-B (the latter two in small amounts)	TCT-C, TCT-D, ALM	7094, 7115, 7298, 8819, 9310, 9555, 10060	Harzianum A
CBS 112445 = IBT 40868	*T. turrialbense*	Costa Rica: Turrialba	Soil	ALM F30, TCT-A, TCT-B, TCP	TCT-A, TCT-B, ALM	7091, 7112, 7267, 8748, 9142, 9302, 9546	Harzianum A, traces of trichodermin

[a] *ALM F30/F50* Alamethicin F30/F50, *TCP* trichocompactin, *TBV-A* trichobrevin A, *TBV-B* trichobrevin B, *TCT-A* trichocryptin A, *TCT-B* trichocryptin B, *TCT-C* trichocryptin C, *TCT-D* trichocryptin D, *TFR* trichoferin, *HCP* hypocompactin, *HRC* hyporodicin, *TKO* trichokonin, *n.d.* not done, i. e. those strains have not been analyzed for peptaibiotics and hydrophobins

[b] For a complete list of ALMs F30/F50 produced by *Trichoderma arundinaceum* NRRL 3199 see Kirschbaum et al. (2003). Further truncated peptaibiotics from *Trichoderma arundinaceum* NRRL 3199 were listed by Psurek et al. (2006)

[c] MALDI TOF mass data have mass accuracy of 0.1%

Table 2 Isolates and GenBank accession numbers

Isolate	Species	*tef1*	*rpb2*	ITS
CBS 119573	*T. arundinaceum*	EU338280	EU338308	AY154943
NRRL 3199	*T. arundinaceum*	EU338279	EU338307	EU330932
CBS 121153	*T. arundinaceum*	EU338278	EU338306	EU330931
CBS 119577	*T. arundinaceum*	EU338277	EU338305	AY154921
CBS 119578	*T. arundinaceum*	EU338276	EU338304	AY154921
CBS 119575 T	*T. arundinaceum*	EU338275	EU338303	AY154921
CBS 119574	*T. arundinaceum*	EU338274	EU338302	AY154921
ATCC 90237	*T. arundinaceum*	EU338291	EU338326	DQ080074
CBS 1132314	*T. arundinaceum*	EU596602		EU596603
CBS 109720 T	*T. brevicompactum*	EU338299	EU338317	AY324173/AY324183
CBS 112443	*T. brevicompactum*	EU338281	EU338319	AY324174/AY324183
CBS 121154	*T. brevicompactum*	EU338283	EU338310	EU338330
CBS 119570	*T. brevicompactum*	EU338298	EU338316	AY154920
CBS 119569	*T. brevicompactum*	EU338297	EU338315	AY154920
CBS 112444	*T. brevicompactum*	EU338296	EU338314	AY324173/AY324183
CBS 119572	*T. brevicompactum*	EU338295	EU338313	EU330937
G.J.S. 04–380 = MA 4103	*T. brevicompactum*	EU338292	EU338309	EU330935
IBT 40841	*T. brevicompactum*	EU338294	EU338312	AY154920
CBS 119571	*T. brevicompactum*	EU338293	EU338311	AY154920
CBS 112446	*T. brevicompactum*	EU338273	EU338301	AY324173/AY324183
CBS 112447	*T. brevicompactum*	EU338300	EU338318	EU330942
CBS 114249	*H. candida*	AY737742	AY391899	AY737757
CBS 114232	*H. catoptron*	AY737726	AY391900	AY737766
CBS 114245	*H. ceracea*	AY937437	AF545508	EU330953
CBS 114576	*H. ceramica*	AY737738	AF545510	AY737764
G.J.S. 90–97 = IMI 352471	*H. cf. rufa VE*	DQ307530	EU341808	DQ315449
G.J.S. 98-1	*H. chlorospora*	AY737737	AY391906	AY737762
G.J.S. 94-67	*H. chromosperma*	AY737728	AY391912	AY737774
G.J.S. 97-237	*H. cinnamomea*	AY737732	AY391920	AY737759
DAOM 139758	*H. citrinoviride*	EU338334	EU338338	EU330960
P.C. 21	*H. costaricensis*	AY737741	AY391921	AY737754
CBS 111146	*H. cremea*	AY737736	AF545511	AY737760
CBS 111148	*H. cuneispora*	AY737727	AF545512	AY737763
CBS 119053	*H. dingleyae*	AF348117	EU341803	DQ313151
CBS 119089	*H. dorotheae*	DQ307536	EU248602	DQ313144
CBS 111147	*H. estonica*	AY737733	AF545514	AY737767
G.J.S. 02-78	*H. intricata*	EU248630	EU241505	EU264002
G.J.S. 90-22 = IMI 393966	*H. lixii*	AF443933	AY391925	AF443915
CBS 102037	*H. lutea*	AY737731	AY489662	AY737773
CBS 114236	*H. melanomagna*	AY737751	AY391926	AY737770
CBS 114330	*H. nigrovirens*	AY737744	AF545518	AY737777
CBS 115283	*H. pezizoides*	AY937438	EU248608	DQ000632
CBS 114071	*H. phyllostachydis*	AY737745	AF545513	EU330959
CBS 814.68	*H. pilulifera*	AY737747	AF545519	Z48813
CBS 121320 = DIS 119fT	*T. protrudens*	EU338289	EU338322	EU330946
HY 8	*H. psychrophila*	AY737752	AF545520	EU330957
G.J.S. 89–120	*H. rodmanii*	EU338285	EU338323	EU330947
CBS 120895	*H. rodmanii*	EU338286	EU338324	EU330948
CBS 109719	*H. rodmanii*	EU338290	EU338325	EU330949
DAOM 167636	*H. semiorbis*	AY737750	AF545522	AY737758
CBS 112888	*H. stilbohypoxyli*	AY376062	EU341805	AY380915
CBS 114248	*H. straminea*	AY737746	AY391945	AY737765
G.J.S. 85–228	*H. sulawesensis*	AY737730	AY391954	AY737753
CBS 111145	*H. surrotunda*	AY737734	AF545540	AY737769
CBS 114234	*H. thailandica*	AY737748	AY391957	AY737772
CBS 114237	*H. thelephoricola*	AY737735	AY391958	AY737776

Table 2 (continued)

Isolate	Species	*tef1*	*rpb2*	ITS
CBS 112445	*T. turrialbense*	EU338284	EU338321	AY324173/AY324183
BBA 72294	*T. turrialbense*	EU338282	EU338320	EU330944
G.J.S. 99–130	*H. victoriensis*	EU338331	EU338336	EU330952
PC 278	*H. virescentiflava*	AY737749	AY391059	AY737768
DAOM 100525	*T. aggressivum*	AF348095	AF545541	AF057600
G.J.S. 90–7	*T. asperellum*	EU338333	EU338337	EU330956
CBS 142.95	*T. atroviride*	AF456891	EU341801	AF456917
DAOM 167161	*T. fertile*	AY750881	AF545546	DQ083018
DAOM 167652	*T. flavofuscum*	AY750891	AF545547	EU330955
DAOM 167057	*T. hamatum*	AY750893	AF545548	Z48816
CBS 988.97	*T. koningii*	DQ289007	EU248600	DQ323409
DAOM 222105	*T. koningiopsis*	AY376042	EU341810	AY380901
DAOM 166989	*T. longibrachiatum*	EU338335	EU338339	EU330961
DAOM 167069	*T. minutisporum*	AY750883	EU341809	DQ083015
DAOM 167085	*T. oblongisporum*	AY750884	AY545551	DQ083020
DAOM 166162	*T. pubescens*	AY750887	AF545552	DQ083016
G.J.S. 03–74	*T. scalesiae*	DQ841726	EU252007	DQ841742
DAOM 183974	*T. spirale*	AY750890	AF545553	DQ083014
DAOM 166121	*T. erinaceus*	DQ109547	EU248604	DQ109534
DAOM 166121	*T. strigosum*	AF487668	AF545556	AF487657
G.J.S. 00–108	*T. stromaticum*	AY937436	EU341807	DQ083013
DAOM 178713A	*T. tomentosum*	AY750882	AF545557	DQ085432
G.J.S. 01–287	*T. virens*	AY750894	EU341804	DQ083023
CBS 101526	*T. viride*	AY376053	EU248599	X93979
CBS 438.95	*T. viride*	DQ307522	EU341806	DQ315438
CBS 333.72	*T. viridescens*	DQ307523	EU341802	DQ315441
G.J.S. 74–83	*H. lutea*	EU338287	EU338327	EU330950
G.J.S. 85–26	*H. lutea*	EU338288	EU338328	EU330951
DIS 219C	*Trichoderma sp.*	EU338332	EU338329	EU330954

PCR amplifications were performed in a solution that contained: 2.5µl of 10X PCR Buffer (New England Biolab, Ipswich, Mass.) with $MgCl_2$ to a final concentration of 1.5 mM, 0.2 mM dNTPs, 0.2 µM of forward and reverse primers, 1.25 units of Taq Polymerase (New England Biolab), and 10–50 ng of genomic DNA and double-distilled water for a total volume to 25µl per reaction. The reactions were placed in a PTC-200 MJ Research thermocycler (Waltham, Mass.) using a touchdown program (Don et al. 1991). The touchdown PCR was initiated with a 2-min denaturation at 94°C followed by an initial 15 cycles of PCR amplification. The annealing temperature in the first amplification cycle was 65°C, which was reduced 1°C per cycle over the next 15 cycles. An additional 35 cycles were performed, each consisting of 30-s denaturation at 94°C, 30-s annealing at 48°C and 1-min extension at 72°C concluding with 10-min extension at 72°C. The resulting products were purified with ExoSAP-it kit (USB, Cleveland, Ohio) using the manufacturer's protocol. The purified amplicons were sequenced directly using the BigDye Terminator v3.1 chemistry in a 16 capillary automated DNA sequencer (ABI 3100; Applied Biosystems, Foster City, Calif.). For each locus, both strands were sequenced using the primers used in producing the amplicons. In the case of *rpb2*, two additional internal primers RPB-432F (5'-ATGATCAACAGAGGYATGGA) and RPB-450R (5′-TCCATRCCTCTGTTTGATCAT) were used in sequencing reactions. Sequences were edited and assembled using Sequencher 4.1 (Gene Codes, Madison, Wis.). Clustal X 1.81 (Thompson et al. 1997) was used to align the sequences; the alignment was adjusted manually with McClade version 3.06 software (Maddison and Maddison 2005).

Sequence analyses To determine the phylogenetic position of the Brevicompactum clade, the sequence alignment of the three gene sections for 66 isolates of *Trichoderma* species (Table 2) was analysed with maximum parsimony (MP), neighbour-joining (NJ) and Bayesian inference (BI). The MP analysis was carried out with PAUP* version b10 (Swofford 2002) using a heuristic search, with a starting tree obtained via 1000 random stepwise addition sequences, tree-bisection-reconnection as the branch-swapping algorithm, and MULTREES on. PAUP* was also used to

construct NJ trees, with a distance set to Kimura 2-parameter model. Bootstrap values for MP and NJ trees were calculated from 1,000 replicates. Two members of *Trichoderma* sect. *Longibrachiatum* were used as outgroup species. GenBank accession numbers are given in Table 2.

MrBayes 3.0 b4 (Huelsenbeck 2000; Huelsenbeck et al. 2001) was used to reconstruct phylogenetic trees based on the Bayesian approach (Mau et al. 1999; Rannala and Yang 1996). The Bayesian analysis used a different model of evolution for each of the three loci (ITS, *tef1*, *rpb2*). The models of DNA substitution for *rpb2* and *tef1* were determined previously (Chaverri and Samuels 2003; Chaverri et al. 2005) with Modeltest 3.6 (Posada and Crandall 1998). The parameters estimated for ITS by Modeltest were: general time reversible (GTR + I + G, nst = 6) model with gamma distributions and invariable sites; base frequencies = 0.2082, 0.3400, 0.2485; rates (Rmat) = 1.7117, 2.4357, 2.0885, 0.6750, 4.7081; gamma shape = 0.7900; proportion invariable sites (pinvar) = 0.6037. Four chains and 5,000,000 Markov chain-Monte Carlo generations were run, and the current tree was saved to a file every 100 generations. Stability of likelihood scores was confirmed with the software TRACER version 1.2.1 (Rambaut and Drummond 2004), which traces the parameter against the generation number. Once stability was reached both in terms of likelihood scores and parameter estimation, the first 5,000 trees were discarded (as burn-in).

Topological incongruence for the trees based on individual genes was examined with a reciprocal 70% bootstrap (BP) or a 95% posterior probability (PP) threshold (Mason-Gamer and Kellogg 1996; Reeb et al. 2004) to determine whether the sequences from the three genes should be combined in a single analysis. Bootstrap values were generated with neighbour joining (NJ) with 1,000 replicates and a maximum likelihood distance. Posterior probabilities were calculated with Bayesian analysis in MrBayes. A conflict was assumed to be significant if two relationships for the same taxa, one being monophyletic and the other non-monophyletic, both with BP = 70% and PP = 95%, were observed on each ITS, *tef1* and *rpb2* majority-rule consensus trees. The three partitions could be combined if no significant conflicts were detected.

The culture G.J.S. 85-26 (*H. lutea*) was used as an outgroup because this species was shown to be the closest to the Brevicompactum clade.

Secondary metabolites

Peptaibiotics: HPLC-ESI-Ion-Trap-Mass spectroscopy

Cultivation of strains All subcultures and main cultures used for peptaibiomics were grown at room temperature (23–26°C) under ambient daylight on PDA (Difco, Becton Dickinson, Heidelberg, Germany). Peptaibiotics studied are listed in Tables 1, 3, 4, 5, 6 and 7.

Subcultures were grown on PDA for 4 days and used for inoculation of the main culture.

Extraction After 6 days cultivation, fungal cultures were extracted with a mixture of 1:1 (*v/v*) CH_2Cl_2:MeOH, evaporated in vacuo, and cleaned over Sep-Pak C_{18} cartridges as described by Krause et al. (2006).

HPLC-UV-ESI-Ion-Trap- MS measurements

Analyses were performed on an Agilent 1100 HPLC equipped with Kromasil KR100 column, (150 mm × 4.6 mm i. d., 3.5 µm) held at 35°C. The UV detector was set at 205 nm (Krause et al. 2006; Degenkolb et al. 2006a, b).

Online HPLC/ESI-MS was performed on a LCQ ion trap MS (Thermo Finnigan MAT, San José, Calif.) using Excalibur v.1.2 software. Sequence analysis was carried out in the positive ESI mode in centroid mode with an accuracy of ± *m/z* 0.5. A collision induced dissociation (CID) energy of 0% was used for scanning molecular masses ($[M+H]^+$/$[M+Na]^+$) and fragments resulting from cleavage of the extremely labile Aib-Pro bond. CID energies of 45% and 65% were used for generating series of characteristic "in-source"-fragment ions. The collision energy for MS^n experiments was set between 25 and 65 V, depending on the precursor ion, typically at 45 V. Fragment ion series were assigned in accordance with the previously used nomenclature. In cases where the isomeric amino acids Leu/Ile or Val/Iva (Iva, isovaline) could not be distinguished, the abbreviations Lxx and Vxx were used instead (Krause et al. 2006; Degenkolb et al. 2006a, b).

Detection of DL-Alaol by GC/MS measurements For GC/MS measurements, a GC-A17 coupled to a QP-5000 MS (Shimadzu, Kyoto) was used. The instrument was equipped with a Chirasil-L-Val (i.e., *N*-propionyl-L-valine-*tert*-butylamide polysiloxane) capillary column, 25 m × 0.25 mm i.d. (Varian-Chrompack, Darmstadt). Helium was used as the carrier gas. EI mass spectra were recorded at 70 eV. A subfraction of 1 mg of the methanolic extract, also used for HPLC and LC/MS measurements, was dried under a cold stream of N_2 and hydrolyzed in a ReactiVial with 6 N HCl at 110°C for 18 h. The chirality of Alaol was determined after derivatization of the dried hydrolysate with *N*-pentafluoropropionic anhydride (PFPAA) by GC/MS in SIM mode at *m/z* 190−191. *N*-pentafluoropropionyl derivatives of L-Alaol and DL-Alaol were used as standard samples (Küsters and Portmann 1994). The following

Table 3 Peptaibiotic patterns of strains from the *Trichoderma brevicompactum* complex (excluding *Hypocra rodmanii*)

Species	Strain	Peptaibiotics: molecular weight					
		ALM	TCP	TCT-A	TCT-B	TBV	TFR
Trichoderma brevicompactum	CBS 109720 = IBT 40866 = DAOM 231232 (ex-type)	1964 [**1**][a] 1,978 [**2**, **3**], 1992 [**4**]	726 [5, 6]; 740 [**7**, 8]; 754 [**9**, 10]	1125 [19, **20**, **21**]; 1139 [22, **23**]	1210 [11, 12]; 1224 [13, **14**]; 1238 [15, **16**]; 1252 [17, **18**]	n.d.	n.d.
	CBS 119569 = IBT 40839	1964 [**1**], 1,978 [**2**, **3**], 1992 [**4**]	726 [5]; 740 [**7**, **8**] 754 [9, 10]	1153 [24, 25]; 1167 [26, **27**, 28]; 1181 [29, 30]	n.d.	n.d.	n.d.
	CBS 119570 = IBT 40840	1964 [**1**], 1,978 [**2**, **3**], 1992 [**4**]	726 [5]; 740 [7, **8**]; 754 [9, 10]	1153 [24, 25]; 1167 [26, **27**, 28]; 1181 [29, 30]	n.d.	n.d.	n.d.
	CBS 112444 = IBT 40861	1964 [**1**], 1,978 [**2**, **3**], 1992 [**4**]	740 [**7**, **8**]; 754 [9, 10]	1111 [80, 81]; 1125 [**20**, **21**]; 1139 [**23**]; 1153 [82]	1210 [11]; 1,224 [13, 14]; 1238 [**16**, 83, 84, 85]; 1252 [**17**, **18**]	n.d.	1207 [**64**]
	CBS 112446 = IBT 40862	1963 [**76**], 1964 [**1**], 1977 [77], 1978 [**2**, **3**], 1992 [**4**]	740 [7, **8**]; 754 [9, 10]	1111 [80, 81]; 1125 [20, 21]; 1139 [**23**]	1210 [11]; 1224 [13, 14]; 1238 [**16**, 83, 84, 85]; 1252 [**17**, **18**]	n.d.	1207 [**64**]; 1193 [**66**, **67**, 68]
	CBS 112447	1963 [**76**], 1964 [**1**], 1977 [**77**], 1978 [**2**, **3**], 1992 [**4**]	740 [7, 8]; 754 [9, 10]	1111 [80, 81]; 1125 [20, 21]; 1139 [**23**]; 1153 [25]	1210 [11]; 1224 [13, 14]; 1238 [**16**, 83, 84, 85]; 1252 [17, 18]	n.d.	1207 [**64**], 1193 [**66**, **67**, 68]
	CBS 121154 = G.J.S. 05–355	1963 [**76**]; 1977 [77]; 1977 [78]; 1991 [79]; 1950 [31]; 1964 [**1**], 1978 [**2**, **3**], 1992 [**4**]	726 [5]; 740 [7, 8]; 754 [9, 10]	1125 [86, 87, 88, 89]; 1139 [**90**]; 1153 [**91**]	n.d.	1127 [52]; 1141 [53, 54]; 1157 [61, 62] (in trace amounts)	1207 [**64**]; 1193 [**66**, 68]
Trichoderma turrialbense	CBS 112445 = IBT 40868 (ex-type)	1950 [31]; 1964 [**1**], 1978 [**2**, **3**], 1992 [**4**]	726 [5, 6]; 740 [7, 8]; 754 [9, **10**]	1139 [22, **23**]; 1153 [24, **25**]; 1167 [26, **27**, 28]	1224 [13, 14]; 1238 [**15**, **16**]; 1252 [17, 18]; 1266 [**33**, **34**, 35, 36]; 1280 [37, 38]	n.d.	n.d.
	CBS 122554 = BBA 72294	1963 [**76**]; 1977 [77]; 1977 [78]; 1991 [79]; 1964 [**1**], 1978 [**2**, **3**], 1992 [**4**]	740 [7, **8**]; 754 [9, 10]	1097 [92]; 1111 [93]; 1125 [**94**]	1196 [95]; 1210 [96, 97]; 1224 [**98**, **99**, **100**, **101**]; 1238 [102, 103]	1127 [52]; 1,141 [53]; 1157 [62]	1207 [64]
Trichoderma arundinaceum	CBS 119575 = IBT 40842 = G. J.S. 05–180 (ex-type)	1963 [**76**]; 1977 [**77**]; 1977 [**78**]; 1991 [79]; 1964 [**1**], 1978 [**2**, **3**], 1992 [**4**]	740 [7, 8]; 776 [9, 10]; 770 [**39**]	n.d.	n.d.	1127 [50-52]; 1143 [58, 59]; 1141 [**53**, **54**]; 1157 [60, 61, **62**]	1207 [64]
	CBS 119576 = ATCC 90237 = IBT 9471	1964 [**1**], 1978 [**2**, **3**], 1992 [**4**, 63]	726 [5, 6]; 740 [7, 8]; 756 [**10**]; 770 [39, 41]; 784 [42, 43]	n.d.	1238 [15, 16]; 1252 [17, 18]; 1266 [33–36] (in trace amounts)	1099 [44–47]; 1113 [48, 49]; 1127 [50–52]; 1141 [53, 54]; 1129 [55–57]; 1143 [58, 59]; 1157 [60–62]	1207 [64]

Table 3 (continued)

Species	Strain	Peptaibiotics: molecular weight					
		ALM	TCP	TCT-A	TCT-B	TBV	TFR
	NRRL 3199	1964 [**1**], 1978 [**2**, **3**], 1992 [**4**]	740 [70]; 754 [71, 72]; 756 [73]; 770 [74, 75]	n.d.	n.d.	1099 [44–47]; 1113 [48, 49]; 1127 [50–52]; 1141 [53, 54]; 1129 [55–57]; 1143 [58, 59]; 1157 [60–62]	1207 [64]; 1193 [66–69]
	CBS 119577 = IBT 40863	1964 [**1**], 1978 [**2**, **3**], 1992 [**4**]	726 [5, 6]; 740 [7, 8]; 754 [9, 10]	n.d.	n.d.	1099 [44–47]; 1113 [48, 49]; 1127 [50–52]; 1141 [53, 54]; 1129 [55–57]; 1143 [58, 59]; 1157 [60–62]	1207 [64]
	CBS 121153 = G.J.S. 90–2	1963 [**76**]; 1977 [77]; 1977 [**78**]; 1991 [79]; 1964 [**1**], 1978 [**2**, **3**], 1992 [**4**]	754 [10]; 770 [**39**, **41**]	n.d.	n.d.	1113 [48, 49]; 1127 [52]; 1141 [53, 54]; 1129 [57]; 1143 [58, 59]; 1157 [60–62]	1207 [64]
Trichoderma protrudens	CBS 121320 = DIS 119f (ex-type)	1963 [**76**]; 1977 [77]; 1977 [**78**]; 1991 [79]; 1964 [**1**], 1978 [**2**, **3**], 1992 [**4**]	754 [10]; 770 [**39**, **41**]	n.d.	n.d.	1113 [48, 49]; 1127 [52]; 1141 [53, 54]; 1129 [**57**]; 1143 [**58**, **59**]; 1157 [60, **61**, **62**]; 1171 [104–106]	1207 [**64**]; 1193 [65, 66, 68]

[a] Consecutive numbering for recurrent sequences from [1]–[75] is adopted from Degenkolb et al. (2006a); new compounds are listed in ascending order from [76] on. Numbers in bold indicate major compounds in the HPLC elution profiles produced by an individual strain
ALM F30/F50 Alamethicin F30/F50, *TCP* trichocompactin, *TBV* trichobrevin A and B, *TCT-A* trichocryptin A, *TCT-B* trichocryptin B, *TFR* trichoferin, *n.d.* not detected. For ALMs, TCPs, and TFRs, the predominant $[M+H]^+$ ions are listed; for TCTs and TBVs, the predominant $[M+Na]^+$ ions

modified temperature program was used for GC separation: injector and interface temperature, 250°C each; initial temperature, 65°C, 4 min hold; 3°C/min until reaching 100°C, 3.5 min hold; 40°C/min until reaching 190°C, 5 min hold. The pressure program was as follows: initial pressure 3.2 kPa, 4 min hold; 0.2 kPa/ min until reaching 7 kPa, 3 min hold. The split ratio was set 30:1.

Peptaibiotics: MALDI-TOF analysis

Growth conditions Cultures were routinely grown at 25°C on malt extract (Oxoid, Wesel, Germany) agar plates and prepared on day 6 in the sporulation phase. Peptaibiotics from MALDI-TOF MS analysis are summarized in Table 1.

Extraction and preparation of mycelium for MALDI-TOF analysis A few µg of mycelium were directly spotted onto target wells of a 100-position sample plate and immediately mixed with 1 µl of matrix solution [10 mg/ml dihydroxybenzoic acid (DHB, from Anagnostec, Golm, Germany) in acetonitrile / methanol / water (1: 1:1, *v/v*) and 0.3% trifluoroacetic acid]. The sample matrix mixture was allowed to air-dry prior to analysis.

MS analysis by MALDI-TOF MS

Low-molecular mass peptides were measured on a VOYAGER DE-PRO - time of flight mass spectrometer from Applied Biosystems using a nitrogen laser beam ($\lambda = 337$ nm), with the MS in the delayed extraction mode, allowing the determination of monoisotopic mass values. A low mass gate of 800 Da improved the measurement by filtering out the most intensive matrix ions. The mass spectrometer was used in the positive ion detection and reflector mode.

Table 4 Sequences of new 11- and 12-residue peptaibiotics of different strains from the *Trichoderma brevicompactum* complex (excluding *Hypocrea rodmanii*)

Peptaibiotic[a]	Molecular weight ([M+Na]$^+$)		Residue											
			1	2	3	4	5	6	7	8	9	10	11	12
TCT-A_VIa [80]	1111	Ac	Vxx	Aib	Pro	Vxx	Aib	Pro	Aib	Vxx	Aib	Pro	Lxxol	
TCT-A_VIb [81]	1111	Ac	Lxx	Aib	Pro	Vxx	Aib	Pro	Aib	Aib	Aib	Pro	Lxxol	
TCT-A_IIIc [82]	1153	Ac	Lxx	Aib	Pro	Lxx	Aib	Pro	Lxx	Aib	Aib	Pro	Lxxol	
TCT-B_IIIc [83]	1238	Ac	Lxx	Aib	Pro	Vxx	Vxx	Aib	Pro	Aib	Lxx	Aib	Pro	Lxxol
TCT-B_IIId [84]	1238	Ac	Vxx	Aib	Pro	Vxx	Lxx	Aib	Pro	Aib	Lxx	Aib	Pro	Lxxol
TCT-B_IIIe [85]	1238	Ac	Lxx	Aib	Pro	Vxx	Lxx	Aib	Pro	Aib	Vxx	Aib	Pro	Lxxol
TCT-A_Ic [86]	1125	Ac	Vxx	Aib	Pro	Lxx	Aib	Pro	Lxx	Aib	Aib	Pro	Vxxol	
TCT-A_Id [87]	1125	Ac	Lxx	Aib	Pro	Lxx	Aib	Pro	Lxx	Aib	Aib	Pro	Aibol	
TCT-A_Ie [88]	1125	Ac	Vxx	Aib	Pro	Lxx	Aib	Pro	Lxx	Aib	Aib	Pro	Vxxol	
TCT-A_1f [89]	1125	Ac	Lxx	Aib	Pro	Lxx	Aib	Pro	Vxx	Aib	Aib	Pro	Vxxol	
TCT-A_IIc [90]	1139	Ac	Lxx	Aib	Pro	Lxx	Aib	Pro	Lxx	Aib	Aib	Pro	Vxxol	
TCT-A_IIIc [91]	1153	Ac	Lxx	Aib	Pro	Lxx	Aib	Pro	Lxx	Aib	Aib	Pro	Lxxol	
TCT-C_Ia [92]	1097	Ac	Vxx	Aib	Pro	Vxx	Aib	Pro	Lxx	Vxx	Aib	Pro	Alaol	
TCT-C_IIa [93]	1111	Ac	Vxx	Aib	Pro	Vxx	Aib	Pro	Lxx	Lxx	Aib	Pro	Alaol	
TCT-C_IIIa [94]	1125	Ac	Lxx	Aib	Pro	Vxx	Aib	Pro	Lxx	Lxx	Aib	Pro	Alaol	
TCT-D_Ia [95]	1196	Ac	Vxx	Aib	Pro	Vxx	Vxx	Aib	Pro	Lxx	Vxx	Aib	Pro	Alaol
TCT-D_IIa [96]	1210	Ac	Vxx	Aib	Pro	Vxx	Vxx	Aib	Pro	Lxx	Lxx	Aib	Pro	Alaol
TCT-D_IIb [97]	1210	Ac	Lxx	Aib	Pro	Vxx	Vxx	Aib	Pro	Lxx	Vxx	Aib	Pro	Alaol
TCT-D_IIIa [98]	1224	Ac	Lxx	Aib	Pro	Vxx	Vxx	Aib	Pro	Lxx	Lxx	Aib	Pro	Alaol
TCT-D_IIIb [99]	1224	Ac	Vxx	Aib	Pro	Vxx	Lxx	Aib	Pro	Lxx	Lxx	Aib	Pro	Alaol
TCT-D_IIIc [100]	1224	Ac	Lxx	Aib	Pro	Vxx	Vxx	Aib	Pro	Lxx	Lxx	Aib	Pro	Alaol
TCT-D_IIId [101]	1224	Ac	Lxx	Aib	Pro	Vxx	Vxx	Aib	Pro	Lxx	Lxx	Aib	Pro	Alaol
TCT-D_IVa [102]	1238	Ac	Lxx	Aib	Pro	Vxx	Lxx	Aib	Pro	Lxx	Lxx	Aib	Pro	Alaol
TCT-D_IVb [103]	1238	Ac	Lxx	Aib	Pro	Vxx	Lxx	Aib	Pro	Lxx	Lxx	Aib	Pro	Alaol
TBV-B_IVa [104]	1171	Ac	Aib	Ser	Lxx	Lxx	Aib	Pro	Lxx	Lxx	Aib	Pro	Lxxol	
TBV-B_IVb [105]	1171	Ac	Aib	Ser	Lxx	Lxx	Aib	Pro	Lxx	Lxx	Aib	Pro	Lxxol	
TBV-B_IVc [106]	1171	Ac	Aib	Ser	Lxx	Lxx	Aib	Pro	Lxx	Lxx	Aib	Pro	Lxxol	

[a] The *N*-terminal sequences AcVxx-Aib and AcLxx-Aib were tentatively assigned from sequence homologies with those trichocryptins/trichobrevins previously reported by Degenkolb et al (2006a)

Characterization by MALDI-TOF MS analysis was performed on the same MALDI instrument in linear delayed extraction mode using an acceleration voltage of 20 kV and a low mass gate of 1,500 Da. Spectra for individual specimens were compiled, averaging results from at least 100 shots taken across the width of the specimen for *m/z* 2,000–20,000.

Mycotoxin and secondary metabolite profiling

Cultivation and extraction Liquid cultivations were performed in 25-ml Blue cap bottles containing 4 ml potato-dextrose broth (Difco) for 10 days in darkness. Cultures were extracted over night using 15 ml ethyl acetate, which was then evaporated in vacuo and redissolved in 500µl acetonitrile /water (2:1, v/v) and filtered through a 0.45-µm PTFE syringe filter (Nielsen et al. 2005). Plate cultures were grown on oatmeal agar and PDA (Difco) for 10 days in darkness at 25°C, and a 0.6-cm^2 agar culture was cut out and transferred to a 2-ml vial along with the 10-cm^2 culture mat which was scraped off using a scalpel. The sample was ultrasonicated with 0.75 ml acetonitrile for 1 h, and filtered through a 0.45-µm PTFE syringe filter.

HPLC-DAD-ESI-TOF-MS Analysis was performed on an Agilent 1100 system equipped with a photo diode array detector (DAD), and a Luna C_{18} II column (Phenomenex, Torrance, Calif.) and coupled to a LCT orthogonal time-of-flight MS (Waters-Micromass, Manchester, UK), with a Z-spray ESI source and a LockSpray probe (Nielsen et al. 2005).

Samples were analyzed in positive ESI$^+$ and ESI$^-$ using a water-acetonitrile gradient system starting from either 5% acetonitrile, which was increased linearly to 100% in 23 min holding for 5 min, or 15% acetonitrile, which was increased linearly to 100% in 20 min holding for 5 min (Nielsen et al. 2005). In both ESI$^+$ and ESI$^-$ two scan functions (1 s each) were used: the first with a potential

Table 5 Sequences of new 7-residue hypocompactins (HCP), of 14-residue hypocrodicins (HRC), and 19-residue trichokonins (TKO) produced by *Hypocrea rodmanii*

Peptaibiotic	Residue																		
	(MW)[a]	1	2	3	4	5	6	7	8	9	10	11	12	13	14	15	16	17	18	19
HCP-I [107]	738	[125][b]	Gly	Ala	Lxx	Aib	Gly	Lxx	Lxxol											
HCP-II [108]	752	[125][b]	Gly	Ala	Lxx	Vxx	Gly	Lxx	Lxxol											
HCP-III [109]	766	[125][b]	[182]c	Vxx	Lxx	Aib	Gly	Lxx	Lxxol											
HCP-IV [110]	780	[125][b]	[182][c]	Vxx	Lxx	Vxx	Gly	Lxx	Lxxol											
HCP-V [111]	814			[329][d]	Lxx	Aib	Gly	Lxx	Lxxol											
HCP-VI [112]	828			[329][d]	Lxx	Vxx	Gly	Lxx	Lxxol											
HRC-A [113]	1437	Ac	Aib	Gln	Vxx	Aib	Pro	Vxx	Vxx	Aib	Pro	Aib	Lxx	Aib	Pro	Lxxol				
HRC-B [114]	1451	Ac	Aib	Gln	Lxx	Aib	Pro	Vxx	Vxx	Aib	Pro	Aib	Lxx	Aib	Pro	Lxxol				
HRC-C [115]	1465	Ac	Aib	Gln	Lxx	Aib	Pro	Vxx	Lxx	Aib	Pro	Aib	Lxx	Aib	Pro	Lxxol				
HRC-D [116]	1380	Ac	Aib	Gly	Lxx	Aib	Pro	Vxx	Vxx	Aib	Pro	Aib	Lxx	Aib	Pro	Lxxol				
HRC-E [117]	1394	Ac	Aib	Ala	Lxx	Aib	Pro	Vxx	Vxx	Aib	Pro	Aib	Lxx	Aib	Pro	Lxxol				
TKO-V [118]	1866	Ac	Aib	Ala	Aib	Ala	Aib	Gln	Aib	Vxx	Aib	Gly	Lxx	Aib	Pro	Vxx	Aib	Aib	Gln	Gln	Pheol
TKO [119]	1880	Ac	Aib	Aib	Ala	Ala	Aib	Gln	Aib	Vxx	Aib	Gly	Lxx	Aib	Pro	Vxx	Aib	Vxx	Gln	Gln	Pheol

[a] Molecular weight (MW) refers to the $[M+H]^+$ ions in the case of HCPs and TKOs, but to $[M+Na]^+$ in the case of HRCs

[b] Tentatively assigned as C_8 fatty acid residue (*n*-octenoyl or homologue), according to structural homologies. See text for details

[c] Tentatively assigned as Gly residue

[d] Only partial sequences can be given because of low abundance of *N*-terminal fragment ions

difference of 14 V between the skimmers scanning *m/z* 100 to 900, the second with 40 V between the skimmers scanning *m/z* 100–2,200.

Data analysis was performed as described previously (Nielsen et al. 2005). Unknown peaks were matched against an internal reference standard database (~730 compounds) as well as the 33,557 compounds in Antibase 2007 (Laatsch 2007).

Results

For ease of discussion, the new names that will be introduced below are used in this and the "Discussion" sections.

Phylogeny

To position *T. brevicompactum* and its relatives within *Trichoderma*, we sequenced parts of three genes *tef1*, *rpb2,* and ITS (Fig. 1). The alignment of three loci included a total of 2,369 characters in the analyses (848 for *rpb2*, 837 for *tef1*, 684 for ITS), including insertions and deletions. Ambiguously-aligned regions were manually excluded from the analyses (356 characters). In the maximum parsimony analyses, the consistency and homoplasy indices for the combined dataset were, respectively, 0.333 and 0.667. Of the included characters, *rpb2* provided the most parsimony informative characters (34%), followed by ITS (20.8%), and *tef1* (19.4%); *tef1* provided the least informative characters, in part because most of the ambiguously-aligned characters were in the large intron of *tef1*.

The reciprocal 70% BP and 95% PP thresholds for individual loci show that the topologies of the three genes are congruent (results not shown) and therefore the partitions were combined in a single tree (Fig. 1). Figure 1 represents a Bayesian phylogram with the best log likelihood (LnL = −22,426.97). Bootstrap results from the MP and NJ analyses are indicated in Fig. 2 but trees are not shown. The results of all BI, MP, and NJ analyses show high BP and PP values for the clade that includes *T. brevicompactum, T. protrudens, T. turrialbense, T. arundinaceum*, and *H. rodmanii*, hereafter the Brevicompactum clade. These five species received high bootstrap support in parsimony analysis and high posterior probabilities in Bayesian analysis.

Results of the phylogenetic analyses reveal high BP and PP for previously described clades/lineages (Kindermann et al. 1998; Chaverri and Samuels 2003; Samuels 2006; International Subcommission on *Trichoderma* and *Hypocrea* Taxonomy: http://www.isth.info/biodiversity/index.php). The Brevicompactum clade is distinct from other known lineages and thus represents a separate lineage

Table 6 Structural variations of peptaibiotics from the *Trichoderma brevicompactum* complex (excluding *H. rodmanii*)

Peptaibiotic	Residue																			
		1	2	3	4	5	6	7	8	9	10	11	12	13	14	15	16	17	18	19	20
ALM F30	Ac	Aib	Pro	Aib	Ala	Aib	Ala	Gln Glu	Aib	Aib Vxx Lxx	Aib	Gly	Vxx Lxx	Aib	Pro	Vxx	Aib	Aib	Glu	Gln	Pheol
ALM F50	Ac	Aib	Pro	Aib	Ala Aib	Aib	Ala Aib	Gln	Aib	Vxx	Aib	Gly	Lxx	Aib	Pro	Vxx	Aib	Aib	Gln	Gln	Pheol
TCP	Oc	Gly	Ala	Lxx	Aib Vxx	Gly Ala Ser	Vxx Lxx	Lxxol													
TBV	Ac	Aib	Ala Ser	Aib Vxx	Aib Vxx Lxx	Aib	Pro	Lxx	Lxx	Aib	Pro	Alaol Aibol Vxxol Lxxol									
TCT-A	Ac	Vxx Lxx	Aib	Pro	Vxx Lxx	Aib	Pro	Aib Vxx Lxx	Aib Vxx Lxx	Aib	Pro	Lxxol									
TCT-B	Ac	Vxx Lxx	Aib	Pro	Vxx	Vxx Lxx	Aib	Pro	Aib Lxx	Aib Vxx Lxx	Aib	Pro	Lxxol								
TCT-C	Ac	Vxx Lxx	Aib	Pro	Vxx	Aib	Pro	Lxx	Vxx Lxx	Aib	Pro	Alaol									
TCT-D	Ac	Vxx Lxx	Aib	Pro	Vxx	Vxx Lxx	Aib	Pro	Lxx	Vxx Lxx	Aib	Pro	Alaol								
TFR	MDA	Pro	AHMOD Desmethyl-AHMOD	Ala	Aib	Aib Vxx	Aib Vxx Lxx	Gly Ala Aib	Aib	Aib	AAE AMAE										

ALM Alamethicin (F30: acidic, F50: neutral), *TCP* trichocompactin, *TBV* trichobrevin, *TCT* trichocryptin (subfamilies A–D), *TFR* trichoferin, *Oc* n-octanoy,; *MDA* 2-methyldecanoic acid, *AHMOD* 2-amino-4-methyl-6-hydroxy-8-oxo-decanoic acid, *AMAE* 2-[(2′-aminopropyl)-methylamino]-ethanol, *AAE* 2-(2′-aminopropyl)amino-ethanol

Table 7 Peptaibiotics, mycotoxins and hydrophobins

Number	Pseudomolecular ion ($[M+H]^+$or $[M+Na]^+$) of peptaibiotics and hydrophobins[a]
I. ALAMETHECINS (ALM)	
1	1964
2	1978
3	1978
4	1992
31	1950
76	1963
77	1977
78	1977
79	1991
II. TRICHOCOMPACTIN (TCP)	
5	726
6	726
7	740
8	740
9	754
10	754
40	756
39	770
41	770
42	784
43	784
70	740
71	754
72	754
73	756
74	770
75	770
III. TRI0CHOCRYPTIN-A (TCT-A)	
19	1125
20	1125
21	1125
22	1139
23	1139
24	1153
25	1153
26	1167
27	1167
28	1167
29	1181
30	1181
80	1111
81	1111
82	1153
86	1125
87	1125
88	1125
89	1125
90	1139
91	1153
IV. TRI0CHOCRYPTIN-B (TCT-B)	
11	1210
12	1210
13	1224
14	1224
15	1238
16	1238
17	1252
18	1252
33	1266
34	1266
35	1266
36	1266
83	1238
84	1238
85	1238
V. TRICHOCRYPTIN-C (11-residue peptaibols with C-terminal Alaol) (TCT-C)	
92	1097
93	1111
94	1125
VI. TRICHOCRYPTIN-D (12-residue peptaibols with C-terminal Alaol) TCT-D	
95	1196
96	1210
97	1210
98	1224
99	1224
100	1224
101	1224
102	1238
103	1238
VII. TRICHOBREVIN (TBV)	
44	1099
45	1099
46	1099
47	1099
48	1113
49	1113
50	1127
51	1127
52	1127
53	1141
54	1141
55	1129
56	1129
57	1129
58	1143
59	1143
60	1157
61	1157
62	1157
104	1171
105	1171
106	1171
VIII. TRICHOFERIN (TFR)	
64	1207
65	1193
66	1193
67	1193

Table 7 (continued)

Number	Pseudomolecular ion ([M+H]$^+$or [M+Na]$^+$) of peptaibiotics and hydrophobins[a]
68	1193
69	1193
IX. HYPOCOMPACTIN (HPC)	
107	738
108	752
109	766
110	780
111	714
112	728
X. HYPORODICIN (HRC)	
113	1437
114	1451
115	1465
116	1380
117	1394
XI. TRICHOKONIN ((TKO)	
118	1866
119	1880
HYDROPHOBIN BIOMARKERS (HPH)	
300	6658
301	6879
302	6943
303	7118
304	7289
305	7319
306	8755
307	9499
308	9567
TRICHOTHECENES	
400	Trichodermin TDERMIN)
401	Harzianum A (HARZ_A)

Consecutive numbering from 1 to 75 according to Degenkolb et al. 2006a
[a] For details, see text

within *Trichoderma*/*Hypocrea*, as was suggested by Kraus et al. (2004) for the single species *T. brevicompactum*.

Because of low bootstrap support (Fig. 1), the Brevicompactum clade is in an unresolved polytomy with *H. victoriensis* and the Viride, Minutisporum, Megalocitrina, and Lutea Clades. However, based on branch length the closest relative to the Brevicompactum clade is the Lutea clade (Fig. 1).

For convenience, we included only representative cultures of members of the Brevicompactum clade in Fig. 1. In order to clarify the interrelationships of members of the Brevicompactum clade, we analyzed all 28 isolates that we know belong in that clade in our subsequent analyses (Fig. 2a–d) (the 29th, CBS 113214, was received too late to include in the phylogenetic analysis). We adopted the phylogenetic species recognition of Dettman et al. (2003). Briefly a clade is recognized as an independent evolutionary lineage if it satisfies either of two criteria: (1) genealogical concordance: the clade is present in the majority of the single-locus trees; or (2) genealogical nonconcordance: the clade is well supported in at least one single-locus tree and is not contradicted in any other single-locus tree at the same level of support. We sequenced three unlinked loci: *tef1* (Fig. 2b), *rpb2* (Fig. 2c), and ITS (Fig. 2c). The properties of the data set for each gene and the combined multi locus sequence (MLS; Fig. 2a) are given in Table 2. In this second analysis, the sequences varied strikingly in their variability; *tef1* had the highest number of parsimony informative characters (144 out of 596 or 24%) followed by *rpb2* (14.6%) and ITS (2.2%).

Figure 2a represents a Bayesian inference majority-rule consensus tree based on MLS. This tree shows a strongly supported Brevicompactum clade (9) that is divided into two sister subclades: *Hypocrea rodmanii* (7) and the Brevicompactum complex (8), each of which was highly supported in the combined data set and in the individual gene trees based on *tef1* and *rpb2* (Fig. 2b,c). The *T. brevicompactum* complex was divided further into a polytomy comprising three main clades: 1 (*T. brevicompactum*, *T. turrialbense*), 2 (*T. arundinaceum*), and the single culture CBS 121320 (*T. protrudens*). Subclades 1 and 2 were also highly supported in the individual gene trees (Fig. 2b,c). The *T. brevicompactum* clade (3) again showed two supported subclades (4, 5); the ex-type culture of *T. brevicompactum* (CBS 109720) is in subclade 4. Subclade 4 did not have support in the *rbp2* tree (Fig. 2c) but subclade 5 received strong support in both of the individual gene trees (Fig. 2b,c). The two members of subclade 5 (CBS 112446, CBS 112447) differed by only one allele despite their widely divergent geographic origins (India and Mexico). There was no support for taxonomic separation of clade 3 from morphology, secondary metabolites or biogeography.

The two isolates of node 6 (*T. turrialbense*) originated from the same area in Costa Rica. This clade is highly supported in MLS, *tef1* and *rpb2*. Despite a strong sister relationship with *T. brevicompactum* s. str. (clade 1), it differs from *T. brevicompactum* in producing harzianum A and in subtle morphological characters (Table 8).

The other large clade (clade 2, *T. arundinaceum*) consisted of 8 isolates. This clade had high support in the MLS, *tef1* and *rpb2* trees. Despite their diverse geographic origins, their sequences were highly homogenous. Such a high homogeneity among isolates of one species having such diverse origin is uncommon in *Trichoderma*.

Trichoderma protrudens, which was found as an endophyte in sapwood of *Theobroma cacao* in India, had strong sister relationship to clades 1 and 2 in MLS (Fig. 2a) and the single gene trees (Fig. 2b,c). The ITS sequence for this isolate differed from *T. brevicompactum* and *T. turrialbense* by a 1-bp insertion.

The three isolates of *Hypocrea rodmanii* (clade 7) were collected in the Mid Atlantic states (Maryland and Virginia)

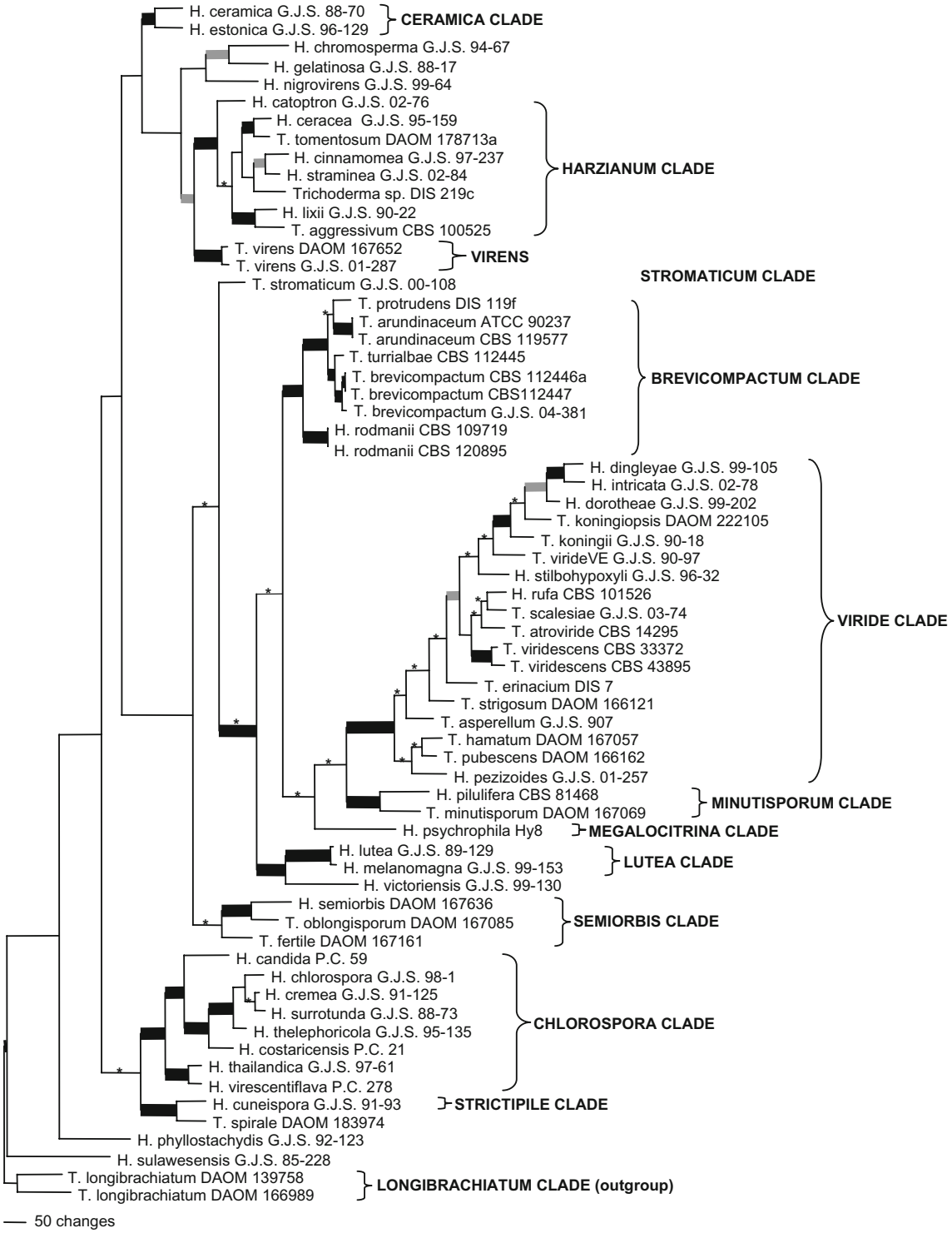

Fig. 1 Bayesian phylogram of combined ITS, *tef1*, and *rpb2* sequence data. The tree presented had the best log likelihood (LnL=−22,426.97) in the Bayesian analysis. *Thick black lines* represent nodes with posterior probability >90%, and Parsimony and Neighbour-Joining bootstraps >70%. *Thick gray lines* represent nodes with posterior probability >90%, Neighbor-Joining bootstrap >70%, and Parsimony bootstrap <70%. Nodes with *asterisks* (*) represent clades with posterior probabilities >90%. Clade/lineage names based in part on: Samuels 2006; Chaverri and Samuels 2003; and ISTH (http://www.isth.info/biodiversity/index.php)

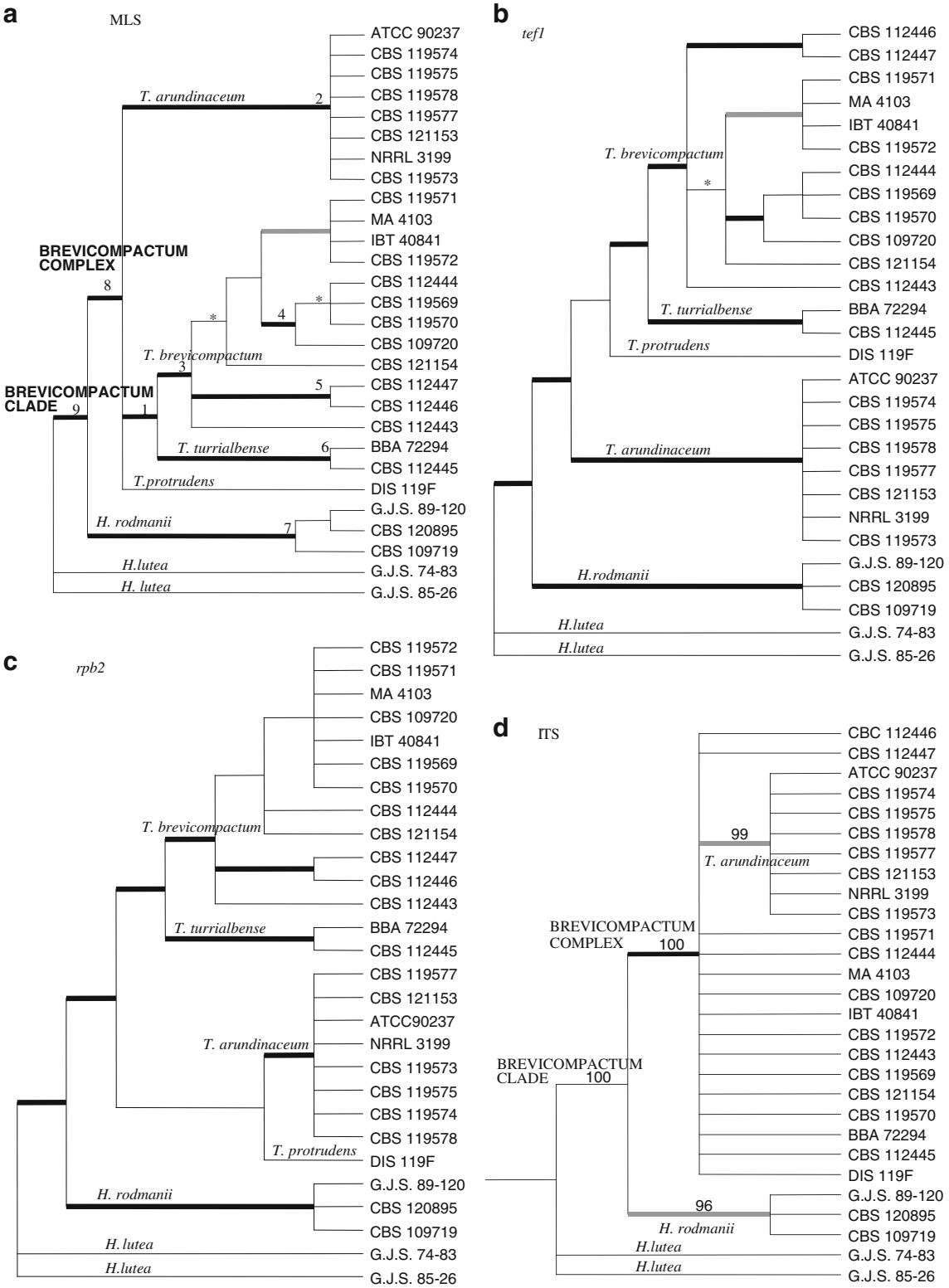

Fig. 2 Majority-rule (50%) consensus tree resulting from Bayesian analysis of **a** combined 3-gene, **b** *tef1,* **c** *rpb2* and **d** ITS dataset. Branches with *thick black lines* represent clades with posterior probability (PP) ≥ 0.95 and bootstrap Maximum parsimony (BS-MP) and Bootstrap Neighbour-Joining (BS-NJ) values ≥ 70%. *Thick gray lines* represent clades with PP ≥ 0.95 and BS-MP or BS-NJ or both < 70%. *Asterisks* (*) represent clades with PP ≥0.90. *Numbers* on nodes correspond with node numbers used in the text

Table 8 Continuous characters of morphology and colony

Character		Taxa				
		Trichoderma arundinaceum	*Trichoderma brevicompactum*	*Trichoderma protrudens*	*Hypocrea rodmanii*	*Trichoderma turrialbense*
Dominant distribution		Cosmopolitan, temperate and tropical	Cosmopolitan, temperate and tropical	India: Kerala	USA: MD, VA	Costa Rica
Conidia length (μm)		(2.2)2.7–3.5(5.0)	(2.2)2.7–3.0(3.7)	(2.5)2.7–3.2(3.5)	(1.7)2.0–2.5(2.7)	(2.2)2.5–3.0(3.2)
95% CI		3.1–3.2	2.9–3.0	2.9–3.0	2.2–2.3	2.7–2.8
		n=270	*n*=330.	*n*=30	*n*=60	
Width (μm)		(1.7)2.5–3.0(3.5)	(2.0)2.2–2.7(3.0)	(2.2)2.5–2.7(3.0)	(1.7)2.0–2.2(2.5)	(2.0)2.2–2.7(3.0)
95% CI		2.6–2.7	2.5–2.6	2.5–2.7	2.0–2.1	2.5–2.6
		n =270	*n*=330	*n*=30	*n*=60	*n*=60
L/W		(0.9−)1.0−1.4(−1.7)	(0.9)1.1–1.3(1.4)	(1.0)1.0–1.3(1.5)	(0.9)1.0–1.2(1.4)	(0.8)1.0–1.1(1.5)
95% CI		1.16–1.20	1.16–1.19	1.1–1.2	1.07–1.12	1.06–1.10
		n = 270	*n*=330	*n*=30	*n*=60	*n*=60
Phialides length (μm)		(3.7)4.5–7.0(12.7)	(3.7)4.7–6.7(15.0)	(4.0)5.5–9.0(12.0)	(3.0)4.0–5.5(7.0)	(3.7)4.5–6.7(12.0)
95% CI		5.5–5.7	5.6–5.9	6.7–8.0	4.5–4.9	5.3–5.9
		n=270	*n*=330	*n*=30	*n*=60	*n*=60
Max. width (μm)		(2.0)3.0–4.0(4.5)	(2.5)3.0–3.7(4.5)	(2.2)2.5–3.0(3.2)	(2.5)2.7–3.2(3.7)	(2.5)2.7–3.7(4.2)
95% CI		3.4–3.5	3.3–3.4	2.7–3.0	2.9–3.1	3.1–3.3
		n=270	*n*=330	*n*=30	*n*=60	*n*=60
Base (μm)		(1.2)2.0–3.0(3.7)	(1.3)2.0–2.7(3.7)	(1.5)1.7–2.7(3.2)	(1.0)1.5–2.2(2.5)	(1.5)2.0–2.7(3.7)
95% CI		2.5–2.6	2.4–2.5	2.1–2.3	1.7–2.0	2.3–2.5
		n=270	*n*=330	*n*=60	*n*=30	*n*=60
Length/width		(1.1)1.2–2.2(5.2)	(1.1)1.3–2.2(5.1)	(1.4)1.8–3.4(5.0)	(1.0)1.3–1.7(2.4)	(1.2)1.3–2.3(4.3)
95% CI		1.6–1.8	1.7–1.8	2.4–2.9	1.5–1.7	1.7–1.9
		n=270	*n*=330	*n*=30	*n*=60	*n*=60
Width of supporting cell (μm)		(2.0)3.0–4.2(6.0)	(1.7)2.7–4.0(5.7)	(2.2)2.5–3.0(3.2)	(2.2)3.0–4.0(4.5)	(2.0)2.5–3.5(4.2)
95% CI		3.5–3.6	3.3–3.5	2.6–2.8	3.3–3.5	3.0–3.3
		n=270	*n*=330	*n*=30	*n*=60	*n*=60
Ratio phialide length/width of supporting cell		(0.8)1.1–2.3(6.5)	(1.0)1.3–2.3(4.8)	(1.5)2.0–3.5(6.5)	(0.8)1.1–1.7(2.5)	(0.9)1,2–2.6(6.0)
95% CI		1.6–1.7	1.7–1.8	2.5−3.0	1.4–1.5	1.7–2.1
		n=270	*n*=330	*n*=30	*n*=60	*n*=60
Ratio phialide width/width of supporting cell		(0.5)0.8–1.2(1.6)	(0.6)0.8–1.2(1.7)	(0.7)0.9–1.3(1.4)	(0.6)0.7–1.1(1.4)	(0.6)0.9–1.3(1.8)
95% CI		0.97–1.01	1.0–1.1	1.0–1.1	0.9–1.0	1.0–1.1
		n=270	*n*=330	*n*=30	*n* - 60	*n*=60
Colony radius PDA 72 H (mm)						
15°C	Range	2–6	0–6	1–3	3–7	0–5
	Mean	5	2		6	3
	SD	1	2		2	2
	n	7	11	1	2	2
	CI	4–5	2–3		5–8	1–5
20°C	Range	9–37	14–39	17–28	29–33	21–36
	Mean	32	30		31	25
	SD	7	7		2	6
	n	7	11		2	2
	CI	29–35	27–33	20–36	29–32	
25°C	Range	32–48	30–50	30–38	31–40	35–45
	Mean	41	42		35	40
	SD	4	5		4	4
	n	7	11	1	2	2
	CI	39–45	40–44		32–39	40–44

Table 8 (continued)

Character		Taxa				
		Trichoderma arundinaceum	*Trichoderma brevicompactum*	*Trichoderma protrudens*	*Hypocrea rodmanii*	*Trichoderma turrialbense*
Dominant distribution		Cosmopolitan, temperate and tropical	Cosmopolitan, temperate and tropical	India: Kerala	USA: MD, VA	Costa Rica
30°C	Range	40–69	36–60	52–58	35–42	44–63
	Mean	54	52		37	56
	SD	7	6		3	7
	n	7	11	1	2	2
	CI	51–57	50–54		36–42	50–54
37°C	Range	0–18	0–30	23−45	0	3–38
	Mean	8	7			11
	SD	7	10			15
	n	7	11	1	2	2
	CI	6–12	4–10			4–10
Colony radius SNA 72 H (mm)						
15°C	Range	1–8	0–5	5–7	2–4	2–5
	Mean	4	1.5		3	2
	SD	2	2		1	1.5
	n	7	11	1	2	3
	CI	–5	1–2		2–4	13–21
20°C	Range	0–39	12–34	19–29	10–19	21–38
	Mean	30	24		17	26
	SD	5	5		4	7
	n	7	11	1	2	2
	CI	27–32	22–26			20–35
	CI					
25°C	Range	32–48	19–48	30–41	13–28	38–50
	Mean	41	35		22	44
	SD	4	11		5	4
	n	7	1	1	2	2
	CI	39–43	33–37		16–27	40–48
30°C	Range	40–55	20–56	39–47	7–26	54–59
	Mean	47	41		19	56
	SD	5	9		7	2
	n	7	11	1	2	2
		45–50	38–45		11–26	54–59
37°C	Range	0–22	0–25	16–27	0	1–45
	Mean	7	5			14
	SD	5	7			19
	n	7	11	1	2	2
	CI	5–9	2–7			0–25
Temperature of first appearance of green conidia on PDA grown in intermittent light						
		20−25°C	25(−30)°C	30°C	20−25°C	20−25°C

and formed a highly supported clade (7) in MLS, *tef1* and *rpb2* that was sister to the Brevicompactum complex. In the ITS tree (Fig. 2d), this clade received strong support in Bayesian analysis, but its bootstrap support was low (Fig. 2d).

In brief, phylogenetically, *T. brevicompactum* (Fig. 2a, clade 3), *T. arundinaceum* (Fig. 2a, clade 2), *T. turrialbense* (Fig. 2a, clade 6), *T. protrudens* (Fig. 2a) and *H. rodmanii* (Fig. 2a, clade 7) have support in the majority (2/3) of the three individual gene trees and thus meet the genealogical concordance criteria of Dettman et al. (2003) for recognizing species. *Trichoderma protrudens* was consistently independent of all other lineages in all of the analyses. ITS sequences were able to discriminate unequivocally *H. rodmanii* and *T. arundinaceum*; but *T. brevicompactum*, *T. turrialbense,* and *T. protrudens* were indistinguishable by ITS. The present work confirms the reidentification as *T.*

arundinaceum of three *Trichoderma/Hypocrea* strains that have been reported in the peptaibiotic or mycotoxin literature. Culture NRRL 3199 is cited as *T. viride* in U.S. Patent 3833723 (Coats et al. 1974) for production of alamethicin and has become the standard source for alamethicins (e.g., Kirschbaum et al. 2003). Culture ATCC 90237 was reported in the literature, as *T. harzianum,* as the original source of harzianum A (Corley et al. 1994). Culture CBS 113214, a soil isolate, was reported by Lee et al. (2005, as F000527) as a likely new *Hypocrea* sp. that produces harzianum A.

Peptaibiotics

Peptaibiotics: HPLC-ESI-Ion-Trap-MS

General Remarks The patterns of peptaibiotics produced by *T. brevicompactum* CBS 109720, CBS 119569, CBS 119570, *T. arundinaceum* CBS 119576, CBS 119577, NRRL 3199 and *T. turrialbense* CBS 112445 (as *T.* cf. *brevicompactum*) were investigated earlier (Degenkolb et al. 2006a). To maintain conformity and to prevent confusion about the identity of recurrent sequences mentioned throughout the text and in tables, we adopt the consecutive numbering of peptaibiotics from **1** to **75** previously introduced by Degenkolb et al. (2006a). Consequently, numbering of additional, mostly new sequences proceeds consecutively from substance **76–119**. The peptaibiotics pattern of the above seven strains is shown in Table 3. New sequences of peptaibiotics detected in the *Trichoderma* strains (excluding *T./H. rodmanii*) are listed in Table 4, sequences of peptaibiotics from *T./H. rodmanii* in Table 5, and general sequences ("building schemes") of peptaibiotics found in the Brevicompactum clade are listed in Table 6. All strains of *T. brevicompactum*, *T. arundinaceum*, *T. turrialbense*, and *T. protrudens* listed in Table 1 produced a number of 20-residue peptaibols, alamethicins (ALMs), as major components. The alamethicins, which are the most thoroughly investigated peptaibols, were recently reviewed (Leitgeb et al. 2007).

Peptaibiomics of Trichoderma brevicompactum Some intraspecific variation among the ALM profiles was observed. ALMs F30 [**1–4**] were produced by four strains, whereas the remaining three strains produced a mixture of the acidic ALMs F30 and the neutral ALMs F50/5, F50/6a, F50/7, and F50/8b [**76–79**]. It appears, however, that in cases where both subgroups of ALMs were produced, ALMs F30 dominated over ALMs F50. These results confirm the observation of Kirschbaum et al. (2003) who described a time-dependent formation of ALM subgroups by *T. arundinaceum* NRRL 3199. The latter produced the neutral ALM F50 (Gln^{18}-Gln^{19}) at the beginning of the fermentation; after about 5 d the ALM F50 concentration decreased whereas the concentration of the acidic ALM F30 (Glu^{18}-Gln^{19}) increased.

The second most abundant group were the 11-residue trichocryptins A [**19–30**, **80**, **81**, **86–91**]. They represent deletion sequences of the 12-residue trichocryptins B [**11–18**, **83–85**], lacking the amino acid residue in position 5, which is either Lxx or Vxx. Again, there is intraspecific variation in the pattern of trichocryptins produced. The trichocryptins A are found in every investigated strain but chain length varied, depending on the amino acids in the exchange position 1, 4, 7, and 8. The trichocryptins B display the same building scheme as trichcryptins A but carry an additional Vxx residue in position 4. Variable amino acids are therefore located in position 1, 5, 8, and 9.

Trichoferins (TFR) are a group of minor, 10-residue lipoaminopeptides produced by four of the seven strains. The major component, TFR A [**64**], is produced by each of the four trichoferin-positive strains, but there is some intraspecific variation in the pattern of the four minor homologues, TFR C-E [**66–68**]. Notably, trace amounts of trichobrevins [**52–54**, **61**, **62**] were found in CBS 121154 but not in any of the other six strains. The pattern of peptaibiotics produced by that strain is less complex than in any other *T. brevicompactum* strain investigated.

Peptaibiomics of Trichoderma turrialbense Trichoderma turrialbense is distinguished from *T. brevicompactum* mainly by the production of different trichothecenes as pointed out above. Like *T. brevicompactum*, *T. turrialbense* produces ALMs F30 [**1–4**] as the major group of peptaibiotics, although larger amounts of ALMs F50 [**76–79**] are also present in CBS 122554 but not in CBS 112445. Trichocryptins A [**23–28**] and B [**13–18**, **33–38**] were found in CBS 112445, being the only strain to produce major amounts of trichocryptins B, which display $[M+Na]^+$ ions at *m/z* 1266 [**33–36**] and 1280 [**37**, **38**]. In contrast, *T. turrialbense* CBS 122554 produced four 11-residue trichocryptins C [**92–95**] and eight 12-residue trichocryptins D [**96–103**], the former representing deletion sequences of the latter. As shown in Table 6, both of these novel subgroups exhibit high structural homology with trichocryptins A and B, but they carry an L-alaninol (Alaol) residue at their *C*-terminus. This is the first report to unambiguously prove the presence of L-Alaol as a *C*-terminal constituent of peptaibiotics. Small amounts of trichobrevins A [**52**, **53**] and B [**62**] and trichoferin A [**64**] were also detected in strain CBS 122554. From its pattern of peptaibiotics, the new species *T. turrialbense* is intermediate between *T. brevicompactum* and *T. arundinaceum*.

Peptaibiomics of Trichoderma arundinaceum This includes strain NRRL 3199, a patent strain originally reported as "*T.*

viride" and generally considered to be the classical commercial source of ALMs (Kirschbaum et al. 2003; Leitgeb et al. 2007). The 12-residue trichobrevins (TBV, **44–62**) were recognized as the second most abundant group of peptaibiotics of *T. arundinaceum*. Depending on the strain investigated, TBV B-IIIb [**61**] and B-IIIc [**62**], or A-IVa [**53**] and A-IV-B [**54**] were observed as the predominant compounds. Thus, the common presence of both alamethicins and trichobrevins as the two major groups of peptaibiotics was recognized as the most important feature distinguishing *T. brevicompactum*/*T. turrialbense* from *T. arundinaceum*/*T. protrudens*. Trace amounts of trichocryptins B were also detected in strain CBS 119576.

Peptaibiomics of Trichoderma protrudens The pattern of peptaibiotics produced by CBS 121320 is quantitatively identical to that of all five strains of *T. arundinaceum* studied. CBS 121320 produced three new, positionally isomeric minor compounds, the 11-residue trichobrevins B-IVa [**104–106**], in small, but in somewhat larger amounts than in *T. arundinaceum*, enabling us to sequence them.

Additional minor components, such as 7-residue trichocompactins III b (**10**), Va (**39**), and Vb (**41**), as well as four 10-residue lipoaminopeptides, trichoferins A (**64**), B (**65**), C (**66**), and E (**68**), were found.

Peptaibiomics of Hypocrea rodmanii Hypocrea rodmanii did not produce any of the peptaibiotics typical of the *Trichoderma* species treated above. The most conspicuous difference is the absence of alamethicins F30/F50, trichocryptins, trichobrevins, and trichoferins, which were the distinctive peptaibiotics of *T. brevicompactum*, *T. arundinaceum*, *T. turrialbense* and *T. protrudens*.

Both investigated strains of *Hypocrea rodmanii* produced six new 7-residue lipopeptaibols, named hypocompactins (HCP) I-VI [**107–112**]. Four of them, HCPs I-IV [**107–110**], exhibit homology with four 7-residue lipostrigocins A1-A4 from *T.* cf. *strigosum* CBS 119777 (Degenkolb et al. 2006b) and the 7-residue trichocompactins produced by *T. brevicompactum*, *T. turrialbense*, *T. arundinaceum*, and *T. protrudens*. We assume that the *N*-terminal Gly of hypocompactins I-IV has been blocked by a C_8 mono-unsaturated, branched or non-branched fatty acid, probably *n*-octenoyl. This is based on LC/high-resolution CID-MS data (K.F. Nielsen and T. Degenkolb, unpublished data) and structural homologies with the lipostrigocins, trichogin GA IV from *T. longibrachiatum* M 3431 (Auvin-Guette et al. 1992), and trikoningin KB I from *T. koningii* 903589 (Auvin-Guette et al. 1993), all carrying an *N*-terminal *n*-octanoyl-Aib residue. This assumption is further supported by the presence of a *cis*-4-decenoyl residue bound to Gly in the trichodecenins I and II. The producer of the latter two lipopeptaibols was reported as *T. viride* (Fujita et al. 1994), but neither details of taxonomic identification nor a strain accession number were given. Hypocompactins V and VI [**111**, **112**] could only be sequenced partially because of the very low intensities of the *N*-terminal *b*-type fragment ions. The hypothesis of *N*-terminal *n*-octenoyl-Gly in HCP I-IV leads to the hypothesis that *n*-octanoyl-Gly (Oc-Gly) might be present in the all TCPs, as supported by LC/high-resolution CID-MS data (K.F. Nielsen and T. Degenkolb, unpublished data).

Hypocrea rodmanii CBS 120895 and CBS 109719 produced compounds [**113**–**117**] representing five new 14-residue peptaibols, hyporodicins (HRC) A–E. All of them carry the *C*-terminal octapeptide Vxx-Aib-Pro-Aib-Lxx-Aib-Pro-Lxxol. This *C*-terminus has also been identified in some of the trichobrevins and trichocryptins; and it was first reported for the 14-residue harzianins HC-I and HC-VI from *T. harzianum*, strains M-90361 and M-903603, with Vxx = Val and Lxx = Leu (Rebuffat et al. 1995). The close relationship of the hyporodicins [**113**–**117**], with harzianins HC is further supported by the structure of the *N*-terminal pentapeptide Ac-Aib-Gln-Lxx-Aib-Pro found in [**113**–**115**]: the same sequence with Lxx = Leu has been reported previously for harzianins HC-X, HC-XIII, and HC-XV (Rebuffat et al. 1995).

Two 19-residue peptaibols, the compounds [**118**] and [**119**], were produced. Compound [**118**] exhibited the same fragmentation pattern as trichokonin V (TKO-V) from a fungicolous strain of *T. koningii* that was isolated from a fruiting body of *Ganoderma lucidum* (Huang et al. 1995). Consequently, it could be identical with trichokonin V, or represent a positional isomer. The second trichokonin-like homologue carries a Vxx residue instead of Aib in position 16 of the peptide chain. Thus, compound [**119**] might represent a deletion sequence of trichokonin VII (Huang et al. 1995), as it lacks the Ala residue of the former in position 6. Peptaibols with the same *C*-terminal sequences were described from *T. koningii* LCP984209 (Landreau et al. 2002), a marine strain that was isolated as a contaminant from the cockle *Cerastoderma edule* (Sallenave et al. 1999).

Typing of strains by intact cell MALDI-TOF mass spectrometry (ICMS) and hydrophobins

Sporulating mycelium of strains grown on PDA was subjected on day 6 to intact cell mass spectrometry (ICMS). Patterns in the high mass metabolite range of 1,000 to 2,000 Da and in the low mass proteome region of 4,000 to 12,000 Da were recorded (Tables 1 and 7). The low mass protein region provides molecular ions of hydrophobins, small hydrophobic proteins that are excreted and proteolytically processed. Each spectrum consisted of 3–11 masses

of different intensities, and the mass data were analysed by UPGMA cluster analysis (Pearson Correlation, not shown). The data are grouped into 3 main clusters, *Trichoderma/Hypocrea rodmanii* (CBS 120895), *T.arundinaceum/T. protrudens* (NRRL 3199, CBS 119575, CBS 119576/CBS 121320), and *T. turrialbense* (CBS 122554). A total of 58 different masses were observed. None of the masses recorded for *H. rodmanii* and *T. protrudens* (CBS 121320) were shared by other strains. This supports the conclusion that these isolates represent individual species. *T. arundinaceum* and *T. protrudens* have been grouped by UPGMA cluster analysis or use of the commercial program SARAMIS in one cluster, since the 4 dominant masses and their spacings are fairly similar (CBS 121320 with dominating peaks at m/z 5566, 7188/7249 and 9623, *T. arundinaceum* with corresponding masses of m/z 5605, 7172/7222 and 9650). All *T. arundinaceum* strains share the masses *m/z* 5603, 8648 and 9652, which were not detected in any other strains. These masses can be considered as biomarkers for this species.

More complex is the situation in the *T. brevicompactum/T. turrialbense* cluster. Some of the masses are found in both subclusters, as reflected by the cluster analysis. Inspection of the mass spectra, however, reveals that two of the dominating masses, respectively, in each subcluster are not shared by the other (*m/z* 7092 and 9552 in *T. turrialbense*, *m/z* 6946 and 9572 in *T. brevicompactum*), while two significant masses of the Brevicompactum subcluster are shared as minor peaks in the Turrialbense subcluster (*m/z* 7112, and 8753), and one significant peak (*m/z* 9307) of the Turrialbense subcluster is shared by the Brevicompactum subcluster. Both subclusters share additional minor peaks (*m/z* 7293 and 8815). Analysis of the spectra with the program SARAMIS (Anagnostec) developed for ICMS identification of microbes locates the Turrialbense subcluster within a Brevicompactum cluster. The data suggest that certain hydrophobins may be shared in both subclusters, while others are not. Because hydrophobins are small proteins directly encoded by DNA, identical proteins indicate largely identical gene sequences. Mass data alone do not permit recognition of a species, as we cannot deduce any information on the respective genetic background. Only sequence information on the respective hydrophobins will permit a clear evaluation (Fig. 3).

Mycotoxin and secondary metabolite profilies

Two trichothecene mycotoxins were detected by LC-HRMS in members of the Brevicompactum complex (Table 1), trichodermin and harzianum A. The latter compound was produced by all members of *T. turrialbense, T. protrudens*, and *T. arundinaceum*, whereas *T. brevicompactum* produced trichodermin as previously described (Nielsen et al. 2005). Production of these were 30–100 times higher on PDA than oatmeal agar (OAT).

Besides tricothecenes, several isocoumarins (polyketides) including diaportinol and diaportinic acid (matching authentic reference standards) were detected in shake cultures of *T. turrialbense, T. protrudens*, *T. arundinaceum,* and *T. brevicompactum*.

Trichoderma arundinaceum and *T. protrudens* produced large amounts of an undescribed compound (no likely matches in Antibase 2007), with a $[M-H]^-$ ion of *m/z* 535.1627 and UV max of 200 nm. As this compound did not ionize in ESI^+, it cannot be assigned as a peptide. Notably, it was also observed in *T. brevicompactum* but in 100- to 1,000-fold lower amounts.

All species except *H. rodmanii* produced a unique metabolite with an assumed elementary composition of $C_{10}H_{16}O_4$ ($[M-H]^-$ *m/z* 199.0967 calculated 199.0872 Da, deviation −1.7 ppm) and UV-max 214 nm (no likely matches in Antibase 2007), in ESI^- it displayed a significant loss of CO_2 and showed a $[M-2H + Na]^-$ ion strongly indicating that the molecule contained a carboxylic acid moiety.

Neither trichothecenes nor isocoumarins were detected in *H. rodmanii* (CBS 120895 and CBS 109719), and the only metabolites detected in ESI^+, ESI^-, and UV/VIS were the peptides, which are discussed under Peptaibiomics.

Putative pathways of trichothecene biosynthesis are shown in Fig. 4.

Biogeography

Isolates of *T. brevicompactum* and *T. arundinaceum* are sympatric and probably cosmopolitan. The two known cultures of *T. turrialbense* were collected in Costa Rica, and the only known culture of *T. protrudens* was isolated as an endophyte of the trunk of one *Theobroma cacao* tree in India. *Hypocrea rodmanii* originates from the Mid Atlantic region of the eastern U.S.A. (Maryland, Virginia).

Multidimensional Scaling (MDS)

MDS, a parameter-free data reduction procedure, was performed to detect any grouping of the strains that could be determined by the values of the variables used. Three different analyses were run (Fig. 6).

The first included only morphological data and is presented in Fig. 6a. The stress of the final configuration is 0.1818, which indicates only a moderate fit of the data to the model. While the Brevicompactum and Arundinaceum clades cannot be distinguished based on available morphological and cultural characters, CBS 109719 and CBS 120895 (*H. rodmanii*) form a distinct group, and also CBS 121320 (*T. protrudens*) is clearly distinguishable from all other strains.

The two other analyses were carried out on a subset of cultures for which all metabolite data were available.

When the combined morphological and metabolite characters are used (Fig. 6b), the stress of the final configuration is 0.134 and the MDS performed on the metabolite data alone (Fig. 6c) yields a stress of 0.144, both values slightly better than that obtained with the morphological data alone, but still indicating only a moderate fit of the data to the model. The results of both analyses are very similar and thus confirm the modest contribution of morphological data to the separation of the clades. The scatterplot produced by the MDS with both morphological and metabolite data (Fig. 6b) reveals that isolates tend to group together according to their taxonomy. The major groups (*H. rodmanii*, *T. brevicompactum*, *T. arundinaceum*, and *T. protrudens*) are confirmed, although the separation is not complete. *Hypocrea rodmanii* is separated from all other strains and *Trichoderma protrudens* clusters closer to *T. arundinaceum,* thus reinforcing its phylogenetic similarity of the two species. The two *T. turrialbense* cultures, on the other hand, are widely separated from each other and cluster with *T. brevicompactum* and *T. arundinaceum*. The difference between the two strains of *T. turrialbense* may be explained by differences in trichocryptins C and D. The isolate CBS 121154, *T. brevicompactum* from Cameroon, occupies an intermediate position between *T. arundinaceum*, *T. brevicompactum*, and isolate CBS 122554 of *T. turrialbense* because of its production of trichobrevins [**61**] and [**62**], and trichocompactins [**86–91**].

Species delimitation

The cultures of *H. rodmanii* were derived from isolated single ascospores. Two cultures (CBS 120897, CBS 122581) were not included in the phylogenetic analysis but are undoubtedly representative of this species. Macro-

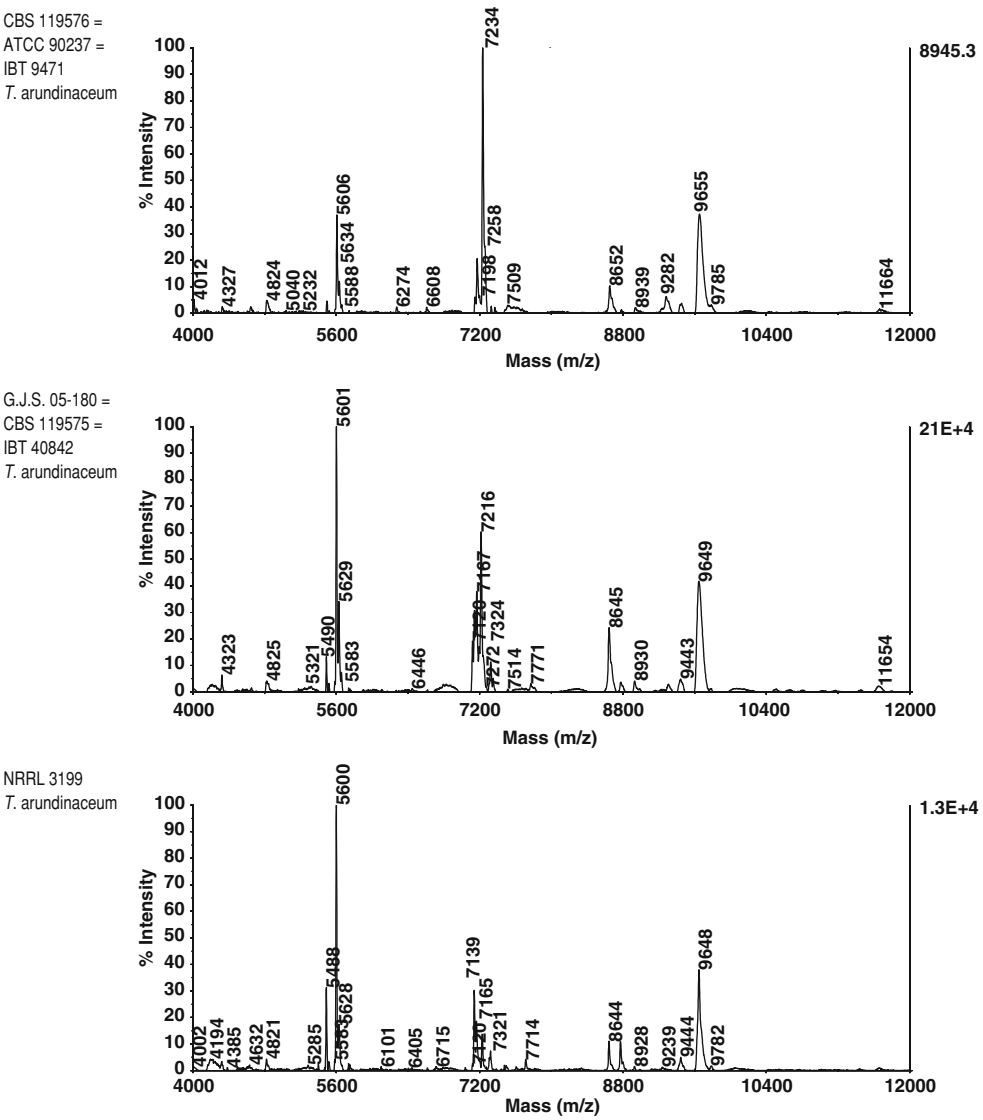

Fig. 3 Intact cell MALDI-TOF mass spectra showing the fingerprint region. One of duplicate or triplicate spectra is shown

and microanatomy of stromata (Figs. 7j-o and 11a-e) are unremarkable in the genus. Ascospores are typical of *Hypocrea* in being hyaline and finely spinulose; the part-ascospores are dimorphic (Fig. 11h, i). There is very little of the stroma morphology or anatomy to distinguish it from other species that have luteous stromata, such as *H. lutea*, which has hyaline ascospores, or *H. straminea* (Chaverri and Samuels 2003), a species that has green ascospores. It is the anamorph that distinguishes this species. Teleomorphs are not known for other members of the Brevicompactum clade.

Two apomorphies combine to characterize the Brevicompactum clade: subglobose conidia and the formation of long white, unbranched or little to frequently branched, conidiophores that project conspicuously from the surface of the pustule (Figs. 8b, 10b, 12c and 13b). These may be sterile over a considerable part of their length but bear one to a few phialides at the tip (e.g., Figs. 8c, 9b, c and 13c). Conidia arise from near their base in a more or less slimy mass; thus, pustules of conidia often appear papillate or lanose. Typical pustules on SNA and CMD are very compact and hemispherical, and free conidiophores within the pustule are not visible when viewed with a stereo microscope. On CMD there is a tendency for pustules to be more extensive, flat and more loosely organized. The papillate aspect is slightly less well developed in *T. turrialbense.* The original description of *T. brevicompactum* (Kraus et al. 2004) described the long extensions as developing in old cultures, but in our experience they are conspicuous elements from an early stage on SNA and CMD. There is a tendency for the projecting conidiophores of *T. brevicompactum, T. turrialbense* and *T. protrudens* to be more branched than in *T. arundinaceum*.

In addition to conidiophores with long extensions, all of the species discussed here produce completely fertile conidiophores that do not have long extensions (e.g., Figs. 8j, 9g

Fig. 3 (continued)

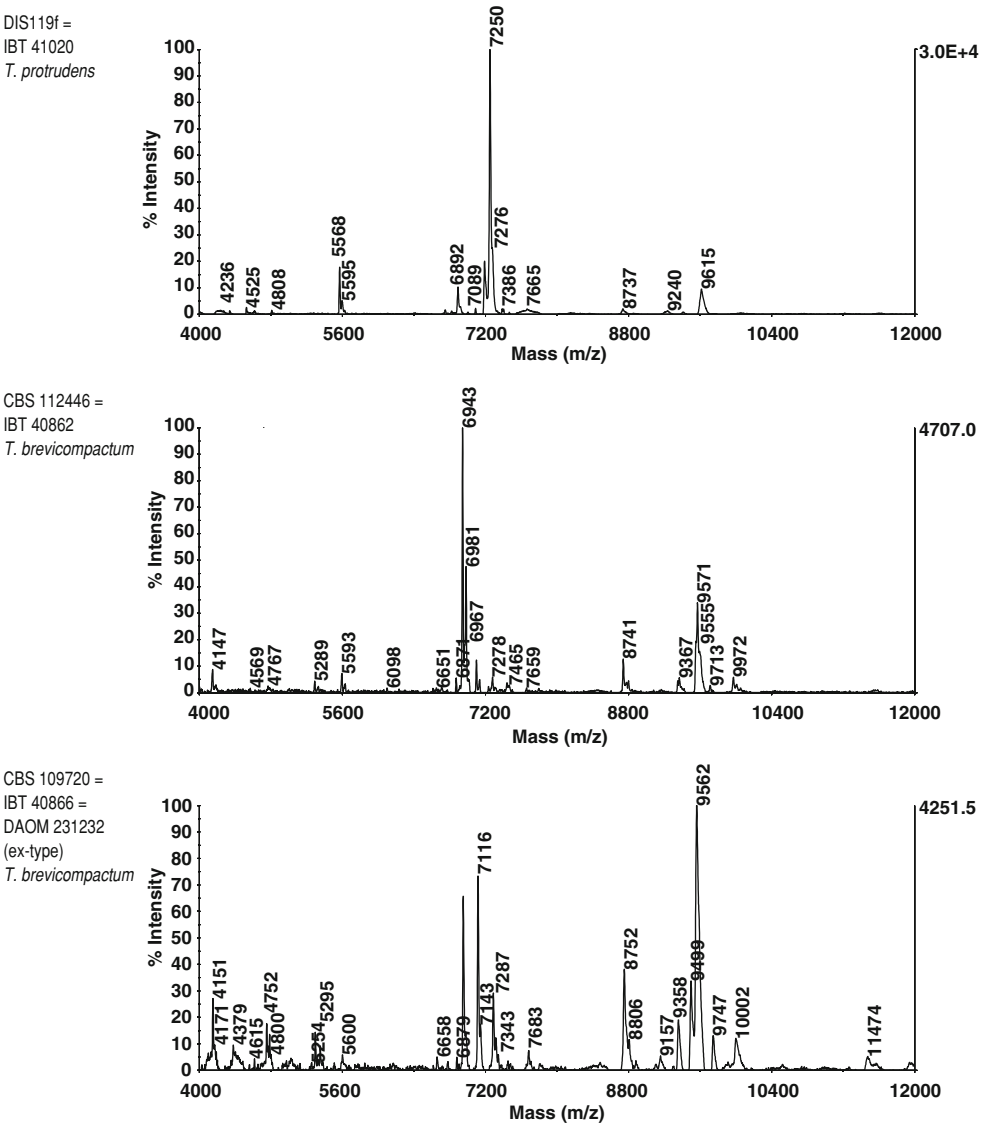

Fig. 3 (continued)

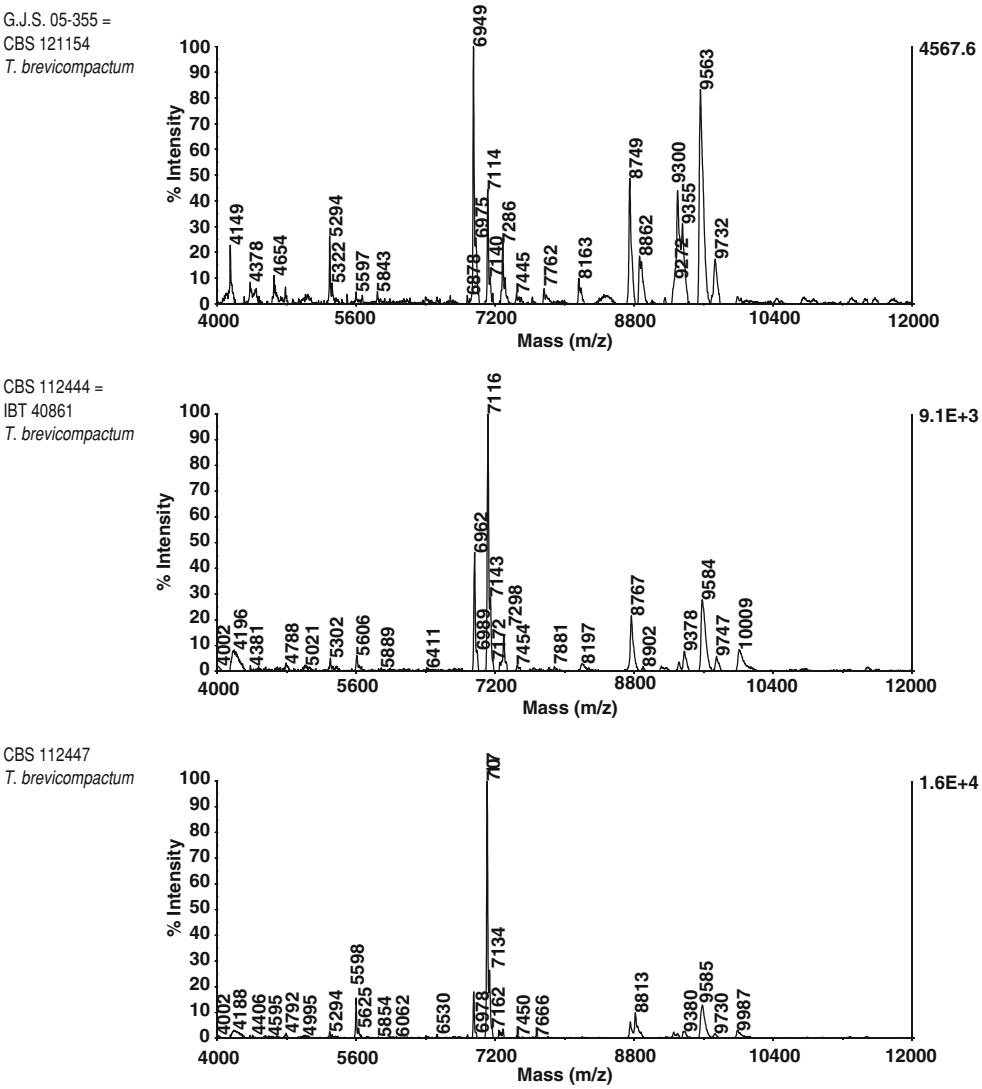

and 10h). These conidiophores resemble *T. harzianum* (Bissett 1991).

Hypocrea rodmanii is separated from the Brevicompactum complex by its slower rate of growth, smaller conidia and phialides, the production of trichokonins, hyporodicins, and hypocompactins. Unlike all members of the Brevicompactum clade, it does not produce alamethicins or trichothecene-type toxins. The small green, globose conidia combine with projecting, partially sterile conidiophores to distinguish this species from all known *Hypocrea* and *Trichoderma* species.

Members of the Brevicompactum complex are not easily separated on the basis of phenotype (Fig. 6; continuous characters are summarized in Table 8).

Trichoderma protrudens is distinguished by its longer phialides, its high growth rate at 37°C, production of harzianum A, and its unique pattern of hydrophobins. *Trichoderma turrialbense* is very closely related to *T. brevicompactum*; we distinguish these species mainly on the basis of production of trichodermin by *T. brevicompactum* and harzianum A by *T. turrialbense. Trichoderma arundinaceum* is distinguished from *T. brevicompactum* by the production of harzianum A and by the lack of a synanamorph in CMD cultures of the former (see below). Overall, the phialides of *T. protrudens* are longer and narrower than in all other species treated, with a consequently larger L/W ratio. The cells that produce phialides are narrowest in *T. protrudens*, 2.5–3.0 µm, as compared to 3–4 µm in the other species. The phialides of *H. rodmanii* are shortest.

No microscopic characters reliably and practically separate *T. brevicompactum, T. turrialbense* and *T. arundinaceum*. Small, but consistent differences in conidial sizes, especially when seen at the 95% confidence intervals and growth rates can be seen in Table 8 and Fig. 5. There is a very slight tendency for conidia of *T. arundinaceum* to be longer and wider than in the other species. *Trichoderma arundinaceum* and *T. brevicompactum* have a larger l/w ratio while the

Fig. 3 (continued)

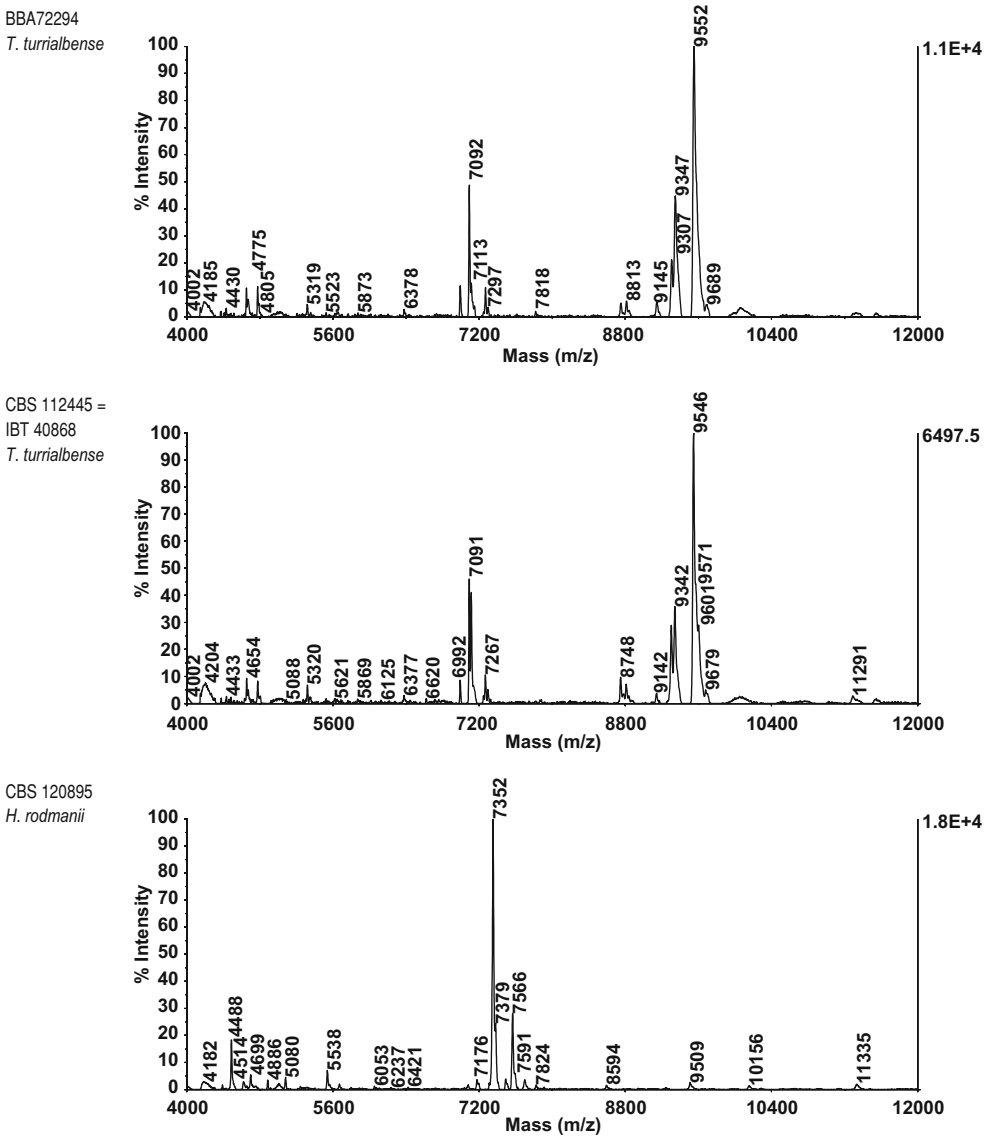

l/w ratio of conidia of *H. rodmanii* and *T. turrialbense* is smaller; the l/w ratio of conidia of *T. prodrudens* is intermediate between the two groups (Fig. 5). *Trichoderma turrialbense* differs from both *T. brevicompactum* and *T. arundinaceum* in having a slightly faster rate of growth at 25 and 30°C on SNA. The formation of, especially, different peptaibiotics in the respective species (trichocryptins in *T. brevicompactum/T. turrialbense* vs trichobrevins in *T. arundinaceum/T. protrudens*), supports a distinction between *T. brevicompactum* and *T. arundinaceum.*

Chemotaxonomic data separate three clusters, *T. protrudens* (a), *T. arundinaceum* (b) and *T. brevicompactum* (c1)/ *T. turrialbense* (c2) due to the presence of one unique non-ribosomal peptide synthtase (NRPS) gene for trichoferin, and high-level expression of trichobrevins. All three groups may produce alamethicins. Trichocryptins A are characteristic for (c1). Major amounts of trichobrevins are found only in (a) and (b), whereas CBS 112154 is the only isolate in (c) to produce traces of trichobrevins. Trichocryptins B are found in (c) only. The structural data of the compounds does not reflect their phylogenetic difference. A comparison of a single domain of all respective alamethicin synthetases would provide this information.

It is thus not possible to clearly differentiate clusters *T. protrudens* from *T. arundinaceum*, or *T. turrialbense* from *T. brevicompactum* by their metabolite profiles, as there is just a single compound, either harzianum A or an unknown peptaibol besides 4 or 5 others, and it might well be that, e.g., new strains of *T. protrudens* producing trichodermin will be discovered. On the other hand, it is very clearly possible to separate *T. protrudens/T. arundinaceum* (a, b) from *T. brevicompactum/T. turrialbense* (c) due to different

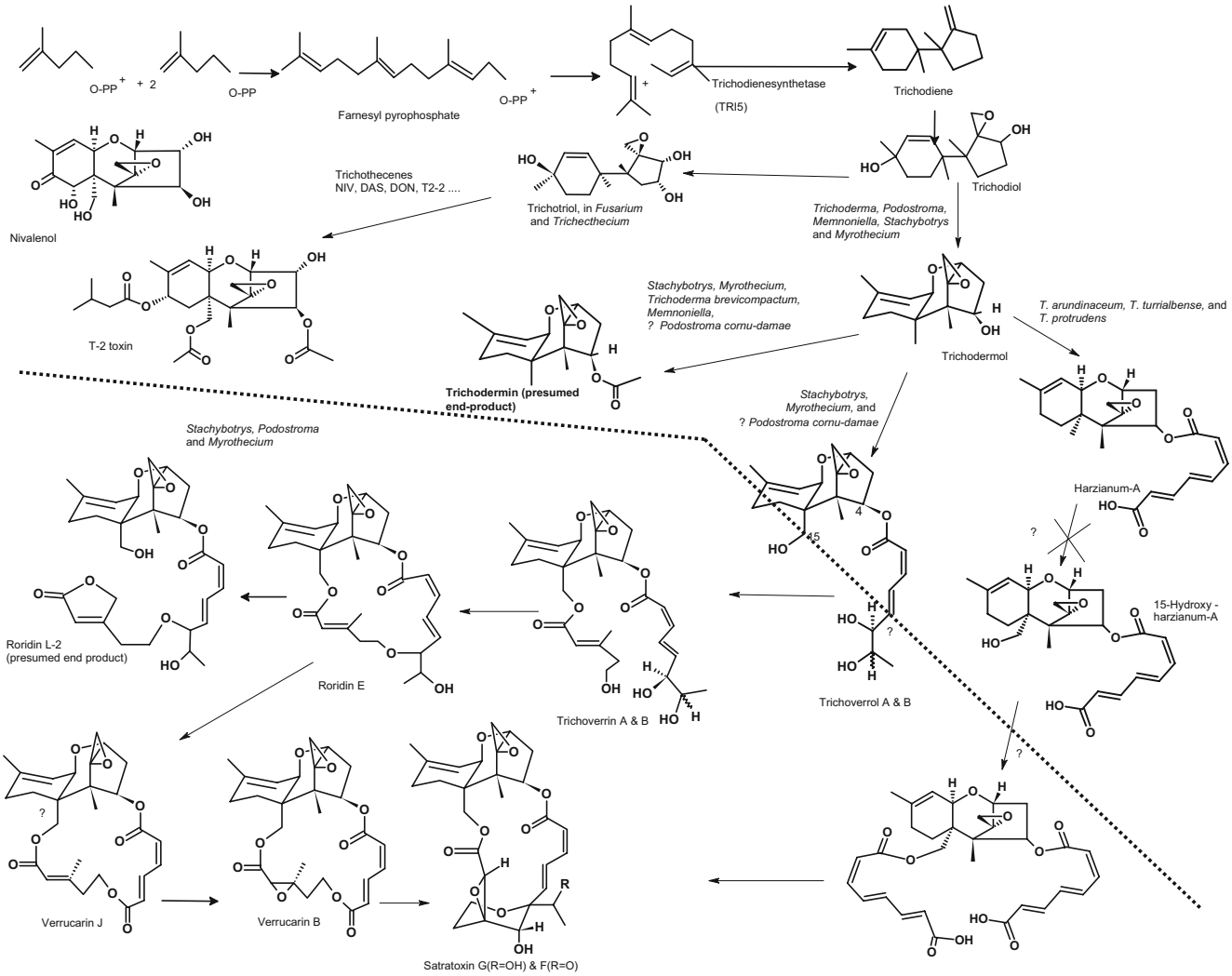

Fig. 4 Overview of putative pathways of trichothecene biosynthesis. Trichodiol is an important branching point with one path leading to trichotriol (T-2 toxin of *Fusarium*), and one leading to trichodermol. Trichodermol is the point of divergence for the simple trichothecene-type toxins trichodermin and harzianum A of *Trichoderma*/*Hypocrea*, and for the macrocyclic trichothecenes of *Myrothecium* and *Stachybotrys*. Because *Trichoderma* lacks the enzyme needed to hydroxylate the 15-position, the second anchor required to form the macrocyclic ring is missing, and either harzianum A or trichodermin are the end products. The identity of the fungus reported as *Podostroma cornu-damae* cannot be confirmed; see the discussion in the text. Simple trichothecene-type toxins are shown above the *dotted line*, and macrocyclic trichothecenes are below the *line*

pattern of trichobrevins (low concentration in c) and trichocryptins B (high concentration in c, trace amounts in *T. arundinaceum* CBS 119576).

The pattern of peptaibiotics of the two strains of *T. turrialbense* is similar but not identical. Both strains produce alamethicins as the major group of peptaibiotics. Trichobrevins are present in only small amounts, if at all, a fact that clearly distinguishes these two strains from *T. arundinaceum*. The major difference between CBS 112445 and CBS 122554 is the presence of 11- and 12-residue trichocryptins C and D in the latter. Trichocryptins C and D terminate in L-alaninol (Alaol), whereas we find Vxxol or Lxxol in trichocryptins A and B. So far, CBS 122554 is the only strain in which we have unambiguously found *C*-terminal Alaol and also the first report of Alaol as a *C*-terminal constituent of peptaibiotics. We did not find Alaol at the *C*-terminus of CBS 112445 trichocryptins. However, that difference is more interesting from a biochemical point of view. The building scheme of all trichcryptins A, B, C, and D is the same, and differences may be explained by positional isomerism.

Discussion

Analyses of partial sequences of *rpb2* indicate that *Trichoderma brevicompactum* represents a separate lineage in *Trichoderma*/*Hypocrea*, which we refer to here as the Brevicompactum clade. Kraus et al. (2004) suggested the

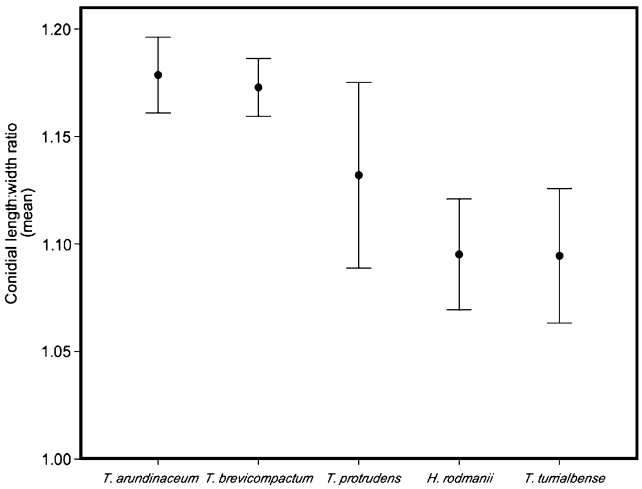

Fig. 5 95% confidence intervals of conidium length/width ratios

phylogenetic distinctiveness of the single species, *T. brevicompactum.* As can be seen from Fig. 1, the Lutea clade is the closest relative of the Brevicompactum clade when branch lengths are considered; this confirms the findings of Kraus et al. (2004).

Additional collections emphasize the two lineages that were seen in the original description of *T. brevicompactum* (Kraus et al. 2004). However, increased sampling has added one new *Hypocrea*, an endophyte in a trunk of cacao in India, and additional *Trichoderma* cultures from diverse geographic sources. The combination of sequences of *tef1, rbp2* and ITS with phenotype data derived from micromorphology, colony morphology and secondary metabolites has led us to recognize five species, of which four are new. Members of the Brevicompactum clade are notable for their subglobose conidia. The only three other species that have smooth, subglobose conidia are *T. harzianum* and *T. aggressivum* (Harzianum clade) and *T. atroviride* (Viride clade); these species are not closely related to each other or to *T. brevicompactum*.

The pattern of peptaibiotics produced by *H. rodmanii* does not identify it as a close relative of *T. brevicompactum* (see Fig. 6c), and it does not produce the trichothecenes or other metabolites that are unique to the Brevicompactum complex. Thus, the apparent relationship of *H. rodmanii* to other members of the clade could be a sampling artefact. With the discovery of additional taxa, the relationship between *H. rodmanii* and members of the Brevicompactum compex may change.

Kraus et al. (2004) cannot be criticized for having recognized only one species. Although they found that *T.* brevicompactum could be distinguished from *H. lutea*, *T. virens* and *T. harzianum* on the basis of carbohydrate utilization, they found virtually no difference among their isolates of *T. brevicompactum.* Our own examination of the morphological and cultural characters of an expanded panel of isolates and analysis using multidimensional scaling revealed only subtle differences. However, the anomalous production of trichothecene-type toxins among the cultures identified by Kraus et al. (2004) as *T. brevicompactum* led us to search for additional phenotypic data from metabolites (peptaibiotics) and physical phenotype.

As studies of species rich genera such as *Trichoderma* expand and include increasing numbers of cultures, more phylogenetic diversity is revealed than can be accounted for by phenotype. In the current work, very small differences in characters such as rate of growth or length/width ratio of conidia are apomorphic for species and combine with metabolic characters in defining species. However 'small' these differences are, they are representative of the species diversity and are taxonomically significant, a point that was made by Hawksworth (2001) with regard to the true diversity of species of fungi.

Although no teleomorph has been discovered for any of the members of the Brevicompactum clade, except for *H. rodmanii*, the moderate diversity among isolates of *T. brevicompactum* suggest recombination. Part of the diversity of *T. brevicompactum* may be due to geographic diversity, as exemplified by CBS 121154 (Cameroon) and CBS 112443 (Papua New Guinea), whereas the remaining cultures are from more or less contiguous continental areas where one might expect genetic interchange. In contrast, *T. arundinaceum* is noteworthy for its apparent lack of phylogenetic diversity despite having essentially the same geographic distribution as most of the *T. brevicompactum* cultures, which suggests that *T. arundinaceum* is clonal. Despite strong morphological similarity and overlapping ranges, the phylogenetic analysis indicates considerable phylogenetic distance with no genetic interchange between the two species.

Kraus et al. (2004) were surprised that *T. brevicompactum* could be closely related to *H. lutea* because of the conspicuous differences in the respective conidiophores, 'pachybasium-like' in *T. brevicompactum* and 'gliocladium-like' in *H. lutea* and its sister species, *H. melanomagna*. However, the morphology of the gliocladium-like anamorphs of *H. lutea* (*Gliocladium viride)*, and *H. melanomagna* is so unusual in the genus as to give no clues about the relationships of these species (see Domsch et al. 2007). No anamorph in *Hypocrea* and no species of *Trichoderma* is strictly similar to *G. viride* in anything other than wet, green pigment and phylogeny. However, gliocladium- or verticillium-like anamorphs occur in unrelated positions of *Trichoderma* either as the primary anamorphs (*T. virens*, *H. gelatinosa*, *T. crassum, H. nigrovirens*) or as synanamorphs of more typical *Trichoderma* species that produce primary conidia in pustules (Chaverri and Samuels 2003). Kraus et al. (2004) did not describe gliocladium- or verticillium-like

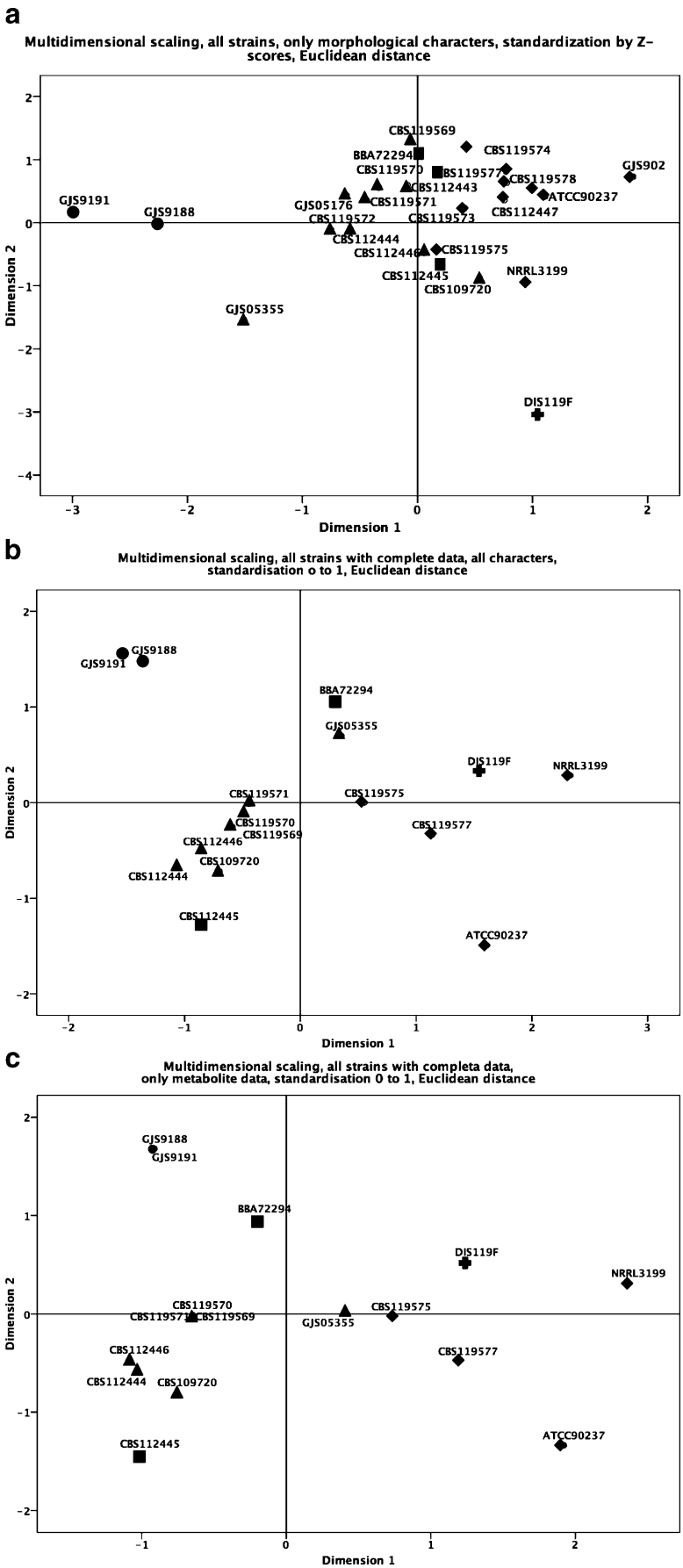

Fig. 6 Results of multidimensional scaling. **a** Morphological characters alone. **b** Combined morphological and metabolic characters. **c** Metabolic characters alone. The following strains lacked metabolic data and thus were excluded from B and C: G.J.S. 05–182, G.J.S. 05–183, G.J.S. 05–184, CBS 112443, G.J.S. 05–178, G.J.S. 05–174, G.J.S. 04–380, G.J.S. 05–176. ♦=*T. arundinaceum,* ▲=*T. brevicompactum,*✚=*T. protrusum,* ●=*H. rodmanii,* ■=*T. turrialbense*

conidiophores for *T. brevicompactum*, but the formation of these conidiophores may depend upon the medium that is used. We did not observe them on PDA and only rarely on SNA whereas on CMD the synanamorph is abundantly formed in all but *T. arundinaceum*. Possibly in *H. lutea* and *T. virens,* where the primary conidiophore is gliocladium-like, the 'true' *Trichoderma* morph has been lost leaving only the synanamorph.

The culture CBS 121320, *T. protrudens,* an endophyte from the trunk of a cacao (*Theobroma cacao*) tree, occupied a unique lineage within the Brevicompactum complex in the phylogenetic analysis (Figs. 1 and 2a–c). In other cases, endophytic *Trichoderma* species are represented by single cultures that occupy unique lineages, sometimes basal to more complex species (e.g., DIS 328gi, G.J.S. 04–40 basal to *T. viride*; Jaklitsch et al. 2006; Hanada et al. 2008) or in the case of *T. koningiopsis* endophytic isolates formed solitary internal lineages or endophyte-pure internal lineages (Samuels et al. 2006). The endophytic habit seems to have limited the ability of the strains living within plant tissue to exchange genetic material with 'freeliving' strains. Perhaps living as an endophyte has compromised their ability to survive in what could be a much more demanding environment outside of the host plant.

The Brevicompactum clade is characterized by the production of simple trichothecene-type mycotoxins. With the exception of *H. rodmanii*, all members of the clade produce either trichodermin or harzianum A. Various species of *Trichoderma* are reported to produce trichothecenes (Nielsen et al. 2005). Corley et al. (1994) characterized harzianum A from a culture that was identified as *T. harzianum* ATCC 90237, which we have re-identified here as *T. arundinaceum.* Lee et al. (2005) reported production of harzianum A by a strain (F000527 = CBS 113214) isolated directly from a soil sample collected in Daejeon, Korea, and identified by DNA sequences as a *Hypocrea* sp. Recently, a new trichothecene homologue, harzianum B, was isolated from the same strain (Jin et al. 2007). We received this strain too late to include in our phylogenetic analysis, but we have identified it also as *T. arundinaceum.* The culture NRRL 3199, a patent strain of unknown provenance identified as *T. viride,* was also shown to produce harzianum A and was re-identified here as *T. arundinaceum*.

A few studies have claimed production of simple trichothecene-type toxins by species of *Trichoderma* (Adams and Hanson 1972; Bamburg and Strong 1969; Watts et al. 1988; Cvetnić and Pepelnjak 1997; see also Sivasithamparam and Ghisalberti 1998 for a review), but in most of the studies, nonspecific analytical methods such as TLC and HPLC were used and no details of taxonomic identification were given. Of these reports, we have only been able to examine the *T. polysporum* strain (IMI 40624) reported by Adams and Hanson (1972). Although we can confirm that it is correctly identified, it did not produce trichothecenes on any of the numerous media that we tested. In contrast to these simple trichothecenes, macrocyclic trichothecenes have been reported from a rare, deadly poisonous, East Asian species, *Podostroma cornu-damae* (Saikawa et al. 2001). However, we cannot confirm the identity of the specimen used by these authors as apparently neither a voucher specimen nor culture were deposited. The Japanese cultures, NBRC 9005 (*P. cornu-damae*) and NBRC 9523 (*P. giganteum*), both of unknown provenances, produce macrocyclic trichothecenes (K.F. Nielsen, unpublished data). The respective ITS and *tef1* of these two cultures are identical, suggesting that there has been contamination of one culture by the other. The sequences place the cultures in the Viride clade (Fig. 1) (K.F. Nielsen and G.J. Samuels, unpublished data). We cannot confirm the production of simple, non-macrocyclic trichothecene mycotoxins, including T-2, by any species of *Trichoderma*/*Hypocrea* outside of the Brevicompactum clade, and the phylogenetic results presented here show that this clade is phylogenetically distant from any species that are used in biological control. In a survey of *Trichoderma* species from all known clades, we have not encountered macrocyclic trichothecenes using a LC-MS approach (K.F. Nielsen, unpublished data.). Despite the production of alamethicins by members of the *T. brevicompactum* clade (Degenkolb et al. 2006a), which could enhance their abilities as biocontrol agents (Corley et al. 1994), the production of trichothecene-type toxins could limit their practical application in integrated crop management schemes.

Recently, Favilla et al. (2006) and Poirier et al. (2007) claimed that the 20-residue peptaibols alamethicin and paracelsin, the 16-residue antiamoebin and other 11-residue trichobrachins (Mohamed-Benkada et al. 2006; Ruiz et al. 2007) were highly toxic in three in vitro invertebrate models, viz. *Crassostrea gigas*, *Artemia salina* and *Daphnia magna*. An alternative explanation of the toxicitiy reported by Favilla et al. (2006) and Poirier et al. (2007) is that the batch of the alamethicin standard that they used (Sigma-Aldrich; product number A-4665) was contaminated with the trichothecene harzianum A. In our own work, we have found that this particular Sigma alamethicin contains harzianum A; and this group of trichothecene-type toxins is highly toxic to *Artemia salina* (K.F. Nielsen, unpublished results). Notably, it took 40 years to recognize that *Trichoderma "viride"* NRRL 3199, which now has been re-identified here as T. *arundinaceum*, also produces harzianum A. Thus, alamethicin samples and standards tested in toxicity assays prior to 2005 could very likely have given false positive results based upon contamination of the samples by trichothecene-type mycotoxins (Degenkolb et al. 2008a). There are no good GLP studies of the toxicity of trichodermin and harzianum A. Trichodermin inhibits the

chain elongation of protein synthesis by binding to the peptidyltransferase (Gilly et al. 1985), whereas the much more potent T-2 toxin from *Fusarium* inhibits initiation of protein synthesis (Liao et al. 1976). There are contradictory results regarding the toxicity of harzianum A: Corley et al. (1994) observed no cytotoxicity in hamster kidney cells whereas Lee et al. (2005) reported this simple trichothecene to be highly toxic to several cell lines.

Harzianum A is especially interesting when considered in light of production of the highly toxic (>10 times more than T-2 toxin) macrocyclic trichothecenes by other hypocrealean fungi, including *Stachybotrys*, *Myrothecium*, and *Podostroma cornu-damae* (syn. *Hypocrea cornu-damae*) noted above (Saikawa et al. 2001). Harzianum A may be a missing link between the simple (trichodermin, T-2 toxin, etc.) and macrocyclic trichothecenes: the missing hydroxyl group on the 15-carbon atom in harzianum A would provide the possibility of attaching an additional octa-(*2Z,4E,6E*)-trienedioic acid (or a related compound) on the C-15. The two arms can then condense to a form a macrocyclic ring (Fig. 4).

Production of isocoumarins by all strains of the Brevicompactum clade, except *H. rodmanii,* (including diaportinol and diaportinic acid) is interesting because this requires the expression of genes for polyketides. However, production of these metabolites is not restricted to the Brevicompactum complex as it is detected throughout *Trichoderma* (K.F. Nielsen, unpublished data) as well as in, e.g., *Penicillium nalgiovense*. Quantitatively, isocoumarins seem to vary considerably from time to time during long-term growth, especially in potato-dextrose broth.

Peptaibiotics are characteristic linear or cyclie α-aminoisobutyrate-containing peptides that are produced mainly by species of *Trichoderma*/*Hypocrea* (for a review, see Degenkolb et al. 2003, 2007, 2008a, b). The Brevicompactum clade is a rich source of new peptaibiotics. Degenkolb et al. (2006a) discovered that 69 of the 75 peptaibiotics produced by species that we describe here as *T. brevicompactum*, *T. arundinaceum* and *T. turrialbense* were new to science. All peptaibiotics consecutively assigned as compounds [**80**]–[**117**] in this study also represent new compounds. All members of the Brevicompactum complex produced the 7-residue trichocompactins (TCP) or 7-residue hypocompactins (HCP). Similar 7- or 8-residue peptaibiotics, mostly lipopeptaibols, were also found in *T. aggressivum* f. *europaeum* CBS 100526, *H. dichromospora* CBS 337.69 (Krause et al. 2006), and *T.* cf. *strigosum* (Degenkolb et al. 2006b); they represent deletion sequences of 10-, 11- or, 12-residue lipopeptaibols. This subgroup of peptaibiotics is biosynthesized by species from different sections and clades of *Trichoderma*; thus its chemotaxonomic relevance is low (Degenkolb et al. 2006b).

Alamethicins and alamethicin-like peptaibols are not restricted to the Brevicompactum complex. They have been found throughout *Trichoderma*, with very similar atroviridins (Oh et al. 2002) and polysporins (New et al. 1996). The respective synthetases can be classified by specificities of their adenylate domains in positions 6, 9, 12, 17 and 20. Most analyses have been carried out with *T. arundinaceum* NRRL 3199, and the alamethicins of the F30/50 type (Kirschbaum et al. 2003) have previously been found in strains CBS 109720, IBT 40839, IBT 40840, CBS 112445, ATCC 90237, and IBT 40863 (Degenkolb et al. 2006a). These represent a special type of synthetase with module 6 preferring Ala against Aib, module 9 strictly Val, module 12 strictly Leu, module 17 preferring Aib against Vxx, and module 20 strictly Pheol.

Hydrophobins are small hydrophobic proteins presumably ubiquitous in filamentous fungi. They are usually secreted and processed, being components of the outer surfaces of walls of hyphae and conidia. Besides their roles in cell wall structure they may mediate interactions between the fungus and the environment such as surface recognition during pathogenic interaction with plants, insects or other fungi, but also in symbiosis. A hydrophobin gene found in a biocontrol strain of *T. asperellum* (T203, Viride clade) enabled the root attachment and colonization that are steps in initiation of a resistance reaction in host the plant to a parasite (Viterbo and Chet 2006). The size of hydrophobins ranges from approximately 75 to 400 amino acid residues containing eight positionally conserved cysteine residues; they can be divided into two classes according to their hydropathy profiles and spacing between the conserved cysteins (Linder et al. 2005). The number of hydrophobin genes detected in fungal genomes may exceed 10, and expression varies with physiological conditions. We here investigated sporulating mycelium under conditions previously applied for class II hydrophobins (Neuhof et al. 2007a). The unique hydrophobin patterns of *H. rodmanii, T. protrudens and T. arundinaceum* identify these as discrete species, while *T. brevicompactum and T. turrialbense* show partially overlapping sets of protein masses. For a review of Class II hydrophobin gene families in *Trichoderma*, see Kubicek et al. (2008).

In a recent intact cell mass spectroscopy (ICMS) study of 32 strains of 29 different species of *Trichoderma/Hypocrea*, hydrophobin patterns specific both at the species and isolate (subspecies) level were observed (Neuhof et al. 2007b). Two to four marker masses of hydrophobins were evaluated for each species. In 21 cases, single masses are shared within experimental errors by two species. A comparison of *H. atroviridis/T. atroviride* mycelium and conidia showed two identical masses. An evaluation of 3

strains of *H. jecorina/T. reesei* revealed three identical masses in one case besides three differing masses, and five differing masses in another case. These differing masses have been attributed in two cases to different post-translational processing of the hydrophobins Hfb1 and Hfb2.

In the case of *T. brevicompactum and T. turrialbense*, the two dominating mass peaks differ, supporting individual species. However, two significant masses of the Brevicompactum group and one mass of the Turrialbense group have also been detected as minor mass peaks in each group respectively. Two additional minor mass peaks are shared as well. These apparent similarities need to be resolved at the sequence level.

Taxonomy

For continuous characters, see Table 8.

1. *Trichoderma arundinaceum* Zafari, Gräf. & Samuels, sp. nov. Figures 7a–c and 8.

Trichodermati brevicompacto G. F. Kraus, C. P. Kubicek & W. Gams simile sed harzianum A produens et in agaro dicto SNA magis celeriter crescens. Conidia subglobosa vel ovoidea, (2.2−)2.7–3.5(−5.0) × (1.7−)2.5–3.0(−3.5) µm.

Teleomorph None known.

Characteristics in culture Optimum temperature for growth on PDA and SNA 30°C. Barely growing at 37°C on PDA or SNA. Colonies grown on PDA sometimes sporulating at 37°C in intermittent light after 72–96 h. On PDA after 5 days at 25°C under intermittent producing conidia in 3 or 4 conspicuous concentric rings, colony margin deeply scalloped. Conidia on PDA yellowish green (K&W 28–30 D-F 8). No pigment diffusing through the agar; no distinctive odour. Colonies grown on SNA in intermittent light forming conidia within 72 (96) h at (25) 30°C. On SNA after 1 week under intermittent light conidia forming abundantly around the colony margin in a broad band, most typically as a continuous lawn, sometimes as discrete, 1.5 mm diam, flat pustules, yellow rarely noted in developing conidia, conidia similar in color to conidia formed on PDA and CMD. Colonies grown on CMD at 25°C under light (12 h cool white fluorescent/12 h darkness) >9 cm diam within one week, conidia green, forming in pustules mainly around the colony margin and to a lesser extent in concentric rings behind the colony margin, similar to the pustules formed on SNA. Pustules formed on CMD and SNA flat, ca. 1 mm diam, remaining discrete or becoming confluent, dense, spiky or papillate from projecting, terminally fertile conidiophores and wet masses of conidia at the base of the projecting conidiophores. Conidiophores on CMD and SNA comprising a broad, more or less conspicuous central axis with lateral and often terminal fertile branches; fertile primary branches profuse, separated by short internodes, typically paired, arising at or near right angles with respect to the main axis, typically increasing in length with distance from the tip; primary branches typically more than 2 cells in length; secondary branches arising at right angles from primary branches, often comprising a single, broad cell; phialides arising in clusters of 3–5 at tips of primary and secondary branches; often a single branch of a conidiophore extending beyond the surface of the pustule, branched or unbranched, straight, smooth, septate, bearing a verticil of a few lageniform phialides at the tip. Phialides slightly enlarged in the middle and lageniform when arising on widely spaced fertile branches or shorter and wider, ampulliform, when arising from crowded fertile branches. Conidia subglobose to ovoidal, (2.2−)2.7–3.5(−5.0) × (1.7−)2.5–3.0(−3.5) µm, smooth, green. Synanamorph not observed on CMD. Chlamydospores not observed on CMD after 1 week at 25°C, intermittent light.

Etymology From Latin '*arundo*,' a reed or cane or anything made of a reed or cane such as a fishing rod, in reference to the long conidiophores that project from the pustules.

Habitat Soil.

Known distribution Iran, Namibia, United States (Miss.).

Holotype Iran: Hamadan, from soil (BPI 878405 ex CBS 119575; ex-type culture CBS 119575).

Additional cultures see Table 1.

2. *Trichoderma brevicompactum* G.F. Kraus, C.P. Kubicek & W. Gams, Mycologia 96: 1063. 2004. Figures 7d–f and 9

Telemorph None known.

Characteristics in culture Optimum temperature for growth on PDA and SNA 30°C. Slowly growing at 37°C, sometimes sporulating on PDA and SNA after 96 h at 37°C. On PDA after 1 week at 25°C under intermittent light producing conidia in several closely spaced, broad, concentric rings; colony margin entire. Conidia on PDA yellowish green (K&W 28–30 D-F 8). No pigment diffusing through the agar; no distinctive odor. Colonies grown on SNA in intermittent light forming conidia within

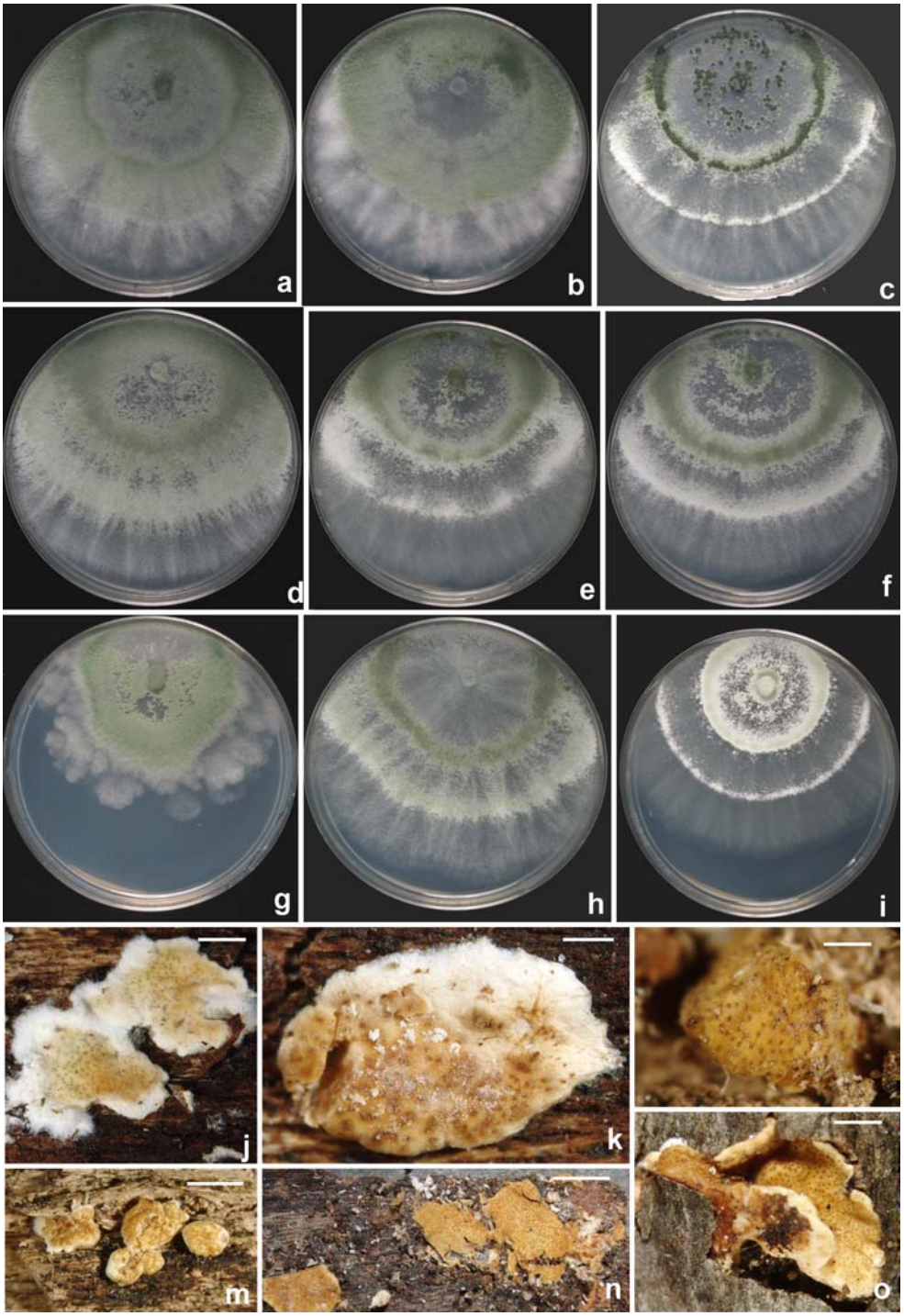

Fig. 7 **a–i** Cultures of *Trichoderma* species and *Hypocrea rodmanii* on PDA 96 h, intermittent light, in 9-cm-diam Petri dishes. **a–c** *T. arundinaceum*. **a** ATCC 90237. **b** NRRL 3199. **c** CBS 119578. **d–f** *T. brevicompactum*. **d** CBS 112444. **e** G.J.S. 04–380. **f** IBT 40841. **g** *T. protrudens*. CBS 121320. **h** *T. turrialbense* CBS 112445. **i** *H. rodmanii* CBS 120895. **j–o** *H. rodmanii*, immature (**j**) and mature (**k–o**) stromata. **j, k** from CBS 122581; **l** from CBS 120897; **m** from G.J.S. 91–90; **n** from CBS 122582; **o** from CBS 1208979. *Scale bars*: **j, k, l, o**=0.5 mm; **m, n**=1 mm

72–96 h at (25) 30°C. On SNA after 1 week under intermittent light conidia forming abundantly around the colony margin and in obscure concentric rings between the margin and the inoculum, rings formed of confluent pustules, complete or broken, conidia at first yellow then similar in color to conidia formed on PDA and CMD grown on SNA in intermittent light forming conidia within 72–96 h at (25) 30°C. On SNA after 1 week under intermittent light conidia forming mainly around the colony margin and to a lesser extent in concentric rings behind the colony margin, similar to the pustules formed on SNA. Pustules formed on CMD and SNA flat, to 2 mm diam, remaining discrete or becoming confluent, tending to be loosely organized, conidial masses appearing to be moist; numerous conspicuous white, usually

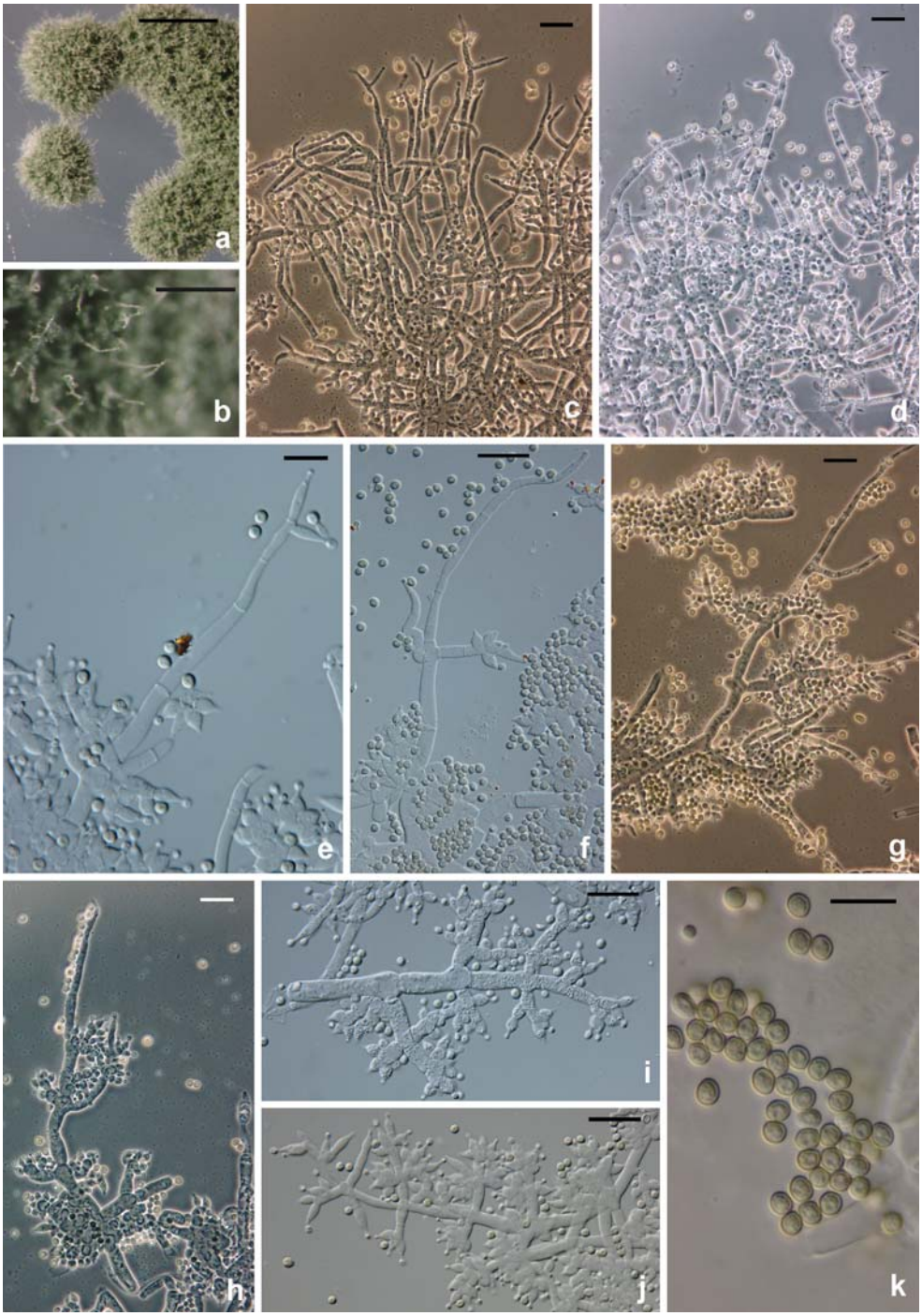

Fig. 8 *Trichoderma arundinaceum*. **a, b** Pustules. Protruding conidiophores seen in **b**. **a** on SNA, **b** on CMD. **c**–**j** Conidiophores. **c, e, f, g, j** from SNA; **d, h, i** from CMD. **k** Conidia, from SNA. **c** = CBS 121153, **d** = CBS 119573, **e, f, j, k** = CBS 119575, **i** = ATCC 90237. *Scale bars*: **a** = 1 mm, **b**=250 μm, **c**–**k**=10 μm

branched, terminally fertile conidiophores protruding from easch pustule. Conidiophores on CMD and SNA comprising a more or less distinct, broad central axis with fertile branches; fertile branches profuse, separated by short internodes, typically paired, arising at or near right angles with respect to the main axis, typically increasing in length with distance from the tip; primary branches often comprising a single, broad cell producing phialides in a dense terminal cluster, or primary branches multicellular and narrower, producing phialides at the tip and rebranching to produce secondary branches terminating in phialides; often a single branch of a conidiophore extending beyond the surface of the pustule, straight, septate, smooth, unbranched or sparingly branched with long internodes between branches, each branch terminating in a verticil of 1–3 phialides or the terminal phialides held in an appressed penicillus of 3–5 on a broad cell.

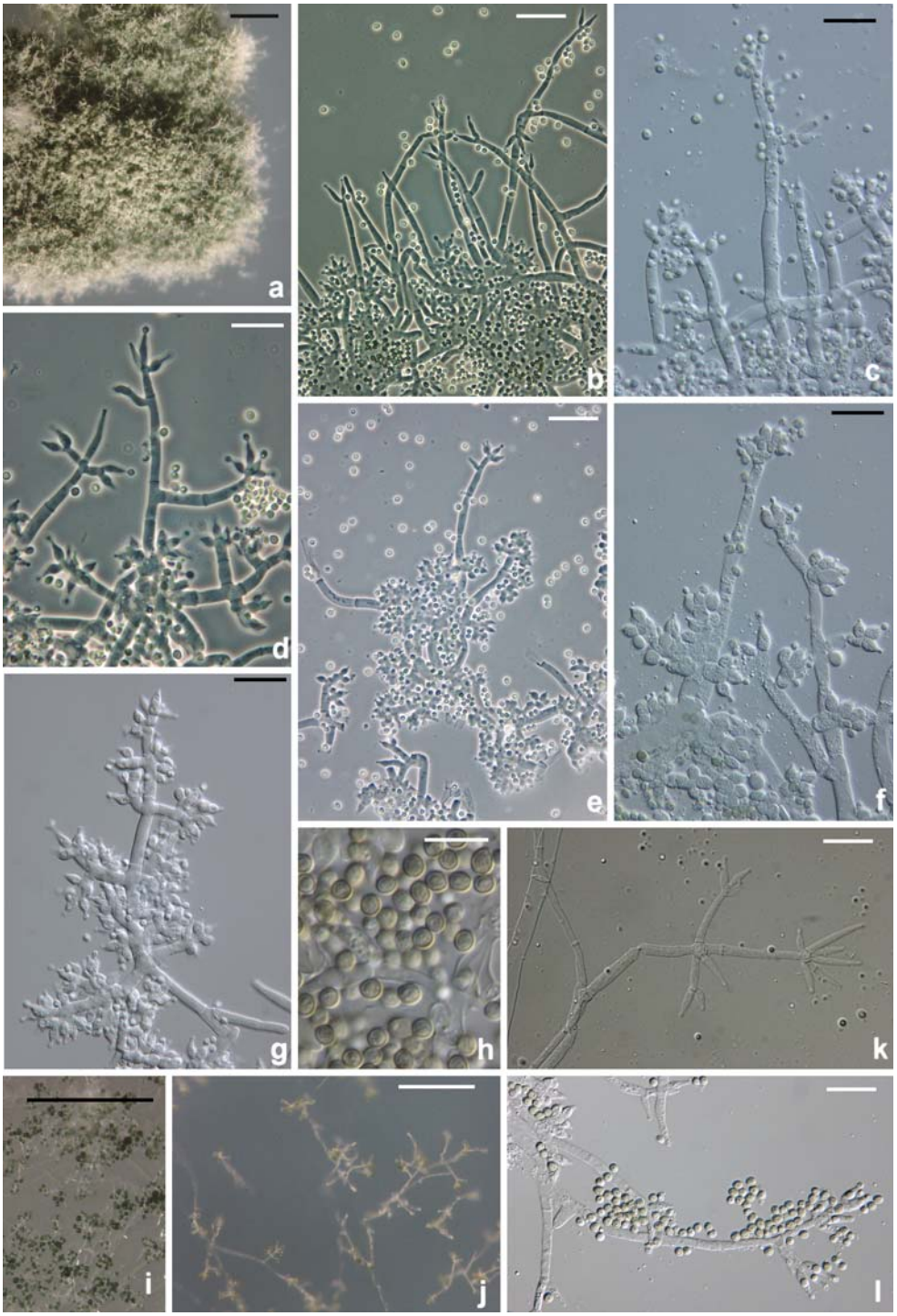

Fig. 9 *Trichoderma brevicompactum*. **a** Pustule on SNA. **b**–**g** Conidiophores taken from pustules. b, d from SNA: c, e-g from CMD. h. Conidia from SNA. **i-l**. Synanamorph on CMD. **a, e** from G.J.S. 04–380, **b** from CBS 109720, **c** from CBS 119570; **d** from CBS 119572, **f** from CBS 119569, **g, j, k** from CBS 112446, **h** from CBS 121154, **i** from CBS 112443, **l** from CBS 112447. *Scale bars*: **a**=0.5 mm, **b–h, k, l**=10 um; **i**=1 mm, **j**=150 μm

Phialides slightly enlarged in the middle and lageniform when arising on widely spaced fertile branches; shorter and wider, ampulliform, when arising from crowded fertile branches. Conidia subglobose, (2.2−)2.7–3.0(−3.7) × (2.0−)2.2–2.7 (−3.0) μm smooth, yellowish green in mass. Synanamorph forming on CMD, verticillium- or gliocladium-like, single conidiophores arising from agar surface and the scant aerial hyphae, conidia held in wet, green heads. Chlamydospores produced only in few cultures on CMD after 1 week at 25°C under intermittent light, terminal, subglobose, (5.7) 8.0–11.0 (13.5) × (5.0) 6.5–9.2 (10.2) μm.

Habitat Soil.

Known distribution St. Vincent and the Grenadines, Caribbean Region (Union Island), India, Iran, Papua-New

Guinea, Peru, United States (N.Y., Wis.), México, Costa Rica, Iran, Colombia. Probably cosmopolitan.

Holotype UNITED STATES, New York, Geneva, New York State Agricultural Experimental Station, isolated from soil in a sunflower field, 20 June 2000, *S. Petzolt & G.E. Harman* (DAOM 231232! Ex-type culture CBS 109720).

Additional cultures examined See Table 1.

3. *Trichoderma protrudens* Samuels & Chaverri, sp. nov. Figures 7g and 10.

Trichodermati arundinaceo Zafari, Gräfenhan & Samuels simile sed phialides longiores et angustiores et in agaro dicto PDA temperatura 37°C magis celeriter crescens. Conidia subglobosa vel ovoidea, (2.5−)2.7–3.2 (−3.5) × (2.2−)2.5–2.7(−3.0) µm.

Teleomorph None known.

Characteristics in culture Optimum temperature for growth on PDA and SNA 30°C; some growth visible at 35°C after 72 h on PDA and SNA. Colonies grown on PDA in intermittent light forming conidia within 72 h at 30°C, on

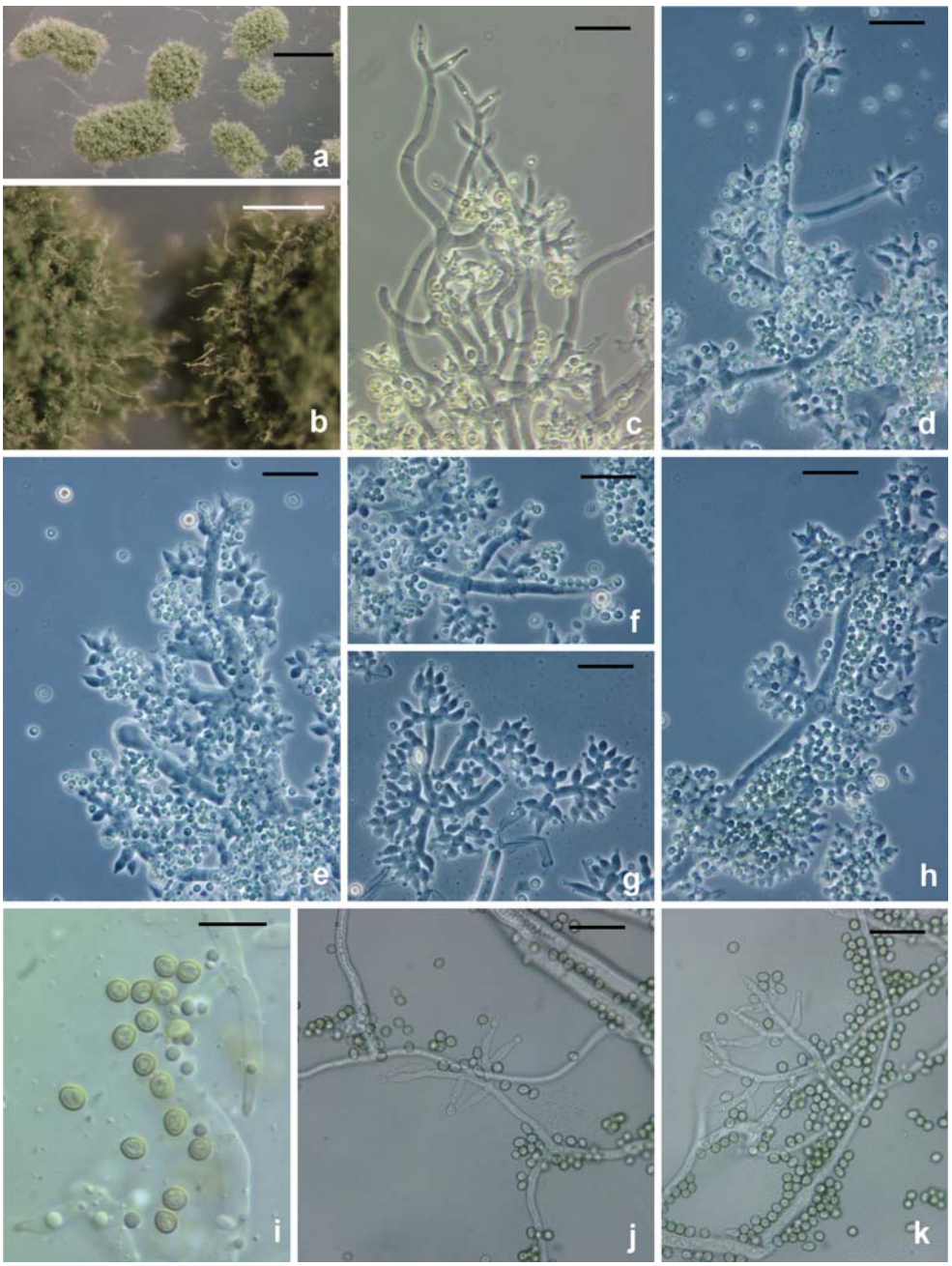

Fig. 10 *Trichoderma protrudens*. **a, b** Pustules. Protruding conidiophores seen in **b**. **a, b** from SNA. **c**–**h** Conidiophores. **c** from CMD; **d, e, f** from SNA; **g, h** from CMD. **i** Conidia, from CMD. **j, k** Synanamorph on CMD. All from CBS 121320. *Scale bars*: **a**=1 mm, **b**=150 µm, **c**–**k**=10 µm

SNA within 96 h at 30°C; sporulating after 72 h in intermittent light on PDA, not sporulating on SNA at 37°C. On PDA after 1 week at 25°C under intermittent light producing conidia in 2 or 3 rather conspicuous concentric rings of coalescing, flat pustules; colony margin scalloped. Conidia on PDA grayish green to dark green (K&W 27 C-F 7). No pigment diffusing through the agar; no distinctive odor. On SNA and CMD after 1 week under intermittent light conidia forming abundantly in the aerial mycelium around the margin of the colony and in discrete, 1–2 mm diam, pustules; pustules more abundant on SNA than on CMD, pustules on SNA formed behind the margin, on CMD in a marginal band; conidia yellowish green (K&W 29 F 8). Pustules on CMD and SNA pulvinate to hemispherical, very compact, conidial masses appearing to be moist; conspicuous long, white, terminally fertile conidiophores arising from each pustule. Conidiophores on CMD and SNA comprising a rather distinct, broad central axis with lateral and often terminal fertile branches; fertile branches profuse, separated by short internodes, typically paired, arising at or near right angles with respect to the main axis, typically increasing in length with distance from the tip; primary branches often comprising a single, broad, cell producing phialides in a dense terminal cluster, or primary branches multicellular and narrower, producing phialides at the tip and rebranching to produce secondary branches with another cluster of phialides; often a single branch of a conidiophore extending beyond the surface of the pustule, straight, septate, smooth, unbranched or sparingly branched, with long internodes between branches, each branch terminating in a verticil of a few phialides. Phialides slightly enlarged in the middle and lageniform when arising on widely spaced fertile branches or shorter and wider, ampulliform, when arising from crowded fertile branches. Synanamorph abundant in the aerial mycelium, verticillium-like, conidia held in wet, green heads. Conidia subglobose to ovoidal, (2.5−)2.7–3.2(−3.5) × (2.2−)2.5–2.7 (−3.0) μm, smooth, deep green in mass. Chlamydospores not observed.

Etymology '*protrudens*' refers to the protruding conidiophores that arise from pustules.

Habitat Isolated as an endophyte from trunk of *Theobroma cacao*.

Known distribution India (Kerala), known only from the type collection.

Holotype INDIA, Kerala, Kannara, Plantation Crops Research Institute, isolated from trunk of 8–10-m-tall tree of *Theobroma cacao,* 5 Nov 1999, *H. C. Evans* CBS 121320 (BPI 878378; ex-type culture CBS 121320).

4. *Hypocrea rodmanii* Samuels & Chaverri, sp. nov. Figures 7j–o, 11 and 12

Stromata lutea, KOH-, 2–3 × 1–2 mm. Ascosporae hyalinae, spinulosae. Pars distalis ascosporarum subglobosa vel globosa, (3.0−)3.2−4.0(−4.5) × (2.7−)3.2–3.7(−4.2) μm; pars proximalis cuneiformis vel oblonga, (3.0−)4.5−4.5 (−7.0) × (2.2−)2.7−3.2(−3.7) μm. Anamorphosis *T. brevicompacto* G. F. Kraus, C. P. Kubicek & W. Gams similis. Conidia subglobosa, (1.7−)2.0–2.5(−2.7) × (2.0−)2.2–2.7(−3.0) μm.

Stromata superficial, sometimes forming below bark, at first semi-effused, light yellow (K&W 4A4-6) with darker ostiola and a white margin, becoming pulvinate, 2–3 × 1–2 mm, ca. 1.5 mm high, darker yellow (4B7–8, 5B6–7), not reacting to KOH, broadly attached with edges slightly free, surface plane, perithecial elevations not evident, ostiola appearing as darker, viscid dots. Cells of the stroma surface in face view angular, ca. 4.5 × 3.7 μm, thin-walled. Surface region of stroma 15–20 μm wide, not pigmented, cells in section *textura epidermoidea*, 2.5–4.5 × 2.5–3.0 μm, walls slightly thickened. Tissue below stroma surface region of intertwined, ca. 2.5 μm wide, thin-walled hyphae. Perithecia elliptic in section, 215–270 μm tall, 150–250 μm diam, ostiolar canal 60–70 μm long (n = 3), perithecial apex not protruding through the stroma surface, cells not distinct from cells of the surrounding stroma surface. Tissue below perithecia *textura epidermoidea*, 8–24 × 6–10 μm, thin-walled. Asci cylindrical, (60) 70–87 (110) × (3.0) 4.0–5.5 (6.5) μm, apex with a shallow ring, 8-spored. Part-ascospores hyaline, finely spinulose, dimorphic; distal part-ascospores subglobose to globose, (3.0) 3.2–4.0 (4.5) × (2.7) 3.2–3.7 (4.2) μm; proximal part-ascospores wedge-shaped to oblong, (3.0) 4.5–4.5 (7.0) × (2.2) 2.7–3.2 (3.7) μm.

Characteristics in culture and anamorph Optimum temperature for growth on PDA 25–30°C and on SNA 20–30°C, not growing at 37°C. Colonies grown on PDA in intermittent light forming conidia within 48 h at 30°C; after 4 days in intermittent light conidial production in 3 or 4 conspicuous, narrow concentric rings of densely aggregated conidia. Conidia on PDA grayish green (K&W 27–28B-C4-6). No pigment diffusing through the agar; no distinctive odor. Conidia not forming on SNA within one week in intermittent light. Colonies grown on CMD at 25°C intermittent light >9 cm diam within one week, conidia forming in a broad ring around the margin in confluent grayish green, cottony pustules; long, sterile hairs arising from the pustules, sometimes hairs producing one phialide at the tip. Conidiophores on CMD comprising a ca. 5-μm-wide main axis from which fertile branches arise near the base; the terminal part of the conidiophore (to 100 μm) septate, straight, thin-walled; apex blunt, sterile or bearing a single,

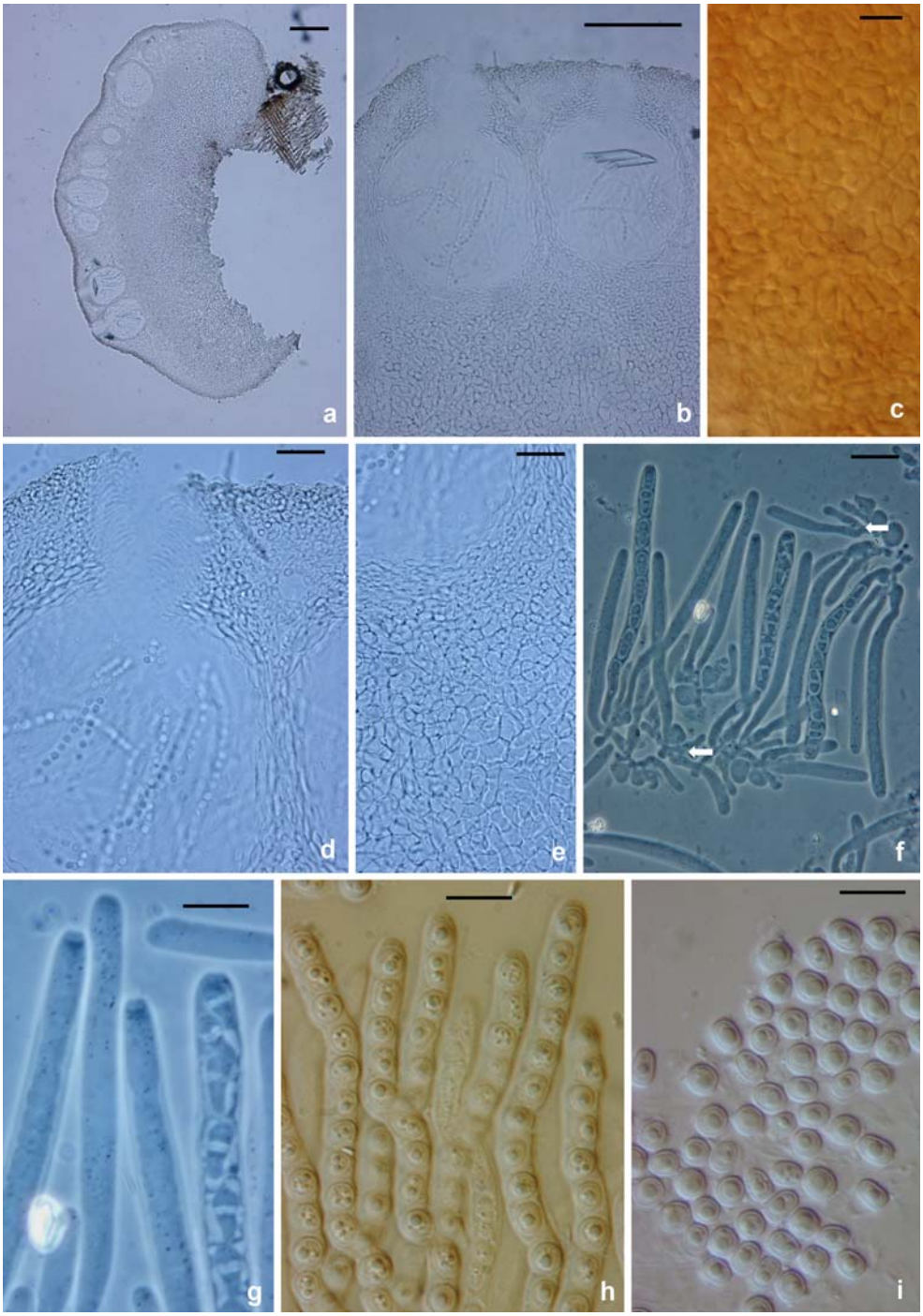

Fig. 11 *Hypocrea rodmanii*, teleomorph. **a** Longitudinal section through a stroma. **b** Median longitudinal section through two perithecia. **c** Cells of the stroma surface in face view. **d** Median longitudinal section through a perithecium showing details of the stroma surface and ostiolar region. **e** Cells of the stroma below perithecia. **f** Young asci showing croziers (*arrows*) and developing ascospores. **g, h** Asci. Apical rings visible in **g**. **i** Discharged ascospores. **a, b, d, e, i** from G.J.S. 91–90; **f, g** from G.J.S. 91–89; **c, h** from G.J.S. 91–88. *Scale bars*: **a, b**=100 μm; **c–f, g-i**=10 μm

terminal phialide. Branches arising at right angles to the main axis at or near 90°, often consisting of one or a few broad cells, or branches longer and of narrower cells; fertile branches often paired, mostly progressively longer with distance from the tip, often rebranching to produce secondary branches; secondary branches typically comprising a single, broad cell with a terminal cluster of phialides. Conidiophores often lacking a sterile elongation, internodes between secondary branches short and phialides densely disposed on short secondary branches. Phialides held in divergent heads of 3–5, ampulliform. Conidia subglobose, (1.7−)2.0–2.5(−2.7) × (2.0−)2.2–2.7(−3.0) μm, smooth, grayish green in mass. Synanamorph not observed. Chlamydospores not observed after 1 week on CMD under intermittent light.

Etymology Hypocrea rodmanii is named in honour of Dr. James E. Rodman, U.S. National Science Foundation, in

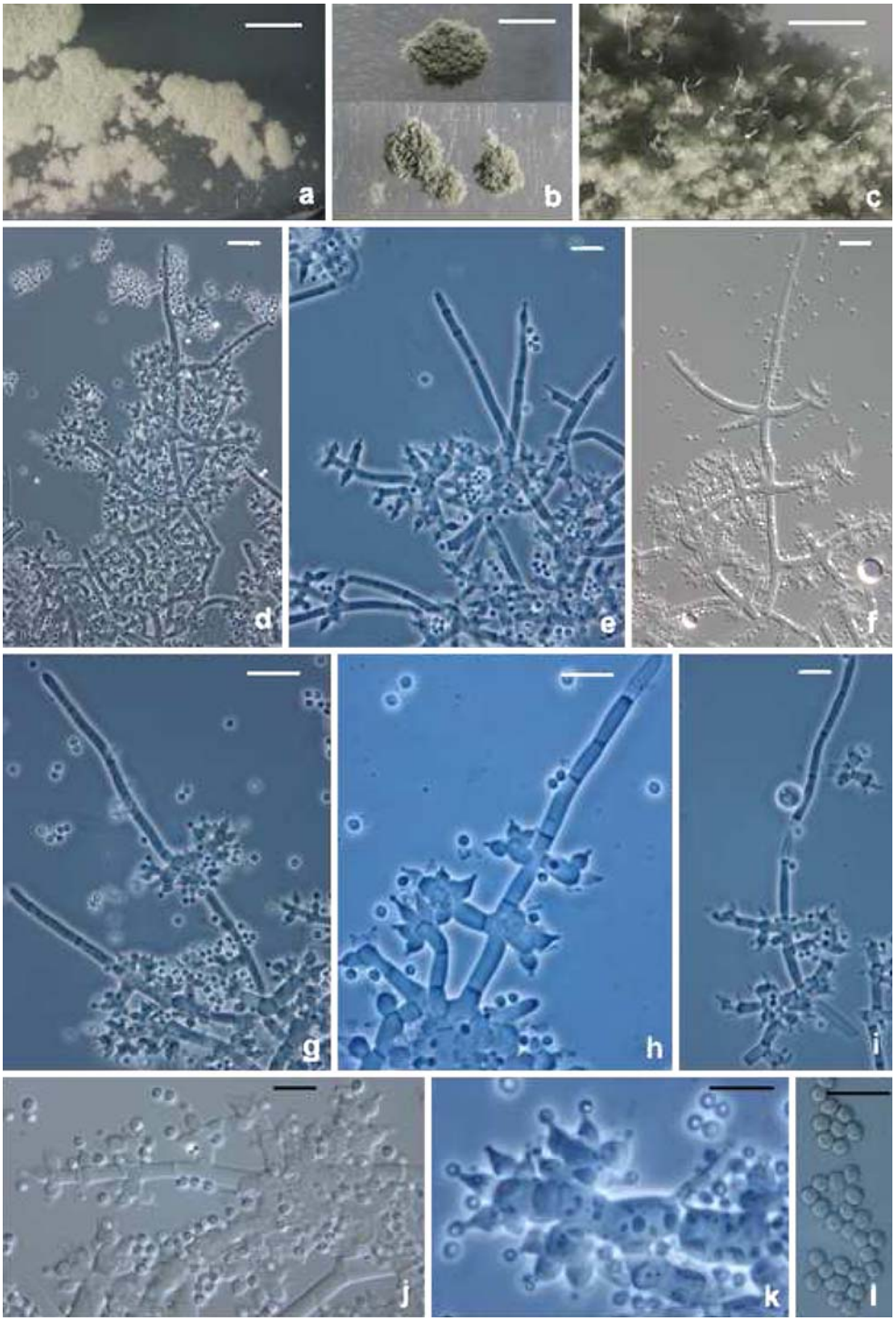

Fig. 12 *Hypocrea rodmanii*, *Trichoderma* anamorph. **a**–**c** Pustules from CMD. **d**–**k** Conidiophores, detail of phialides shown in **k**. **d, e, g–k** from CMD, **f** from SNA. **l** Conidia, from CMD. **a, c, f** from G.J.S. 91–89; **b, d, g, j** from G.J.S. 91–88; e, h, i, k, l from G.J.S. 91–91. *Scale bars*: a, b=1 μm, **c**=150 μm, **d–l**=10 μm

recognition of vision and tenacity in developing the NSF program Partnerships Enhancing Expertise in Taxonomy (PEET), which supported the authors of this species as, respectively, mentor and student.

Habitat On decorticated, rotten wood, often below flaking bark.

Known distribution United States (Maryland, Virginia).

Holotype UNITED STATES, Virginia, Giles County, Cascades Recreation Site, 4 mi N of Pembroke, along Little Stony Creek, 37°02′N, 80°35′W, elev. 838 m, 18 Sep 1991, on branchlets, *G.J. Samuels, C.T. Rogerson, S.M. Huhndorf, S. Rehner & M. Williams* (BPI 1112859, ex-type culture CBS 120895).

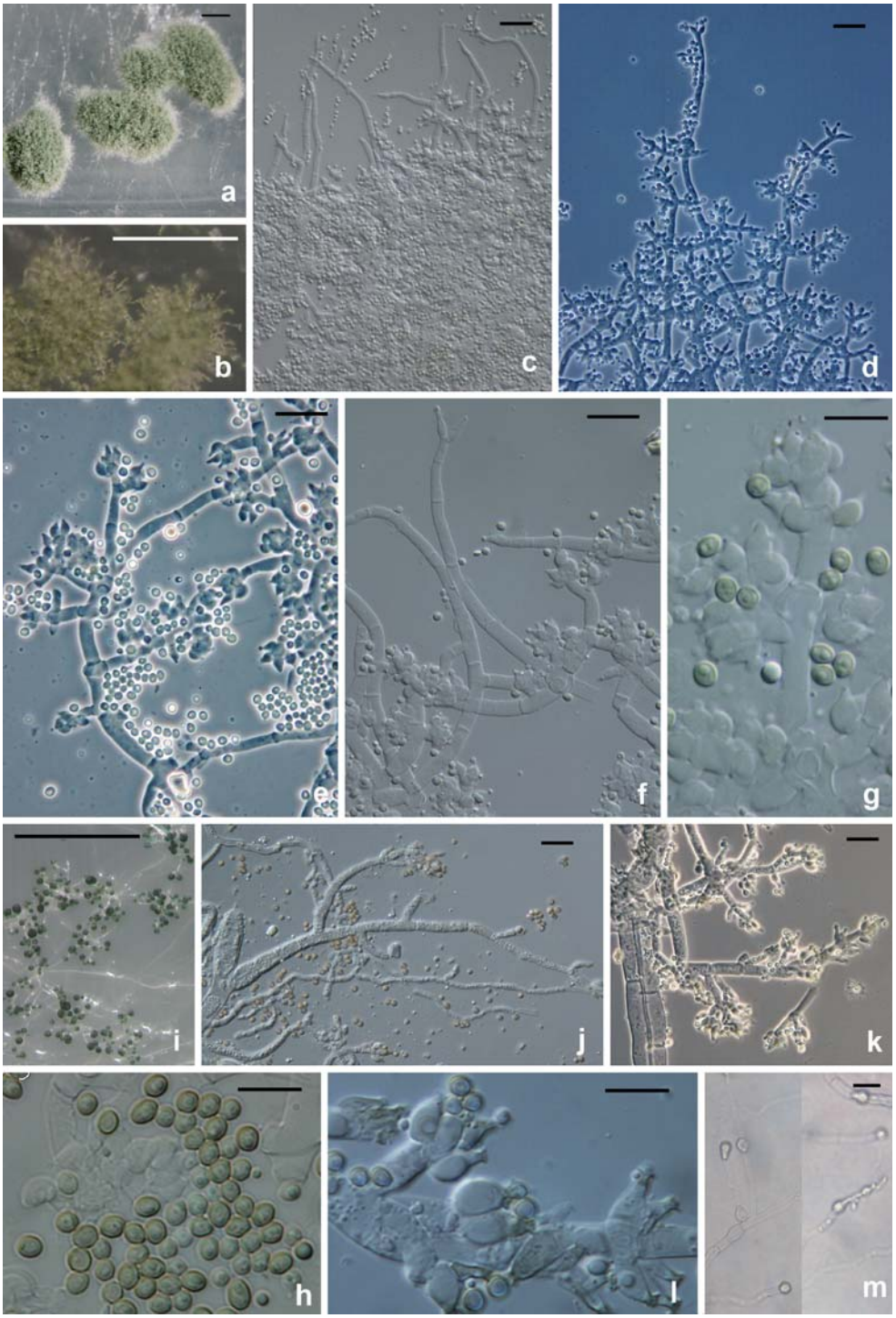

Fig. 13 *Trichoderma turrialbense.* **a, b** Pustules, protruding conidiophores visible in **b**. **a** from CMD, **b** from SNA. **c–g** Conidiophores. **c, d, e, f** from SNA; **g** from CMD. **h** Conidia from SNA. **i–l** Synanamorph on CMD. Details of phialides seen in **l**. **m** Chlamydospores from CMD. **a c, d, f, k, l** = GJS 07–74, **b, e, g, h, j, m** = CBS 112445. *Scale bars*: **a, b**=0.5 mm, **c–m**=10 μm

Additional specimens examined Three specimens with the same collecting data as the holotype (G.J.S. 91-90 = BPI 1112861; BPI 1112862, culture G.J.S. 91-91 = CBS 109719; BPI 1112860, culture G.J.S. 91-89 = CBS 120897; BPI 1112861). Maryland, Garrett County, 5 mi N of Barton, Little Savage River Ravine, on decorticated wood, 23 Sep 1989, *G.J. Samuels (89–120), C.T. Rogerson, W.R. Buck, R.C. Harris* (NY = CBS 122582); same collecting data, *G.J. Samuels (89–116)* (NY = CBS 122581).

Comments The form and pigmentation of the stroma of *H. rodmanii* suggest *H. lutea*, but the anamorph readily distinguishes this species from other known species.

5. *Trichoderma turrialbense* Samuels, Degenkolb, K.F. Nielsen & Gräf. sp. nov. Figures 7h and 13.

Trichodermati brevicompacto G. F. Kraus, C. P. Kubicek & W. Gams simile sed harzianum A produens. Conidia subglobosa, (2.2−)2.5–3.0(−3.2) × (2.0−)2.2–2.7 (−3.0) μm.

Teleomorph None known.

Characteristics in culture Optimum temperature for growth on PDA and SNA 30°C; very little growth at 37°C after 72 h. On PDA forming conidia under intermittent light within 72 h at 30°C, sometimes also sporulating on PDA at 37°C in intermittent light after 96 h. On PDA at 25°C after 5 days under intermittent light producing conidia in broad concentric rings, the oldest conidia in the center and the youngest at the edge of the colony; colony margin even. Conidia on PDA yellowish green (K&W 28–30 D-E 8). No pigment diffusing through the agar; no distinctive odor. Colonies grown on SNA under intermittent light forming conidia only sporadically after 72 h at 30°C. On CMD and SNA after 1 week at 25°C under 12 h cool white fluorescent light/12 h darkness conidia forming abundantly around the colony periphery in more or less conspicuous, compact flat pustules 0.5–1 mm diam, yellow green ('deep green,' K&W 29 E-F 8). Pustules compact or loosely arranged, conidiophores more or less extensively branched, often with long internodes between branches, with a conspicuous main axis; often producing one or a few divergent phialides from the tip; branches arising at right angles to the main axis, short, progressively longer with distance from the tip. Secondary branches arising at right angles from the primary branches, typically unicellular, each terminating in 2−5 divergent or convergent (gliocladium-like) phialides. Phialides ampulliform, shorter and broader when crowded. Conidia subglobose, (2.2−)2.5–3.0(−3.2) × (2.0−)2.2–2.7 (−3.0) μm, smooth, green, appearing to be held in globose wet heads. On CMD and SNA conidiophores of synanamorph arising from surface of agar and from aerial mycelium in abundance, 70–180 μm long, 5–14 μm wide at the base, lateral branches arising at an angle of < 90° with respect to the main axis, terminating in an appressed head of phialides or lower branches producing secondary branches with an appressed head of 2–5 phialides. Phialides ampulliform, 6–7 μm long, 3.0–3.5 μm wide at the widest point, collarette often flared. Chlamydospores not observed on CMD.

Etymology '*turrialbense'* refers to the town of Turrialba, Costa Rica, the only place where this species is known to occur.

Holotype Costa Rica, Turrialba, La Montaña, isolated from soil in a maize field, date not known, S. Danielsen 017, comm. M. Lübeck (BPI 878379, ex-type culture CBS 112445).

Additonal culture examined Costa Rica, Turrialba, isolated from banana roots, date unknown, A. zum Felde S14 comm. R. Sikora (BPI 878380; live culture BBA 72294= CBS 122554).

Comments The culture CBS 112445 was included in the original description of *T. brevicompactum,* where it was reported under the number '4105.' The main distinction between *T. turrialbense* and *T. brevicompactum* is that the main toxin of the former is harzianum A whereas the main toxin of the latter is trichodermin. As can be seen from Table 8, there are slight differences in conidial length, length/width of conidia, width of phialides and cells from which phialides arise. The peptaibiotics pattern of *T. turrialbense* is similar to that of *T. brevicompactum*.

Acknowledgments Dr. James L. Swezey, USDA-ARS, NCAUR, provided culture NRRL 3199. Dr. Harry Evans and CABI-BioScience provided endophytic cultures. CBS and BBA provided additional cultures; we especially acknowledge Ms. Trix Merckx (CBS) for her assistance in receiving and dispatching cultures. Latin descriptions were kindly corrected by Prof. Dr. Ferdinand R. Prostmeier (Justus Liebig Universität, Gießen, Germany). Financial support by the Studienstiftung Mykologie (Cologne, Germany), the Erwin-Stein-Stiftung (Gießen, Germany), the Danish Research Council for Technology and Production Sciences (26-04-0050) and the Centre for Advanced Food Studies (LMC) (Copenhagen, Denmark) is gratefully acknowledged.

References

Adams PM, Hanson JR (1972) Sesquiterpenoid metabolites of *Trichoderma polysporum* and *T. sporulosum*. Phytochemistry 11:423

Auvin-Guette C, Rebuffat S, Prigent Y, Bodo B (1992) Trichogin A IV, an 11-residue lipopeptaibol from *Trichoderma longibrachiatum*. J Am Chem Soc 114:2170–2174

Auvin-Guette C, Rebuffat S, Vuidepot I, Massias M, Bodo B (1993) Structural elucidation of trichokoningins KA and KB, peptaibols from *Trichoderma koningii*. J Chem Soc Perkin Trans I:249–255

Bamburg JR, Strong FM (1969) Mycotoxins of the trichothecane family produced by *Fusarium tricinctum* and *Trichoderma lignorum*. Phytochemistry 8:2405–2410

Bissett J (1991) A revision of the genus *Trichoderma*. III. Section *Pachybasium*. Can J Bot 69:2373–2417

Brückner H, Jung G (1980) Identification of N-acetyl-α-aminobutryic acid after selective trifluoroacetolysis of alamethicin and related peptide antibiotics. Chromatographia 13:170–174

Carbone I, Kohn LM (1999) A method for designing primer sets for speciation studies in filamentous ascomycetes. Mycologia 91:553–556

Chaverri P, Samuels GJ (2003) *Hypocrea*/*Trichoderma* (Ascomycota, Hypocreales, Hypocreaceae): species with green ascospores. Stud Mycol 48:1–116

Chaverri P, Bischoff JF, Hodge KT (2005) A new species of *Hypocrella, H. macrostroma*, and its relationship to other species with large stromata. Mycol Res 109:1268–1275

Coats JH, Meyer CE, Reusser F (1974) Alamethicin and production therefor. Patent U.S.3833723 A61k 21/00 (424–118):1–8

Corley DG, Miller-Wideman M, Durley RC (1994) Isolation and structure of harzianum A: a new trichothecene from *Trichoderma harzianum*. J Nat Prod 57:442–425

Cvetnić Z, Pepelnjak S (1997) Distribution and mycotoxin-producing ability of some fungal isolates from the air. Atmos Environ 31:491–495

Degenkolb T, Berg A, Gams W, Schlegel B, Gräfe U (2003) The occurrence of peptaibols and structurally related peptaibiotics and their mass spectrometric identification *via* diagnostic fragment ions. J Pept Sci 9:666–678

Degenkolb T, Gräfenhan T, Nirenberg HI, Gams W, Brückner H (2006a) *Trichoderma brevicompactum* Complex: Rich source of novel and recurrent plant-protective polypeptide antibiotics. J Agric Food Chem 54:7047–7061

Degenkolb T, Gräfenhan T, Berg A, Nirenberg HI, Gams W, Brückner H (2006b) Peptaibiomics: Screening for polypeptide antibiotics (Peptaibiotics) from plant-protective *Trichoderma* species. Chem Biodivers 3:593–610

Degenkolb T, Kirschbaum J, Brückner H (2007) New sequences, constituents, and producers of peptaibiotics: an updated review. Chem Biodivers 4:1052–1067

Degenkolb T, von Döhren H, Nielsen KF, Samuels GJ, Brückner H (2008a) Recent advances and future prospects in peptaibiotics and mycotoxin research and their importance for chemotaxonomy of *Trichoderma* and *Hypocrea*. Chem Biodivers 5 doi:10.1002/cbdv.200890064 (May 20)

Degenkolb T, Gams W, Brückner H (2008b) Natural *cyclo*-peptaibiotics and related *cyclo*-tetrapeptides: structural diversity and future prospects. Chem Biodivers 5 doi:10.1002/cbdv.200890066

Dettman JR, Jacobson DJ, Taylor JW (2003) A multilocus genealogical approach to phylogenetic species recognition in the model eukaryote *Neurospora*. Evolution 57:2703–2720

Dodd S, Lieckfeldt E, Chaverri P, Overton BE, Samuels GJ (2002) Taxonomy and phylogenetic relationships of two species of *Hypocrea* with *Trichoderma* anamorphs. Mycological Progress 1:409–428

Domsch KH, Gams W, Anderson T-H (2007) Compendium of soil fungi, 2nd taxonomically revised edition by W. Gams. IHW, Eching

Don RH, Cox PT, Wainwright BJ, Baker K, Mattick JS (1991) Touchdown PCR to circumvent spurious priming during gene amplification. Nucleic Acids Res 19:4008

Evans HC, Holmes KA, Thomas SE (2003) Endophytes and mycoparasites associated with an indigenous forest tree, *Theobroma gileri*, in Equador and a preliminary assessment of their potential as biological control agents of cocoa diseases. Mycol Prog 2:149-160

Favilla M, Macchia L, Gallo A, Altomare C (2006) Toxicity assessment of fungal biocontrol agents using two different (*Artemia salina* and *Daphnia magna*) invertebrate bioassays. Food Chem Toxicol 44:1922–1931

Fujita T, Wada S-I, Iida A, Nishimura T, Kanai M, Toyoma N (1994) Fungal metabolites. XIII. Isolation and structure elucidation of new peptaibols, trichodecenins-I and -II from *Trichoderma viride*. Chem Pharm Bull 42:489-494

Gilly M, Benson NR, Pellegrini M (1985) Affinity labeling the ribosome with eukaryotic-specific antibiotics - (bromoacetyl) trichodermin. Biochemistry 24:5787–5792

Godtfredsen WO, Vangedal S (1964) Trichodermin, a new antibiotic related to trichothecin. Proc Chem Soc 1964:188–189

Godtfredsen WO, Vangedal S (1965) Trichodermin, a new sesquiterpene antiobiotic. Acta Chem Scand 19:1088–1102

Gräfenhan T (2006) Epidemiology and biological control of latent grapevine trunk diseases. PhD Thesis. Faculty of Agriculture and Horticulture, Humboldt-University Berlin, Germany. 138 pp

Hanada RE, de Souza JT, Pomella AWV, Hebbar KP, Pereira JO, Ismaiel A, Samuels GJ (2008) *Trichoderma martiale* sp. nov., a new endophyte from sapwood of *Theobroma cacao* with a potential for biological control. Mycol Res (In press)

Hawksworth DL (2001) The magnitude of fungal diversity, the 1.5 million estimate revisited. Mycol Res 105:1422–1432

Huang Q, Tezuka Y, Kikuchi T, Nishi A, Tubaki K, Tanaka K (1995) Studies on metabolites of mycoparasitic fungi. II. Metabolites of *Trichoderma koningii*. Chem Pharm Bull 43:223-229

Huelsenbeck JP (2000) MrBayes: Bayesian inferences of phylogeny (software). University of Rochester, New York

Huelsenbeck JP, Ronquist F, Nielsen ES, Bollback JP (2001) Bayesian inference of phylogeny and its impact on evolutionary biology. Science 294:2310–2314

Jaklitsch WM, Samuels GJ, Dodd SL, Lu B-S, Druzhinina IS (2006) *Hypocrea rufa/Trichoderma viride*: a reassessment, and description of five closely related species with and without warted conidia. Stud Mycol 56:135-177

Jin H-Z, Lee J-H, Zhang W-D, Lee H-B, Hong Y-S, Kim Y-H, Lee J-J (2007) Harzianums A and B produced by a fungal strain, *Hypocrea* sp. F000527, and their cytotoxicity against tumor cell lines. J Asian Nat Prod Res 9:203–207

Kindermann J, El-Ayouti Y, Samuels GJ, Kubicek CP (1998) Phylogeny of the genus *Trichoderma* based on sequence analysis of the internal transcript spacer 1 of the rDNA cluster. Fungal Genet Biol 24:298-309

Kirschbaum J, Krause C, Winzheimer RK, Brückner H (2003) Alamethicin sequences reconsidered and reconciled. J Pept Sci 9:799-809

Kornerup A, Wanscher JH (1978) Methuen handbook of colour, 3rd edn. Eyre Methuen, London

Kraus GF, Druzhinina I, Gams W, Bissett J, Zafari D, Szakacs G, Koptchinski A, Prillinger H, Zare R, Kubicek CP (2004) *Trichoderma brevicompactum* sp. nov. Mycologia 96:1059-1073

Krause C, Kirschbaum J, Brückner H (2006) Peptaibiomics: an advanced, rapid and selective analysis of peptaibiotics/peptaibols by SPE/LC-ES-MS. Amino Acids 30:435-443

Kubicek CP, Baker S, Gamauf C, Kennerley CM, Druzhinina IS (2008) Purifying selection and birth-and-death evolution in the class II hydrophobin gene families of the ascomycete *Trichoderma/Hypocrea*. BMC Evol Biol 8:4 doi:10.1186/1471-2148-8-4

Küsters E, Portmann A (1994) Enantiomeric separation of amino alcohols by gas chromatography on a chiral stationary phase; influence of the perfluoroacetylating reagent on the separation. J High Resolut Chromatogr 17:639-642

Laatsch H (2007) AntiBase 2007. The natural compound identifier. Wiley, Weinheim, Germany

Landreau A, Pouchus YF, Sallenave-Namont C, Biard J-F, Boumard M-C, Robiou Du Pont T, Mondeguer F, Goulard C, Verbist J-F (2002) Combined use of LC/MS and a biological test for rapid identification of marine mycotoxins produced by *Trichoderma koningii*. J Microbiol Methods 48:181-194

Lee HB, Kim Y, Jin HZ, Lee JJ, Kim C-J, Park JY, Jung HS (2005) A new *Hypocrea* strain producing harzianum A cytotoxic to tumour cell lines. Lett Appl Microbiol 40:497-503

Leitgeb B, Szekeres A, Manczinger A, Vágvölgyi C, Kredics L (2007) The history of alamethicin: a review of the most extensively studied peptaibol. Chem Biodivers 4:1027-1051

Liao LL, Grollman AP, Horwitz SB (1976) Mechanism of action of 12,13-epoxytrichothecene, anguidine, an inhibitor of protein-synthesis. Biochim Biophys Acta 454:273–284

Linder MB, Szilvay GR, Nakari-Setälä T, Penttilä ME (2005) Hydrophobins: the protein-amphiphiles of filamentous fungi. FEMS Microbiol Rev 29:877-896

Liu YJ, Whelen S, Hall BD (1999) Phylogenetic relationships among Ascomycetes: Evidence from an RNA polymerase II subunit. Mol Biol Evol 16:1799-1808

Lorito M, Farkas V, Rebuffat S, Bodo B, Kubicek CP (1996) Cell wall synthesis is a major target of mycoparasitic antagonism by *Trichoderma harzianum*. J Bacteriol 178:6382–6385

Maddison DR, Maddison WM (2005) MacClade 4 Analysis of phylogeny and character evolution (version 4.06). Sinauer Associates, Sunderland Mass. http://macclade.org/index.html

Mason-Gamer RJ, Kellogg EA (1996) Testing for phylogenetic conflict among molecular data sets in the tribe Triticeae (Gramineae). Syst Biol 45:524–545

Mau B, Newton M, Larget B (1999) Bayesian phylogenetic inference via Markov chain Monte Carlo methods. Biometrics 55:1–12

Mohamed-Benkada M, Montagu M, Biard JF, Modeguer F, Vérité P, Dalgalarrondo M, Bissett J, Pouchus YF (2006) New short peptaibols from a marine *Trichoderma* strain. Rapid Comm Mass Spectrometry 20:1176–1180

Neuhof T, Dieckmann R, Druzhinina IS, Kubicek CP, von Döhren H (2007a) Intact-cell MALDI-TOF mass spectrometry analysis of peptaibol formation by the genus *Trichoderma*/*Hypocrea*: can molecular phylogeny of species predict peptaibol structures? Microbiology 153:3417-3437

Neuhof T, Dieckmann R, Druzhinina IS, Kubicek CP, Nakari-Setälä T, Penttilä M, von Döhren H (2007b) Direct identification of hydrophobins and their processing in *Trichoderma* using Intact-Cell MALDI-TOF mass spectrometry. FEBS J 274:841-852

New AP, Eckers C, Haskins NJ, Neville WA, Elson S, Hueso-Rodriguez JA, Rivera-Sagredo A (1996) Structures of polysporins A-D, four new peptaibols isolated from *Trichoderma polysporum*. Tetrahedron Lett 37:3039-3042

Nielsen KF, Gräfenhan T, Zafari D, Thrane U (2005) Trichothecene production by *Trichoderma brevicompactum*. J Agric Food Chem 53:8190-8196

Nirenberg H (1976) Untersuchungen über die morphologische und biologische Differenzierung in der *Fusarium*-Sektion Liseola. Mitt Biol Bundesanst Land- Forstwirtsch Berlin-Dahlem 169:1-117

Oh S-U, Yun B-S, Kim J-H, Yoo I-D (2002) Atroviridins A-C and neoatroviridins A-D, novel peptaibol antibiotics produced by *Trichoderma atroviride* F80317. J Antibiot 55:557-564

Poirier L, Quiniou F, Ruiz N, Montagu M, Amiard J-C, Pouchus YF (2007) Toxicity assessment of peptaibols and contaminated sediments on *Crassostrea gigas* embryos. Aquat Toxicol 83:254–262

Posada D, Crandall KA (1998) Modeltest: testing the model of DNA substitution. Bioinformatics 14:917-918

Psurek A, Neusüss C, Degenkolb T, Brückner H, Balaguer E, Imhof D, Scriba GKE (2006) Detection of new amino acid sequences of alamethicins F30 by nonaqueous capillary electrophoresis-mass spectrometry. J Pept Sci 12:279–290

Rambaut A, Drummond A (2004) TRACER v 1.2.1. http://evolve.zoo.ox.ac.uk/software.html?id5tracer

Rannala B, Yang Z (1996) Probability distribution of molecular evolutionary trees: a new method of phylogenetic interference. J Mol Evol 43:304–311

Rebuffat S, Goulard C, Bodo B (1995) Antibiotic peptides from *Trichoderma harzianum*: harzianins HC, proline-rich 14-residue peptaibols. J Chem Soc Perkin Trans I:1849-1855

Reeb V, Lutzoni F, Roux C (2004) Contribution of RPB2 to multilocus phylogenetic studies of the Euascomycetes (Pezizomycotina, Fungi) with special emphasis on lichen-forming Acarosporaceae and evolution of polyspory. Mol Phylogenet Evol 32:1036–1060

Ruiz N, Wielgoz-Collin G, Poirier L, Grovel O, Petit KE, Mohamed-Benkada M, Robiou Du Pont T, Bissett J, Vérité P, Barnathan G, Pouchus YF (2007) New trichobrachins, 11-residue peptaibols from a marine strain of *Trichoderma longibrachiatum*. Peptides 28:1351–1358

Saikawa Y, Okamoto H, Inui T, Makabe M, Okuno T, Suda T, Hashimoto K, Nakata M (2001) Toxic principles of a poisonous mushroom *Podostroma cornu-damae*. Tetrahedron 57:8277–8281

Sallenave C, Pouchus YF, Bardouil M, Lassus P, Roquebert F, Verbist J-F (1999) Bioaccumulation of mycotoxins by shellfish: contamination of mussels by metabolites of a *Trichoderma koningii* strain isolated in the marine environment. Toxicon 37:77–83

Samuels GJ (2006) *Trichoderma*: systematics, the sexual state and ecology. Phytopathology 96:195–206

Samuels GJ, Dodd SL, Gams W, Castlebury LA, Petrini O (2002) *Trichoderma* species associated with the green mold epidemic of commercially grown *Agaricus bisporus*. Mycologia 94:146–170

Samuels GJ, Dodd S, Lu B-S, Petrini O, Schroers H-J, Druzhinina IS (2006) The *Trichoderma koningii* aggregate species. Stud Mycol 56:67–133

Sivasithamparam K, Ghisalberti EL (1998) Secondary metabolism in *Trichoderma* and *Gliocladium*. In: Kubicek CP, Harman GE (eds) *Trichoderma* and *Gliocladium*. Volume 1. Basic biology, taxonomy, and genetics. Francis & Taylor, London, pp 139–191

Swofford DL (2002) PAUP*: Phylogenetic analysis using parsimony (*and other methods). Version 4.06b10. Sinauer Associates, Sunderland, Mass.

Thompson JD, Gibson TJ, Plewniak F, Jeanmougin F, Higgins DG (1997) The ClustalX windows interface; flexible strategies for multiple sequence alignmjent aided by quality analysis tools. Nucleic Acids Res 24:4876–4882

Viterbo A, Chet I (2006) TasHyd1, a new hydrophobin gene from the biocontrol agent *Trichoderma asperellum*, is involved in plant root colonization. Mol Plant Pathol 7:249-258

Watts R, Dahiya J, Chaudhary K, Tauro P (1988) Isolation and characterization of a new antifungal metabolite of *Trichoderma reesei*. Plant Soil 107:81–84

White TJ, Bruns T, Lee S, Taylor J (1990) Amplification and direct sequencing of fungal ribosomal RNA genes for phylogenetics. In: Innis MA, Gelfand DH, Sninsky JJ, White TJ (eds) PCR protocols: aguide to methods and applications. Academic Press, San Diego, pp 315–322